

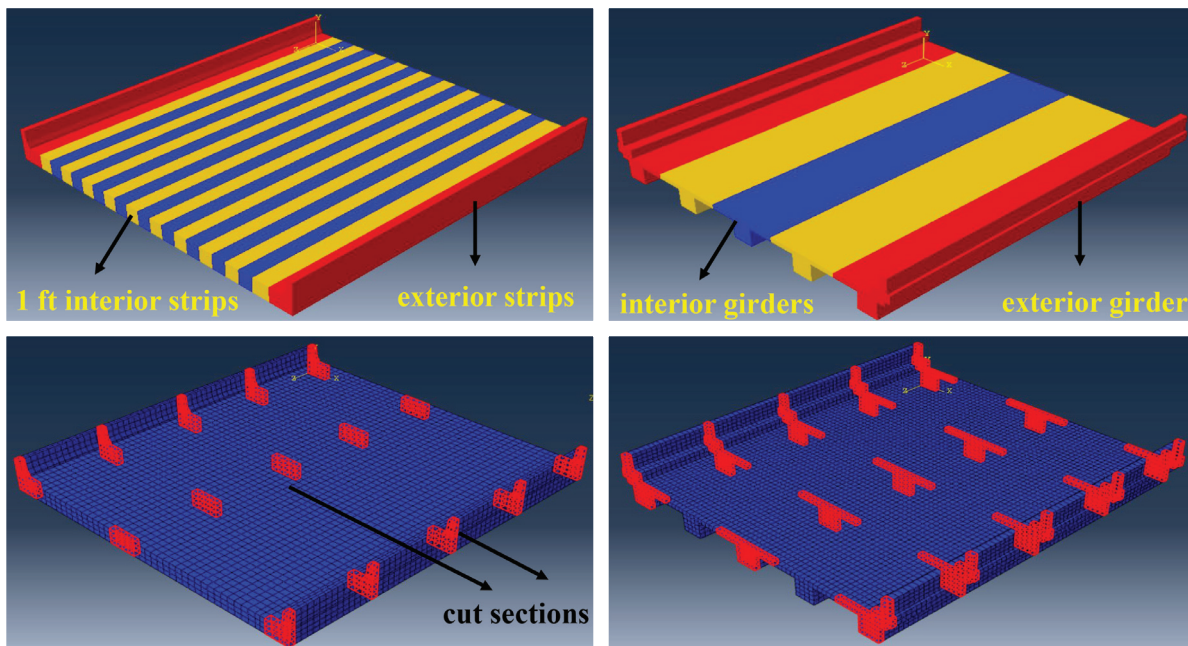
JOINT TRANSPORTATION RESEARCH PROGRAM

INDIANA DEPARTMENT OF TRANSPORTATION
AND PURDUE UNIVERSITY



Strength Assessment of Older Continuous Slab and T-Beam Reinforced Concrete Bridges

Bridge Modeling



**Seungwook Seok, Faezeh Ravazdezh,
Ghadir Haikal, Julio A. Ramirez**

RECOMMENDED CITATION

Seok, S., Ravazdezh, F., Haikal, G., & Ramirez, J. A. (2019). *Strength assessment of older continuous slab and T-beam reinforced concrete bridges* (Joint Transportation Research Program Publication No. FHWA/IN/JTRP-2019/13). West Lafayette, IN: Purdue University. <https://doi.org/10.5703/1288284316924>

AUTHORS

Seungwook Seok
Faezeh Ravazdezh

Graduate Research Assistants
Lyles School of Civil Engineering
Purdue University

Ghadir Haikal, PhD

Assistant Professor of Civil Engineering
Lyles School of Civil Engineering
Purdue University
ghaikal@purdue.edu
Corresponding Author

Julio A. Ramirez, PhD

Karl H. Kettlehut Professor in Civil Engineering
Lyles School of Civil Engineering
Purdue University
(765) 494-2716
ramirez@purdue.edu
Corresponding Author

ACKNOWLEDGMENTS

This project was made possible by the sponsorship of the Joint Transportation Research Program (JTRP) and the Indiana Department of Transportation (INDOT). The authors would like to thank the members of the Study Advisory Committee for their valuable assistance and technical guidance in the course of performing this study.

JOINT TRANSPORTATION RESEARCH PROGRAM

The Joint Transportation Research Program serves as a vehicle for INDOT collaboration with higher education institutions and industry in Indiana to facilitate innovation that results in continuous improvement in the planning, design, construction, operation, management and economic efficiency of the Indiana transportation infrastructure. Further information about JTRP and its current research program is available at <https://engineering.purdue.edu/JTRP.Z>

Published reports of the Joint Transportation Research Program are available at <http://docs.lib.purdue.edu/jtrp/>.

NOTICE

The contents of this report reflect the views of the authors, who are responsible for the facts and the accuracy of the data presented herein. The contents do not necessarily reflect the official views and policies of the Indiana Department of Transportation or the Federal Highway Administration. The report does not constitute a standard, specification, or regulation.

TECHNICAL REPORT DOCUMENTATION PAGE

1. Report No. FHWA/IN/JTRP-2019/13	2. Government Accession No.	3. Recipient's Catalog No.	
4. Title and Subtitle Strength Assessment of Older Continuous Slab and T-Beam Reinforced Concrete Bridges	5. Report Date May 2019		6. Performing Organization Code
	7. Author(s) Seungwook Seok, Faezeh Ravazdezh, Ghadir Haikal, Julio A. Ramirez		8. Performing Organization Report No. FHWA/IN/JTRP-2019/13
9. Performing Organization Name and Address Joint Transportation Research Program Hall for Discovery and Learning Research (DLR), Suite 204 207 S. Martin Jischke Drive West Lafayette, IN 47907	10. Work Unit No.		11. Contract or Grant No. SPR-4120
	12. Sponsoring Agency Name and Address Indiana Department of Transportation (SPR) State Office Building 100 North Senate Avenue Indianapolis, IN 46204		13. Type of Report and Period Covered Final Report
14. Sponsoring Agency Code		15. Supplementary Notes Conducted in cooperation with the U.S. Department of Transportation, Federal Highway Administration.	
16. Abstract <p>This report investigates a new methodology for load rating of older reinforced concrete flat-slab and T-beam bridges in Indiana, using the tools of 3D finite element analysis. The Conventional Load Rating (CLR) method currently in use by INDOT relies on a simplified 2D analysis based on beam theory that may underestimate bridge capacity. Since the actual behavior of a bridge structure is 3D in nature, a 3D computational model is better suited to estimate bridge response for load rating. 3D finite elements models are capable of reflecting actual bridge dimensions, cross sections, and connection configurations. More importantly, with three-dimensional models, the load distribution in the transverse direction of the deck can be explicitly represented, and therefore optimized for maximum impact on load rating. Using 3D models, it is also possible to account for support continuity, variable cross sections, skew factor, edge railings, and other parameters that impact bridge behavior. It is therefore expected that load rating using 3D analysis can result in a more accurate assessment of bridge load carrying capacity compared to CLR by improving demand estimates.</p> <p>A sample of ten representative bridges (five of each type) is selected for this study. The representative bridges were identified based on the statistical distribution of older flat slab and T-beam RC bridges in Indiana. Load rating analysis results for the sample bridges using 3D analysis were compared to ratings obtained using CLR to identify factors contributing to bridge capacity that are not accurately represented with current rating standards. The results show significantly improved rating factors using 3D FE models. A sensitivity study was conducted to assess the impact of select parameters on load rating results and identify potential improvements to current load rating procedures using CLR.</p>			
17. Key Words load rating, AASHTO CLR, 3D finite element analysis, reinforced concrete bridges, flat-slab, T-beam, strength assessment		18. Distribution Statement No restrictions. This document is available through the National Technical Information Service, Springfield, VA 22161.	
19. Security Classif. (of this report) Unclassified	20. Security Classif. (of this page) Unclassified	21. No. of Pages 70 including appendix	22. Price

EXECUTIVE SUMMARY

STRENGTH ASSESSMENT OF OLDER CONTINUOUS SLAB AND T-BEAM REINFORCED CONCRETE BRIDGES

Introduction

This report investigates a new methodology for the load rating of older reinforced concrete flat-slab and T-beam bridges in Indiana, using the tools of 3D finite element analysis. The conventional load rating (CLR) method currently in use by INDOT relies on a simplified 2D analysis based on beam theory that may underestimate bridge capacity. Since the actual behavior of a bridge structure is 3D in nature, a 3D computational model is better suited to estimate bridge carrying capacity for load rating. 3D finite elements models are capable of reflecting actual bridge dimensions, cross sections, and connection configurations. More importantly, with three-dimensional models, the load distribution in the transverse direction of the deck can be explicitly represented, and therefore optimized for maximum impact on load rating. It is also possible to account for support continuity, variable cross sections, skew factor, edge railings, and other factors that impact bridge behavior using 3D models. Therefore, it is expected that load rating using 3D analysis can result in a more accurate assessment of bridge load carrying capacity compared to CLR by improving demand estimates.

A sample of ten representative bridges (five of each type) was selected for this study. The representative bridges were identified based on the statistical distribution of older flat slab and T-beam RC bridges in Indiana. Load rating analysis results for the sample bridges using 3D analysis were compared to ratings obtained using CLR to identify factors contributing to bridge capacity that are not accurately represented with current rating standards. A sensitivity study was conducted on select parameters to assess their impact on load rating results and identify potential improvements to current load rating procedures using CLR.

Findings

Task 1. Selection of representative bridges

Five representative bridges for each bridge type were selected from the NBI database for Indiana. Among many structural/nonstructural features, the following were considered to identify the bridge samples: year built, span length, number of spans, number of lanes, curb-to-curb roadway width, skew angle, and depth of decks (or beams/girders).

Task 2. Bridge strength assessment using conventional rating method

The selected bridges were assessed using the 2D-based CLR methodology currently in practice in Indiana to establish the basis for comparison with the refined 3D FEA results. The rating factors calculated for the sample bridges indicate that some bridges (Sample #2 and Sample #5) exhibit moment deficiency, which makes them candidates for possible retrofitting actions, posting, or replacement, depending on their current traffic count. It is also observed that moment is the controlling effect as a result of locations lacking sufficient steel reinforcement or where reinforcement is only partially developed. In most T-beam bridges, smaller rating factors were obtained for interior girders

compared to exterior ones, mainly due to the larger live load distribution factors (LLDFs) of interior girders.

Task 3. Bridge strength assessment using 3D finite element analysis

For a more detailed assessment of the selected bridges, 3D FEA was conducted with a detailed model of the bridge superstructure geometry (railings, skew angle, slab thickness, girder spacing, etc.). The observed sensitivity of load positioning in lateral direction to evaluate LLDFs indicates that considering one single distribution factor for an entire superstructure and all loading scenarios may not be effective to reflect actual lateral distribution of live loads.

Concrete railings, when properly anchored for monolithic action, play a significant role in allocating a large portion of the response (both moment and shear) to exterior strips/girders, and subsequently decrease the share of interior ones. Therefore, the LLDFs calculated for interior strips/girders are smaller compared to those obtained by the formulation in AASHTO specifications, while distribution factors of exterior strips/girders are larger. It is found that larger LLDF values for exterior strips/girders did not lead to critical rating factors since capacity was also improved due to increased stiffness. In summary, rating factors obtained from 3D FEA are greater than those obtained using the 2D approach for both LFD and LRFD approaches. Greater share of demand absorbed by the edges indicates the importance of considering railings in LLDF evaluation.

Task 4. Sensitivity analysis of geometrical parameters

Bridge geometrical characteristics such as railings, skew angle, slab thickness, supports area, and spacing between the girders were considered as potential factors having an impact on LLDF. Railing height was confirmed as a parameter that produced the most drastic change in moment and shear demands of bridges. Particularly, changes in moment and shear demands for exterior strips were more prominent than those of interior strips. An increase in skew angle was found to cause a reduction in moment and increase in shear for both 1-span and 3-span bridges. The effect of slab thickness of slab bridges was relatively small and slab thickness variation along the bridge length resulted in a slight reduction in moment. Models with area support showed a decrease in both moment and shear when compared to the models with line supports, indicating the importance of area support modeling in 3D FEA. For T-beam bridges, the effect of diaphragm thickness was observed to be negligible. Lastly, T-beam bridges with uneven girder spacing affected moment and shear demand in comparison with those with even girder spacing, and the effect was dependent on the girder spacing scheme, which stresses the importance of the consideration of actual girder spacing in LLDF calculation.

Task 5. Discussion of research findings and proposed implementation

The comparison of rating factors obtained from CLR and 3D FEA indicate that CLR according to AASHTO specifications results in lower estimates of load rating factor in RC slab and T-beam bridges. LLDF is the main parameter affecting the results. Furthermore, a parametric study associated with demand estimation showed a substantial influence of geometric parameters on LLDF. Railing, deck skewness, and support area had substantial beneficial impact on demand response. It follows that neglecting these parameters in LLDF formulation could lead to overestimation of load shares assigned to strips/girders.

Implementation

Based on the study results and conclusions, the following recommendations are presented for consideration and possible implementation.

1. The comparison of rating factors obtained from CLR and 3D FEA indicated that the CLR methodology provided in AASHTO specifications results in lower load rating factor in RC slab and T-beam bridges, and the LLDF was shown to be the main parameter affecting the results. All sample bridges showed an increase in rating factors when evaluated using the 3D FEA-based load rating method compared to CLR values. Notably, three out of four bridges that rated unfavorably, with load rating results below 1 using CLR, showed ratings above 1 with the 3D FEA approach (compare the results of Task 2 and Task 3). The remaining bridge with the rating factor less than "1" (Sample #2) was further improved with the consideration of support area in 3D FE modeling, as shown in Task 4.
2. Given the improved load rating estimates, it is recommended that bridges that exhibit border-line load rating results be analyzed using the 3D FEA-based procedure, while the standard rating methods (CLR) may continue to be used for a conservative estimate of bridge rating.
3. Further improvements can be made to CLR to incorporate 3D effects while maintaining the simplicity of load rating procedures. The presence of railing has a substantial influence on stress distribution in the bridge super-structure, causing higher stress concentrations in exterior strips and reduces stresses in interior ones. It is therefore recommended that, in dead-load demand estimations using CLR, railing weight be allocated entirely to the exterior strips, instead of distributing it evenly across the bridge, as is done current practice using BRR.
4. The study also showed that on the capacity side, an important consideration is the inclusion of the reinforced concrete railing in the estimation of capacity for flexure and shear in RC slab bridges and for flexure in T-beam bridges. Therefore, it is recommended to include reinforced concrete railings properly anchored into the bridge superstructure when determining the capacity of exterior strips and girders.
5. A parametric study associated with demand estimation showed substantial effects of geometric features on LLDF. The study showed that railing height, deck skew, and support area had substantial impacted obtained values of moment and shear. It was also concluded that neglecting these parameters in LLDF formulation could lead to overestimation of load assigned to strips/girders. To simplify the incorporation of these geometric features in load rating calculations by INDOT or structural engineers using current 2D rating methods, a modified LLDF formula, where the effect of these parameters could be taken into account would improve rating estimates. A more extensive parametric study in support of the development of a modified live load rating factor is recommended.

CONTENTS

1. INTRODUCTION	1
1.1 Problem Statement	1
1.2 Research Objective, Scope, and Plan	2
1.3 Report Organization	2
2. SELECTION OF REPRESENTATIVE BRIDGES	2
2.1 Statistical Distribution of the NBI Database for Bridges in Indiana	2
2.2 Representative Bridges	2
3. BRIDGE STRENGTH ASSESSMENT USING CONVENTIONAL LOAD RATING METHOD.	4
3.1 Introduction	4
3.2 Evaluation References.	4
3.3 Loads for Evaluation	4
3.4 Nominal Capacity	7
3.5 Load Rating Procedure.	12
3.6 Summary of Findings	14
4. BRIDGE STRENGTH ASSESSMENT USING 3D FINITE ELEMENT ANALYSIS	15
4.1 Introduction	15
4.2 Modeling Assumptions	15
4.3 Distribution Factor	21
4.4 Capacity Calculation	22
4.5 Rating Factor	24
4.6 Summary of Findings	24
5. SENSITIVITY ANALYSIS OF GEOMETRICAL PARAMETERS.	26
5.1 Introduction	26
5.2 Reference Models	26
5.3 Railing Effect.	27
5.4 Skew Effect	28
5.5 Slab Thickness Effect	28
5.6 Support Area Effect	30
5.7 Diaphragm Effect.	30
5.8 Girder Spacing Effect	30
5.9 Summary of Findings	30
6. DISCUSSION OF RESEARCH FINDINGS	32
6.1 Introduction	32
6.2 Demand Estimation	32
6.3 Effect of Geometrical Parameters.	33
6.4 Capacity Calculation	34
6.5 Improvement in Rating Factors.	36
6.6 Summary of Findings	36
7. SUMMARY AND PROPOSED IMPLEMENTATION	37
7.1 Summary of Findings	37
7.2 Proposed Implementation	37
REFERENCES	38
APPENDIX	
Superstructure Plans and Reinforcement Detailing of Sample Bridges.	39

LIST OF TABLES

Table	Page
Table 2.1 Representative Sample Bridges	4
Table 3.1 Dead Loads on 1-ft. Slab Strip of Flat-Slab Bridges	5
Table 3.2 Dead Loads on Interior and Exterior Girders of T-Beam Bridges	5
Table 3.3 LLDFs for Flat Slab Bridges	8
Table 3.4 LLDFs for T-Beam Bridges	8
Table 3.5 Skew Factors for T-Beam Bridges (LRFR)	8
Table 3.6 Values Considered for Different Factors	13
Table 3.7 Values Considered for Dead Load (A_1) and Live Load (A_2) Factors	13
Table 3.8 Detailed Rating Factor Results: Slab Bridges	13
Table 3.9 Final Rating Factor Results: Slab Bridges	13
Table 3.10 Detailed Rating Factor Results: T-Beam Bridges	14
Table 3.11 Final Rating Factor Results: T-Beam Bridges	14
Table 4.1 3D LLDFs for Different Loading Configurations, Slab Bridges	22
Table 4.2 3D LLDFs for Different Loading Configurations, T-Beam Bridges	23
Table 4.3 3D Results, Rating Factors of Slab Bridges	25
Table 4.4 3D Results, Rating Factors of T-Beam Bridges	25
Table 5.1 Study Parameters and Ranges	26

LIST OF FIGURES

Figure	Page
Figure 1.1 Examples of older reinforced concrete bridges in Indiana: (a) flat slab (b) T-beam	1
Figure 1.2 Research tasks of this project	2
Figure 2.1 Statistical distribution of the structural/nonstructural parameters of flat slab and T-beam bridges provided in the NBI database	3
Figure 3.1 Dead load considerations for flat slab bridges, width cross-section of Sample #4	5
Figure 3.2 Dead load considerations for flat slab bridges, width cross-section of Sample #7	5
Figure 3.3 MATLAB and SAP comparison (Sample #1): (a) moment (b) shear envelopes under DC+DW	6
Figure 3.4 BrR and MATLAB comparison (Sample #5): (a) moment (b) shear envelopes under DC+DW	6
Figure 3.5 HS20 truck and lane loading (LFR)	6
Figure 3.6 HL-93 truck and lane loading (LRFR)	7
Figure 3.7 SAP and MATLAB results comparison: (a) moment (b) shear envelopes under HS20 load for Sample #1	7
Figure 3.8 BrR and SAP results comparison for moment envelope under HS20 load	7
Figure 3.9 BrR and MATLAB results comparison of Sample #5: moment and shear envelopes under (a) axle load (LRFR) (b) lane load (LFR)	8
Figure 3.10 Free body diagram of lever rule method	8
Figure 3.11 Typical beam section of a slab bridge	9
Figure 3.12 Typical beam section of a T-beam bridge: (a) exterior girder (b) interior girder	9
Figure 3.13 Assumed rectangular section for interior girders of T-beam bridges	9
Figure 3.14 Positive and negative moment capacity: (a) beam strip of Sample #3 (slab bridge) (b) interior girder of Sample #7 (T-beam bridge)	9
Figure 3.15 Moment capacity comparison between MATLAB and BrR: (a) Sample #5 (slab bridge) (b) Sample #8 (T-beam bridge)	10
Figure 3.16 Bottom and top reinforcement arrangement over three spans of Sample #3	10
Figure 3.17 Active rebar area improvement when considering partial development length for Sample #1: (a) bottom bars (b) top bars	11
Figure 3.18 Cranked longitudinal reinforcements of Sample #9: (a) arrangement at section view (b) reinforcement configuration	11
Figure 3.19 Shear capacity comparison between MATLAB and BrR for (a) slab bridge Sample #5 (b) T-beam bridge Sample #8 (LRFR approach, axle load)	12
Figure 3.20 Shear capacity comparison between MATLAB and BrR for (a) concrete and (b) steel reinforcement for bridge Sample #8 (LRFR approach, axle load)	12
Figure 3.21 Rating factor comparison for LRFR inventory level of design load rating (Sample #5)	15
Figure 3.22 Rating factor comparison for LRFR inventory level of design load rating (Sample #8)	15
Figure 4.1 Simply supported beams: (a) rectangular (b) T-section	16
Figure 4.2 Moment response with different element types: (a) rectangular (b) T-section	16
Figure 4.3 T-section beam validation with increased length	17
Figure 4.4 Convergence study at beam scale: (a) rectangular beam (b) T-section beam	17
Figure 4.5 Convergence study at bridge scale: (a) slab bridge (b) T-beam bridge	17
Figure 4.6 Bridge sections showing partitioning approach (a) slab bridge (b) T-beam bridge	18
Figure 4.7 Reinforcement modeling (Sample #2)	18
Figure 4.8 Reinforcement effect: (a) longitudinal rebars (b) transverse rebars	19
Figure 4.9 Effect of supports modeling for T-beam: (a) solid-solid (b) shell-shell (c) shell-beam	20
Figure 4.10 Moving load model	20
Figure 4.11 Moment response under moving load: (a) step-by-step results (b) final envelope	21

Figure 4.12 Moving load model verification: (a) one loading step (b) shear envelope	21
Figure 4.13 Dynamic vs. static loading	21
Figure 4.14 Moving truck modeling (Sample #2)	22
Figure 4.15 Sections considered for capacity calculation for exterior (a) strip (b) girder	23
Figure 4.16 Strain distribution: (a) normal (b) shear	23
Figure 4.17 Moment capacity calculation procedure for exterior strips/girders	24
Figure 5.1 Reference models for sensitivity analysis: (a) slab bridge (b) T-beam bridge	26
Figure 5.2 Railing geometries at section of (a) slab bridge (b) T-beam bridge	27
Figure 5.3 Comparison of demand between with and without railings of 40 in. for slab bridge reference model (a) shear (b) moment	27
Figure 5.4 Moment and shear change w.r.t railing height (a) slab bridge (b) T-beam bridge	28
Figure 5.5 Effect of span numbers on demand of slab bridges with railing height of 40 in.	28
Figure 5.6 Moment and shear change w.r.t skew angle (a) slab bridge (b) T-beam bridge	29
Figure 5.7 Effect of span numbers on demand of slab bridges with skew angle of 40 degrees	29
Figure 5.8 Moment and shear change w.r.t slab thickness (slab bridges)	29
Figure 5.9 Slab thickness type (slab bridge): (a) constant thickness (b) variable thickness	30
Figure 5.10 Moment and shear change according to slab thickness type (slab bridge with railing height of 40 in.)	30
Figure 5.11 Support area for (a) 1-span (b) 3-span slab bridge models	31
Figure 5.12 Moment and shear change according to support modeling type for slab bridges with (a) 1 span (b) 3 spans	31
Figure 5.13 Moment and shear change w.r.t diaphragm thickness (T-beam bridge)	31
Figure 5.14 Placement of evenly/unevenly spaced girders at section view of T-beam bridge with (a) even (b) uneven #1 (c) uneven #2 girder spacing	32
Figure 5.15 Moment and shear change according to girder spacing type (T-beam bridges)	32
Figure 6.1 Moment response comparison for interior strips/girders: (a) Sample #1 (b) Sample #7	33
Figure 6.2 LLDFs comparison for interior strips/girders: (a) slab bridge (b) T-beam bridge	34
Figure 6.3 Railing and skew effect: (a) slab bridge (b) T-beam bridge	35
Figure 6.4 Moment reduction for 1-span and 3-span bridges with railing of 40 in.	35
Figure 6.5 Moment capacity of interior and exterior strips/girders: (a) slab (b) T-beam	35
Figure 6.6 2D and 3D rating factor comparison: (a) slab (b-1) interior of T-beam (b-2) exterior of T-beam	36

1. INTRODUCTION

Bridge construction in the 1950s and 1960s favored a continuous reinforced concrete design for two-lane overpasses or bridges across small water streams and roads, using either a flat slab or a variable-depth ribbed (T-beams) system, as shown in Figure 1.1. In Indiana, these bridges represent an important component of the existing network inventory with 2,834 slab bridges and 766 T-beam bridges and are therefore required to satisfy existing specifications when checked for load carrying capacity. Nationally, as more than 30% of existing bridges in the US have exceeded their 50-year design life (American Society of Civil Engineers, 2013), the accurate and reliable evaluation of bridge live load-carrying capacity is of critical importance to state and local government agencies.

The *Manual for Bridge Evaluation* provides a simplified analysis methodology for load rating of bridges (AASHTO, 2011). This methodology, referred to as conventional load rating (CLR), employs a two-dimensional (2D) girder-by-girder analysis, where each individual longitudinal span between two adjacent supports (such as columns) of a bridge is approximated as a simply-supported beam for analysis. CLR is the basis for the bridge analysis program used by Indiana Department of Transportation (INDOT) for load rating of bridges, AASHTOWare Bridge Rating (BrR). It has been reported, however, that the CLR could lead to a costly underestimation of bridge capacity (Cai & Shahawy, 2003; Catbas, Ciloglu, Hasançebi, Popovics, & Aktan, 2003; Sanayei, Reiff, Brenner, & Imbaro, 2016). It is suspected that such conservative

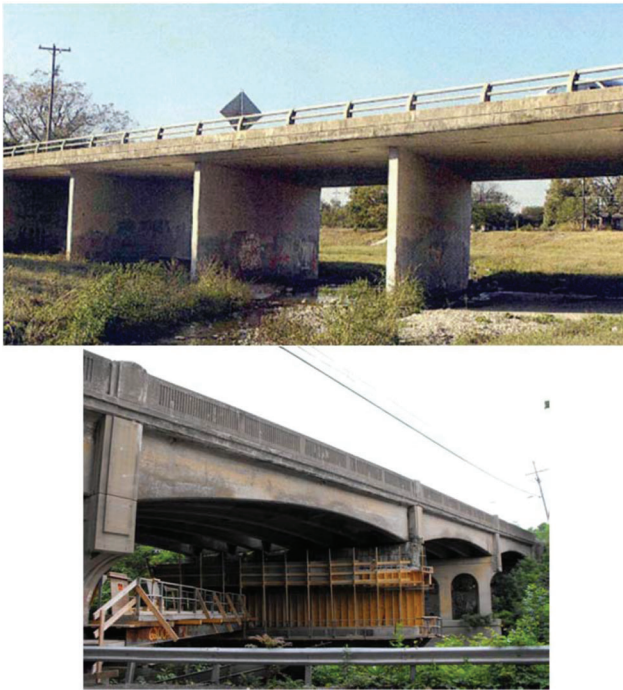


Figure 1.1 Examples of older reinforced concrete bridges in Indiana: (a) flat slab (b) T-beam.

evaluation arises from the rating method's simplified representation of members, supports, and connections. Additionally, nonstructural members such as parapets, railings, sidewalks, etc., are not considered in the evaluation. Due to the large number of flat-slab and T-beam bridges in Indiana, an accurate estimation of load carrying capacity could potentially relieve a large financial burden on the state and further extend bridge life cycles, especially since existing bridges show no signs of structural deficiency and, with proper maintenance, could be expected to serve well in the future.

The CLR is based on the analysis of bridge girders in two dimensions using beam theory. Beam theory is used to model long slender elements that can be represented by their centerline dimensions and loading can be assumed to remain symmetric with respect to the beam centerline. This 2D formulation focuses on bending behavior within the plane where loads are applied. The three-dimensional (3D) effects of load distribution across the bridge width, therefore, cannot be explicitly modeled, and are accounted for using distribution factors. Structural analysis using 2D beam theory has been common practice due to its simplicity and conservative estimates of beam load capacity and was the basis behind a number of structural analysis software, including BrR.

With the increased availability of high-end computational resources, 3D analysis of full-scale structures such as bridges has become increasingly feasible and the tools of 3D computational modeling have been used to great success in the modeling of civil engineering structures under a wide range of loading systems. It has become possible, therefore, to revisit the assumptions of 2D beam theory to investigate the effect of lateral load distribution and bridge components on the load rating of bridges.

1.1 Problem Statement

The standard rating method currently in use by INDOT (i.e., CLR) relies on a simplified 2D analysis based on beam theory may underestimate the capacity of flat slab and T-beam RC bridges. It is important, therefore, to revisit the assumptions and principles of the CLR method to identify potential areas of improvement for more accurate assessment estimate of bridge strength and load distribution.

Since the actual behavior of a bridge structure is 3D in nature, 3D computational model is better suited to estimate bridge carrying capacity for load rating. 3D finite elements models are capable of reflecting actual bridge dimensions, cross sections and connection configurations. More importantly, transverse load distribution is typically accounted for using load distribution factors in two-dimensional bridge analysis for load rating using CLR. With three-dimensional models, the load distribution in the transverse direction of the deck can be explicitly represented, and therefore optimized for maximum impact on load rating. It is also possible to account for support continuity, variable cross sections, edge railings, and other factors that

impact bridge using 3D models. It is therefore expected that, by improving demand estimates, load rating using 3D analysis can result in a more accurate assessment of bridge load carrying capacity compared to CLR.

1.2 Research Objective, Scope, and Plan

The goal of this project is to examine the limits and potential improvements of the 2D-based CLR methodology for flat slab and T-beam RC bridges in Indiana. A refined load rating methodology, based on 3D finite element analysis (FEA), has been employed to realistically account for factors such as lateral load distribution, cross-sections, number of spans, spacing, three-dimensional supports such as diaphragm, support continuity, and edge (railings) effects. These factors are not well considered in CLR and are expected to have a substantial impact on bridge capacity. A sample of ten representative bridges (five of each type) is selected for this study, based on the statistical distribution of older flat slab and T-beam RC bridges in Indiana. Material aspects, including damage and plasticity, are not considered in this report for better comparison CLR, which employs linear elastic analysis. The research tasks conducted for this project are presented in Figure 1.2.

1.3 Report Organization

This report is presented in five chapters. Chapter 1 outlines research background and problem statements followed by research objective, scope, and plan. Chapter 2 discusses the selection of the sample of ten representative bridges, based on the statistical distribution of older flat slab and T-beam RC bridges in Indiana. Chapter 3 explains the framework for the strength assessment of bridges based on CLR procedure and the resulting load rating results for the selected sample bridges. 3D finite element models, loading application, refined load rating procedure, and the relevant load rating results are presented in Chapter 4. Chapter 5 conducts a sensitivity analysis of bridge geometrical parameters, and their effect on demand estimation. Chapter 6 compares the load rating results obtained from conventional load rating and 3D finite element analysis. Potential improvement

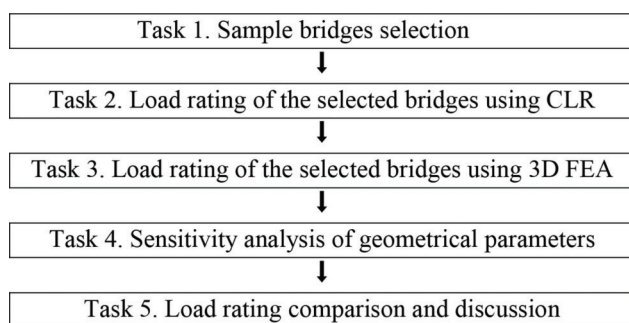


Figure 1.2 Research tasks of this project.

of load distribution factor is discussed in this chapter. Lastly, Chapter 7 summarizes the key results of this project and provides recommendations for future research.

2. SELECTION OF REPRESENTATIVE BRIDGES

2.1 Statistical Distribution of the NBI Database for Bridges in Indiana

A total 2,944 flat slab and 769 T-beam reinforced concrete bridges provided in the National Bridge Inventory (NBI) database for the state of Indiana were surveyed to establish the typical bridge configurations to be considered in the project. Among many structural/nonstructural features, the following were selected to be included to identify the bridge samples (Figure 2.1): year built, span length, number of spans, number of lanes, curb-to-curb roadway width, skew angle, and depth of decks (or beams/girders). These parameters are deemed to have significant impact on the structural behavior. A summary of the study of the database revealed the following:

- *Age of bridges:* About 50% of the reinforced concrete bridges in service in Indiana were constructed before 1970, implying they have exceeded their 50-year design life. Additionally, flat slab bridges have been favored over the recent decades.
- *Maximum span length:* Maximum span lengths for most bridges of the type considered in this study in the NBI fall within the range between 20 and 50 ft. The average maximum span lengths are 31.7 ft. for flat slab bridges, and 45.2 ft. for T-beam bridges.
- *Number of spans:* Among the bridges considered, 3-span bridges predominate, accounting for 66% of the total sample. Single-span bridges are the second largest population, with 23.7% of the total, and 10.3% of the bridges have two or more than four spans. When classified by bridge type, 75.7% of flat slab bridges have three spans, whereas 45.6% of T-beam bridges have one span.
- *Number of lanes:* For both bridge types, two-lane bridges are predominant, accounting for 88.9% of the total. Bridges with other number of lanes occupy only 11.1% of the sample.
- *Curb-to-curb roadway width:* Roadway width of nearly half of the bridges in the database lies within the range from 20 to 30 ft. The second-largest population falls in the 30- to 40-ft. range, with fewer bridges in the 40- to 50-ft. range. This trend is consistent in flat slab and T-beam bridges. The average roadway widths are 33.1 ft. for flat slab bridges, and 30.1 ft. for T-beam bridges.
- *Skew angle:* Half of the bridges have skew angle less than 15 degrees. The second largest skew angle range is between 15 and 30 degrees, accounting for 15.7% of the total. The average skew angles for flat slab and T-beam bridges are 15.7 degrees and 13.3 degrees respectively.

2.2 Representative Bridges

Considering the distribution of parameters shown in Figure 2.1, the representative samples for each type

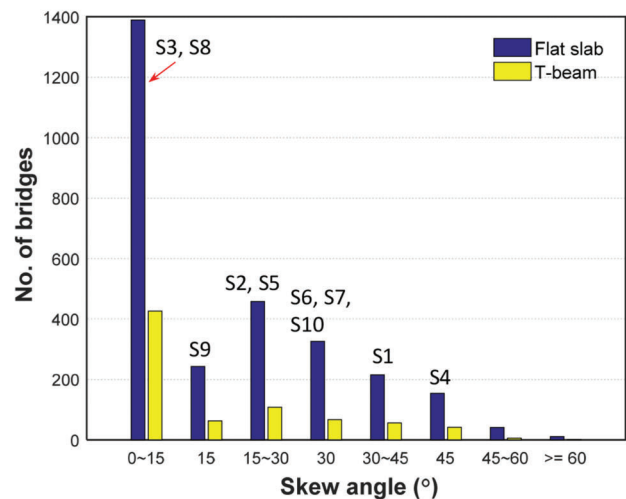
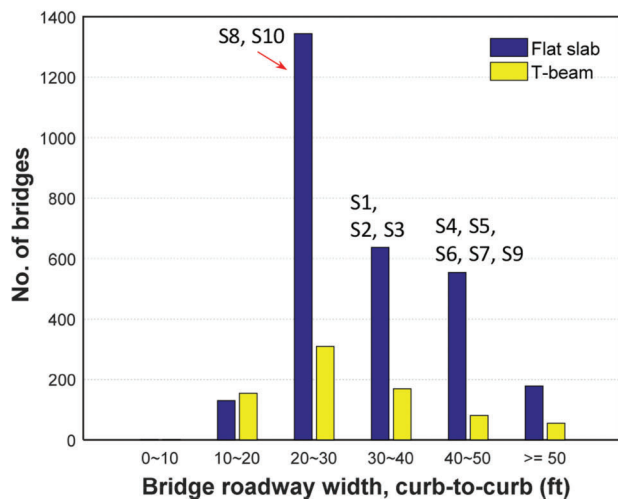
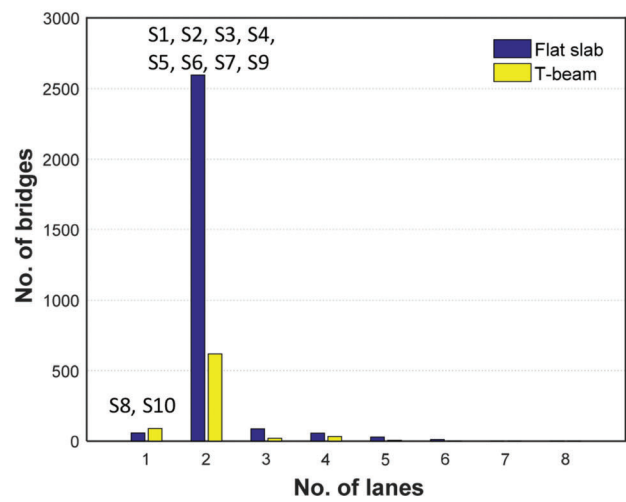
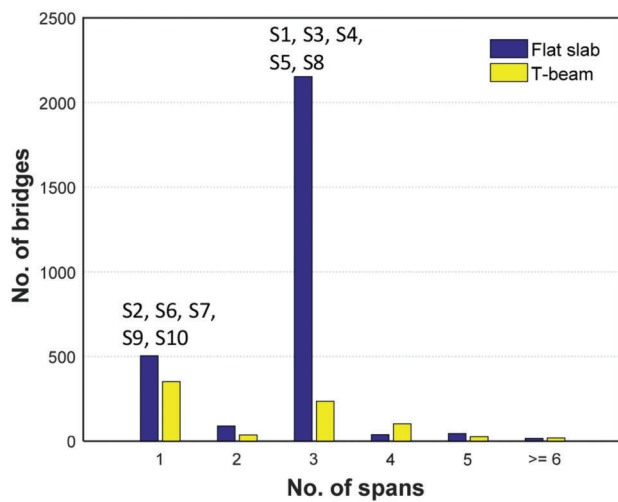
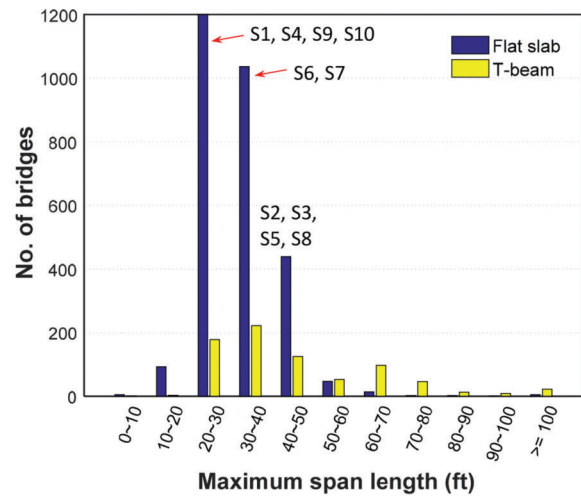
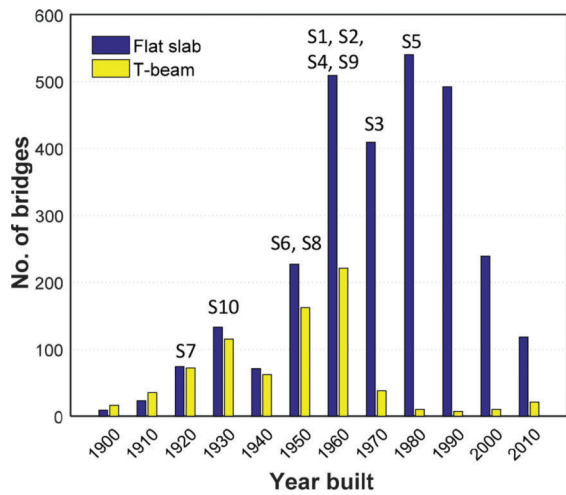


Figure 2.1 Statistical distribution of the structural/nonstructural parameters of flat slab and T-beam bridges provided in the NBI database.

TABLE 2.1
Representative Sample Bridges

Sample No.	Bridge ID	Bridge Type	Year Built	Traffic Volume (AADT)	No. of Spans	Span Length (ft.)	Width, Curb-to-Curb (ft.)	Slab/Girder Thickness (in.)	Skew Angle (degree)
1	I65-198-05476 BSBL	Flat Slab	1968	14,828	3	18-25-18	39.8	14.0	35
2	240-67-06389 A	Flat Slab	1964	2,749	1	48.9	39.4	28.0	20
3	I65-103-05564 DRA	Flat Slab	1970	7,586	3	30-42-30	36.5	22.5*	7
4	057-14-04926 A	Flat Slab	1962	5,919	3	21-28-21	44	14.0	45
5	49-64-6682	Flat Slab	1982	3,730	3	32-42.5-32	46.5	21.0	20
6	031-80-03570 JASB	T-Beam	1951	1,947	1	36	41	7.5/33.2	30
7	150-51-03834 A	T-Beam	1924	1,071	1	38	41	7.2/31.7	30
8	236-61-04121 A	T-Beam	1957	600	3	40	28	6.0/24.0	0
9	I65-124-04285 RLC	T-Beam	1960	1,121	1	28	40	6.5/27.0	15
10	(158)58-47-03027	T-Beam	1938	669	1	28	28	7.7/20.7	30

*Average value of the variable thicknesses along the bridge length (15 in. to 30 in.).

of bridge were determined, such that the selected parameters' values are relatively evenly distributed. Bridges information is summarized in Table 2.1. Figure 2.1 shows the distribution of the selected bridge samples within each category (e.g., S1 represents the Sample 1).

3. BRIDGE STRENGTH ASSESSMENT USING CONVENTIONAL LOAD RATING METHOD

3.1 Introduction

The bridges selected for the representative samples were evaluated using conventional load rating (CLR) methodology as per the AASHTO LRFD and LFD specifications. The CLR methodology employs a 2D girder-by-girder analysis, where each individual longitudinal span between two adjacent supports (such as columns) of a bridge is approximated as a simple supported beam for analysis. Centerline dimensions are used, and the effect of transverse load distribution is incorporated using a distribution factor.

In this study, SAP-2000 was initially used for structural modeling and analysis and then a MATLAB code was developed to provide section-by-section load rating results. Each bridge was modeled estimating span lengths from center-of-support-to-center-of-support to be structurally analyzed under applied loads. Moreover, the superstructure components of the sample bridges were analyzed according to CLR for both moment and shear effects. One sample of each bridge group was analyzed using BrR software and its outputs were compared with results obtained from analysis using SAP-2000 and MATLAB to ensure the validity of the load rating procedure. Assumptions and procedures used in the bridge load rating analyses are given in the subsequent section.

3.2 Evaluation References

Each bridge was analyzed based on the 7th edition of AASHTO LRFD Bridge Design Specifications (for LRFR evaluation) (AASHTO, 2014) and 17th edition of Standard Specifications for Highway Bridges

(for LFR evaluation) (AASHTO, 2002). In addition, the 2nd edition of the *Manual for Bridge Evaluation* (MBE) (AASHTO, 2011) was followed. The load rating was performed with design rating level from LRFR and inventory and operating rating levels from LFR specifications. The main requirements and assumptions of each approach are described in the following subsections.

3.3 Loads for Evaluation

Based on the MBE (AASHTO, 2011), only permanent loads and vehicular loads are considered to be of importance in load rating process and environmental loads such as wind, ice, temperature, stream flow, and earthquake are usually not considered in rating procedures.

3.3.1 Dead Loads: DC and DW

The dead loads were computed based on dimensions obtained from the bridge plans. Unit weights of materials were selected in accordance with LRFR Table 3.5.1-1 and LFR Article 3.3.6. For slab bridges, the weight of a 1-ft. width strip was considered as structural dead load (DC), while for T-beam bridges, the tributary width of the slab and girder were considered as structural dead load. In addition to the 1-ft. strip weight for slab structures, the weights of sidewalk and railing were distributed uniformly over the out-to-out width of the slab bridges, while for T-beam bridges these weights were allocated to exterior girders only. In bridges with variable slab thickness, the average thickness was considered for dead load calculations. For surface-wearing load (DW), the weight of asphalt or plain concrete overlay was computed based on wearing thickness reported in the bridge plans. Figure 3.1 and Figure 3.2 illustrate dead load considerations for flat slab and T-beam bridges, respectively. The values of DC and DW for each bridge group are summarized in Table 3.1 and Table 3.2. Dead loads, DC and DW, were applied as uniform distributed load

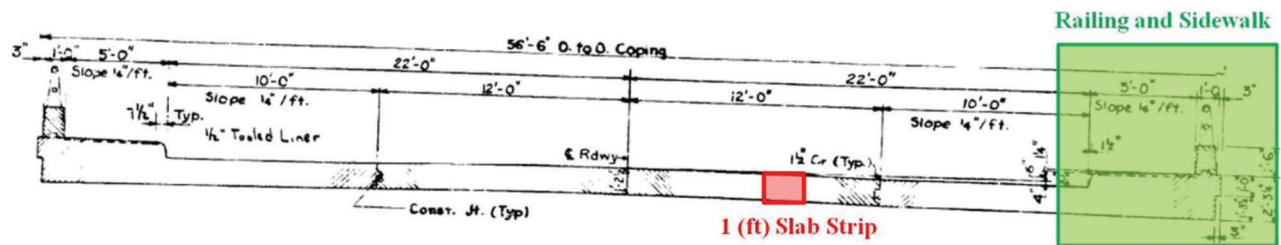


Figure 3.1 Dead load considerations for flat slab bridges, width cross-section of Sample #4.

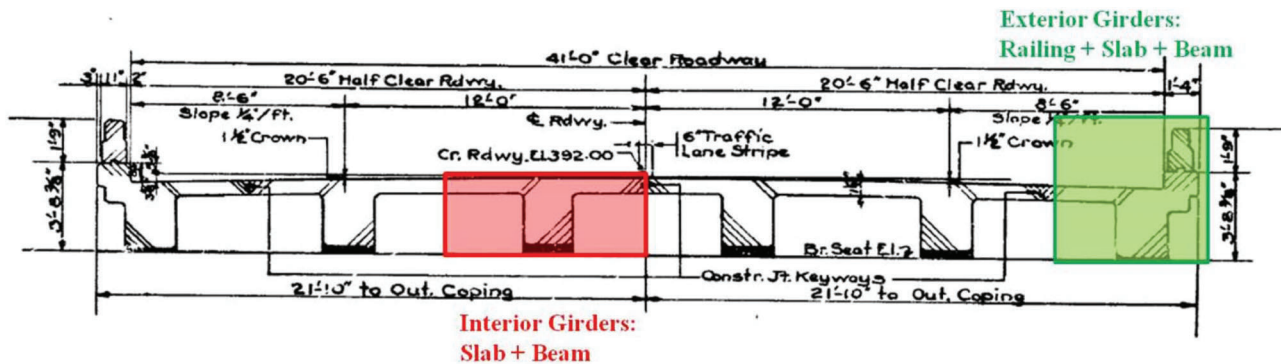


Figure 3.2 Dead load considerations for flat slab bridges, width cross-section of Sample #7.

TABLE 3.1
Dead Loads mon 1-ft. Slab Strip of Flat-Slab Bridges

Sample No.	DC (k/ft.)/1 ft.	DW (k/ft.)/1 ft.
1	0.208	0.012
2	0.390	0.119
3	0.311	0.012
4	0.225	0.030
5	0.288	0.018

TABLE 3.2
Dead Loads on Interior and Exterior Girders of T-Beam Bridges

Sample No.	DC (k/ft.)		DW (k/ft.)	
	Interior Girder	Exterior Girder	Interior Girder	Exterior Girder
6	1.388	1.558	0.024	0.015
7	1.510	1.750	0.024	0.015
8	1.110	1.450	0.210	0.140
9	1.090	1.490	0.023	0.018
10	1.080	1.640	0.043	0.038

on 1-ft. strip flat slab bridges and on individual interior or exterior girder in T-beam bridges. The resultant moment and shear responses were obtained for one of the selected bridges, Sample 1, using both SAP-2000 software and developed MATLAB code. Figure 3.3 shows the consistency of the results. Furthermore, in Figure 3.4, moment and shear responses according to dead load application obtained by MATLAB code are compared to the ones by BrR software for another

sample bridge, Sample 5. These comparisons validate the developed MATLAB code.

3.3.2 Live Loads

Vehicular live loads were selected based on design load and standard load configurations as described in LRFR and LFR, respectively. Figure 3.5 shows the truck load and corresponding lane load for the HS20 truck used in the LFR approach and in Figure 3.6, truck HL-93 and lane load of 0.64 (k/ft.) of the LRFR approach is illustrated. For both approaches, vehicular loadings have been applied in the longitudinal direction transversely occupying a width of 10 (ft.) as specified in both specifications.

3.3.2.1 Live Load Modeling.

To obtain moment and shear envelopes produced by live loads defined in 3.3.2, vehicles were modeled as moving loads using MATLAB code. Afterwards, the results obtained from the code were verified using vehicular modeling in SAP2000 (Figure 3.7). To get the maximum effect for lane loading (LFR), different load combinations were applied to the bridge. Figure 3.8 shows the consistency of results obtained from SAP and BrR for different load patterns for a 3-span slab bridge with a total span of 61 ft. (this slab bridge was used for preliminary study and verification with BrR, and is not among the bridge samples considered in this study). Moreover, Figure 3.9 shows that the analysis results from MATLAB code and BrR under truck loading (LRFR) and lane loading (LFR) for a slab bridge (Sample #5) are in good agreement.

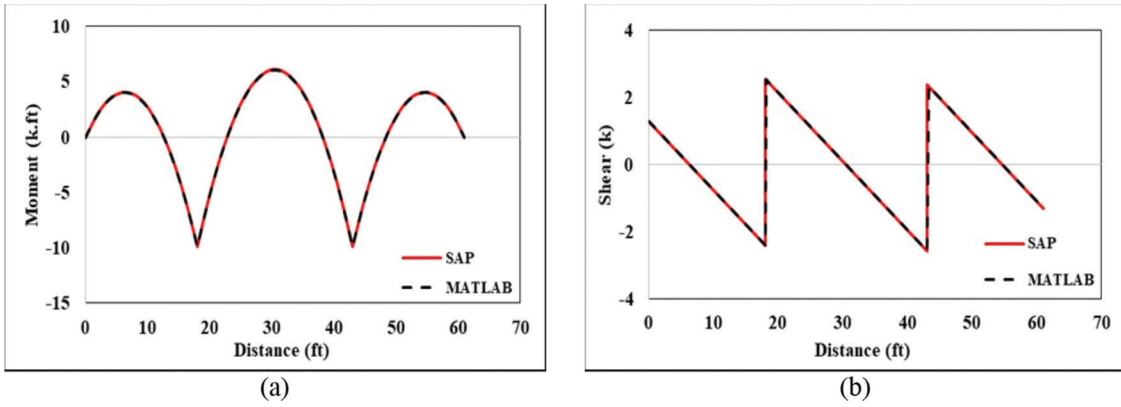


Figure 3.3 MATLAB and SAP comparison (Sample #1): (a) moment (b) shear envelopes under DC+DW.

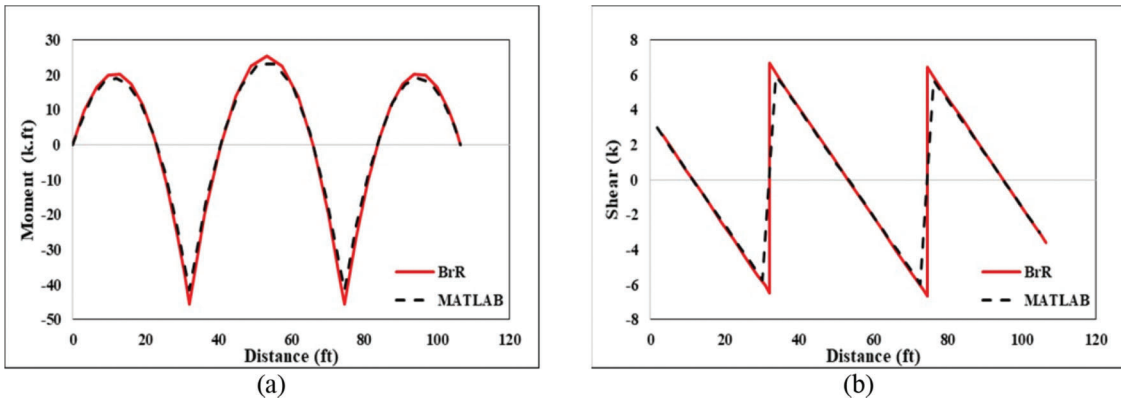


Figure 3.4 BrR and MATLAB comparison (Sample #5): (a) moment (b) shear envelopes under DC+DW.

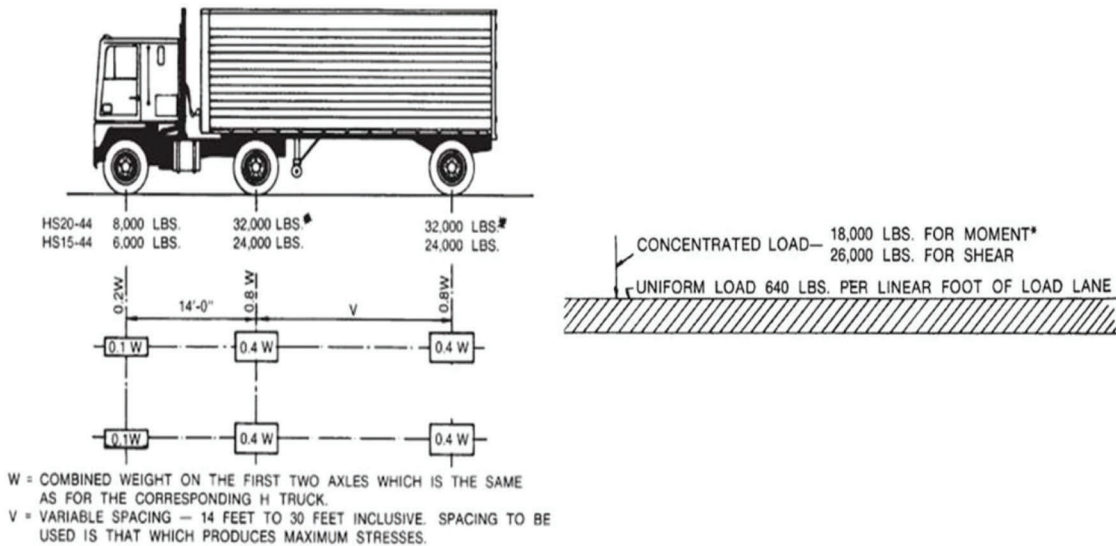


Figure 3.5 HS20 truck and lane loading (LFR).

3.3.2.2 Live Load Distribution Factor (LLDF). For 2D analysis, the live load distribution factor (LLDF) determines the portion of the live load assigned to a 1-ft. strip beam in slab type bridges and to interior or exterior girder in T-beam type bridges. LLDF is

calculated based on specifications provided in Articles 4.6.2.2 and 4.6.2.3 from LRFR and Article 3.23 of LFR specifications. For slab bridges, both LRFR and LFR approaches consider longitudinal strips with an equivalent strip width per lane, E , for both shear and

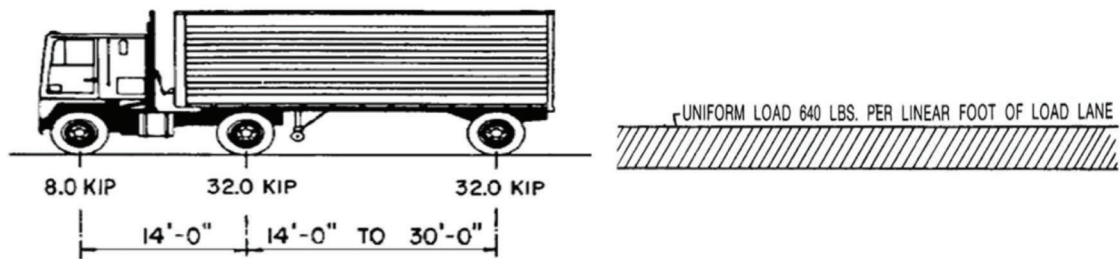


Figure 3.6 HL-93 truck and lane loading (LRFR).

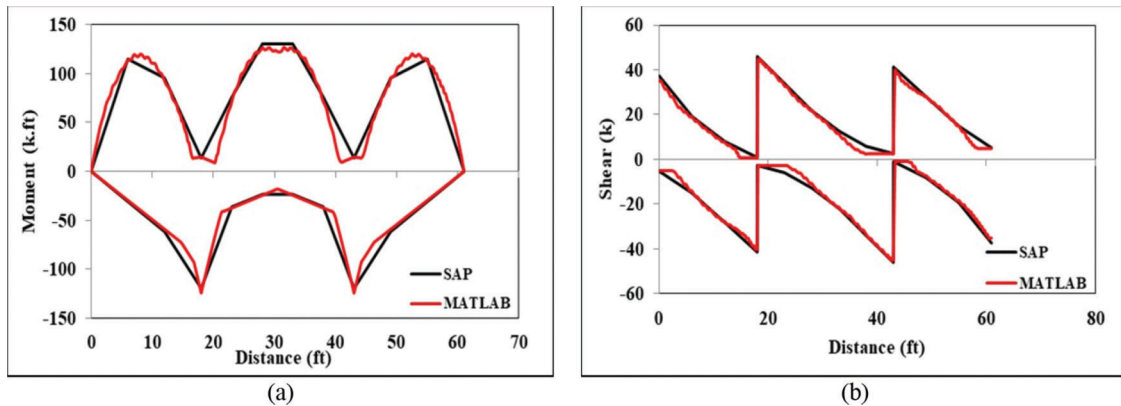


Figure 3.7 SAP and MATLAB results comparison: (a) moment (b) shear envelopes under HS20 load for Sample #1.

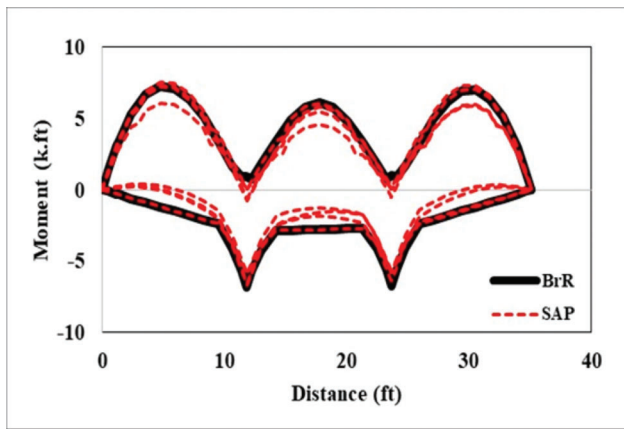


Figure 3.8 BrR and SAP results comparison for moment envelope under HS20 load.

moment. The equivalent strip width was determined by Equation 4.6.2.3-1 (LRFR) and Article 3.24.3.2 (LFR). In order to compute the LLDF for interior and exterior girders in T-beam bridges, equations provided in Tables 4.6.2.2.2b-1, 4.6.2.2.2d-1, 4.6.2.2.3a-1, 4.6.2.2.3b-1 of LRFR and Table 3.23.1 of LFR specifications were used. All T-beam bridges met the requirements to use approximate formulations of LLDF provided in the LRFR Specification. For reference, LFR specifications specify the formula for LLDF based on the span length. However, when the span length is greater than the specified criterion, the lever rule method needs to be

followed. In the lever rule method, truck configuration applied to the bridge width is shown in Figure 3.10. For interior and exterior girders, location of the trucks was selected to produce the maximum effect. LLDF could be also obtained by applying equilibrium of moment about assumed hinge points (interior girder positions). LLDFs for single-lane and multiple-lane loading were compared to identify critical LLDF values for 2D analysis. Finally, all LLDFs are summarized in Table 3.3 and Table 3.4 for slab and T-beam bridges, respectively. It should be noted that multiple presence factors from Table 3.6.1.1.2-1 of LRFR and reduction factor from Article 3.12.1 of LFR were applied to consider the effect of number of loaded lanes. The LLDFs for bridge Sample #5 and Sample #8 have shown a good match with the ones reported by BrR software, which is not included in this report.

For skewed bridges, skew factor was applied to LLDF calculation in accordance to Tables 4.6.2.2.2e-1 and 4.6.2.2.3c-1 of LRFR for moment and shear, respectively. It must be noted that the skew factor was not considered for slab bridges as well as T-beam bridges following LFR specification. Skew factors for the selected T-beam bridges are reported in Table 3.5.

3.4 Nominal Capacity

Nominal flexure and shear capacity of bridge superstructures were calculated in accordance with specifications of both LRFR and LFR approaches. For slab bridges, the capacity of a 1-ft. width beam strip was

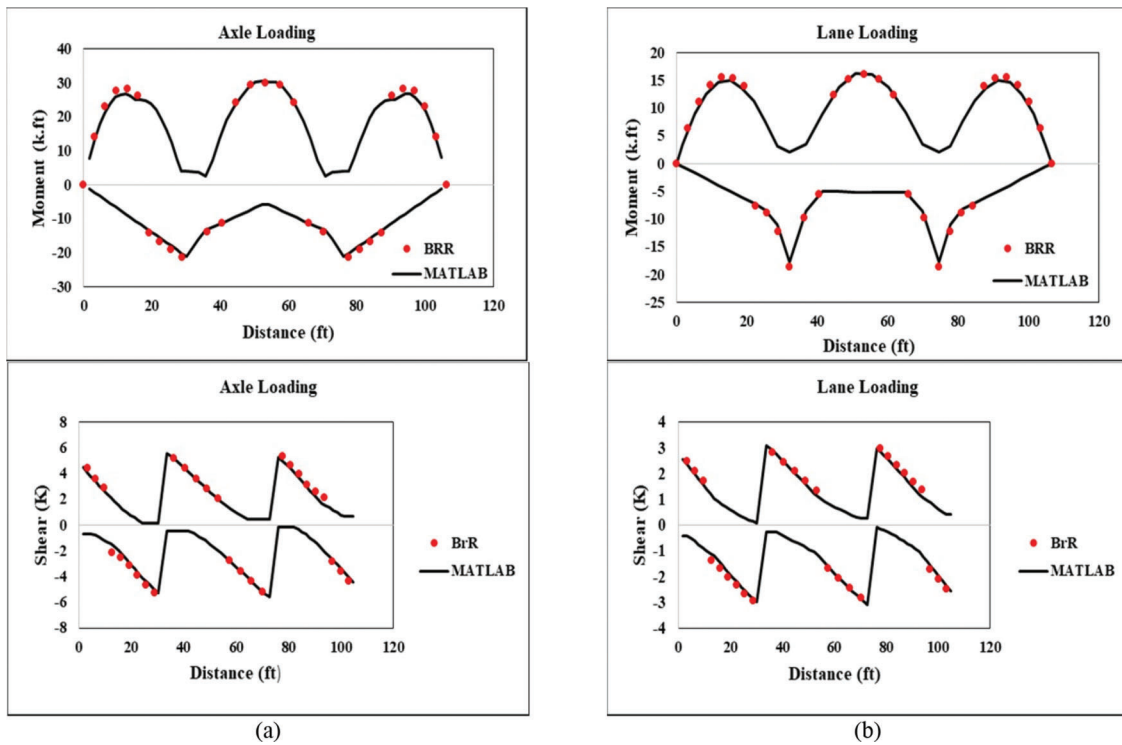


Figure 3.9 BrR and MATLAB results comparison of Sample #5: moment and shear envelopes under (a) axle load (LRFR) (b) lane load (LFR).

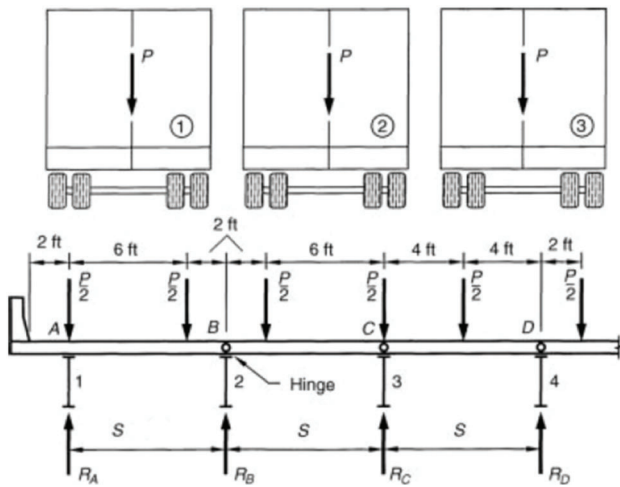


Figure 3.10 Free body diagram of lever rule method (Barker & Puckett, 2013).

TABLE 3.3
LLDFs for Flat Slab Bridges

Sample No.	LRFR ($12/E^1$)	LFR ($1/2E$)
1	0.097	0.098
2	0.080	0.072
3	0.084	0.086
4	0.090	0.095
5	0.086	0.084

¹E is equivalent strip width per lane.

TABLE 3.4
LLDFs for T-Beam Bridges

Sample No.	LRFR				LFR	
	Moment		Shear		Moment and Shear	
	Int.	Ext.	Int.	Ext.	Int.	Ext.
6	0.720	0.634	0.899	0.662	0.750	0.600
7	0.723	0.636	0.882	0.649	0.743	0.590
8	0.693	0.557	0.729	0.485	0.673	0.454
9	0.731	0.619	0.847	0.568	0.730	0.510
10	0.646	0.498	0.836	0.501	0.689	0.430

TABLE 3.5
Skew Factors for T-Beam Bridges (LRFR)

Sample No.	Skew (degree)	Skew Factor (Moment)	Skew Factor (Shear)
6	30	0.944	1.103
7	30	0.942	1.094
8	0	1.000	1.000
9	15	1.000	1.059
10	30	0.951	1.124

calculated. For T-beam bridges, the capacity of each interior and exterior girder was computed based on flexure and shear reinforcement reported in the associated bridge plans. Figure 3.11 and Figure 3.12 show the beam sections considered for capacity calculations for slab type and T-beam type bridges, respectively.

3.4.1 Nominal Flexural Resistance

Specifications of Articles 5.7 (LRFR) and 8.16 (LFR) were followed in order to evaluate the flexural capacity of rectangular and T-section beams. Concrete compressive strength and steel reinforcement yield strength were obtained from information provided in bridge drawings. When no information about concrete and reinforcing steel was available, the values provided in Tables 6A.5.2.1-1 and 6A.5.2.2-1 of MBE (AASHTO, 2011) were used for compressive and yield strength, respectively, based on year of bridge construction. For both LRFR and LFR approaches, rectangular stress block was assumed for compressive stress distribution. For all T-beam bridges, since the compression flange thickness was equal to or greater than the depth of the equivalent rectangular stress block, the section has been considered as a rectangular cross-section. For T-section beams, the effective flange width was computed in accordance with specifications of Article 4.6.2.6 and Article 8.10 of LRFR and LFR, respectively.

Figure 3.13 demonstrates the rectangular section assumed for T-section beams. In moment capacity equations, b_e and b_w were used as section width for positive and negative flexure capacities. Figure 3.14 shows section-by-section positive and negative moment capacities of a slab bridge, Sample #3, as an example of

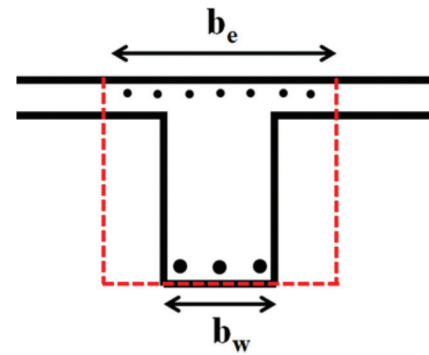
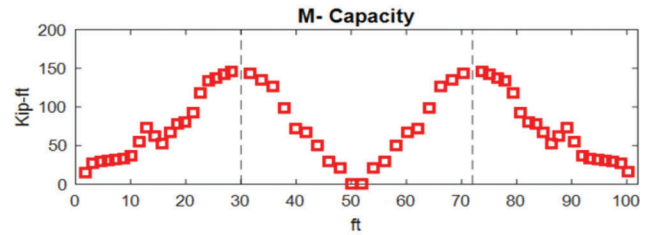
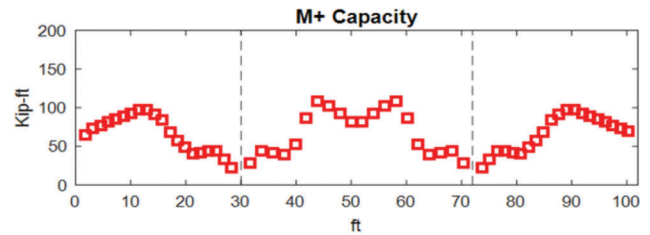
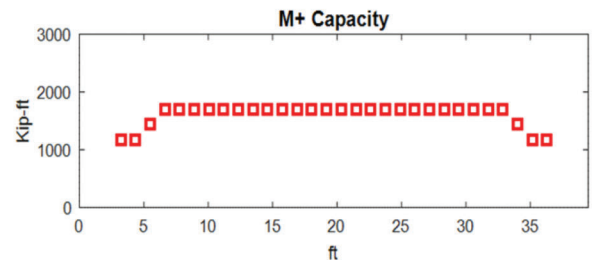


Figure 3.13 Assumed rectangular section for interior girders of T-beam bridges.



(a)



(b)

Figure 3.14 Positive and negative moment capacity: (a) beam strip of Sample #3 (slab bridge) (b) interior girder of Sample #7 (T-beam bridge).

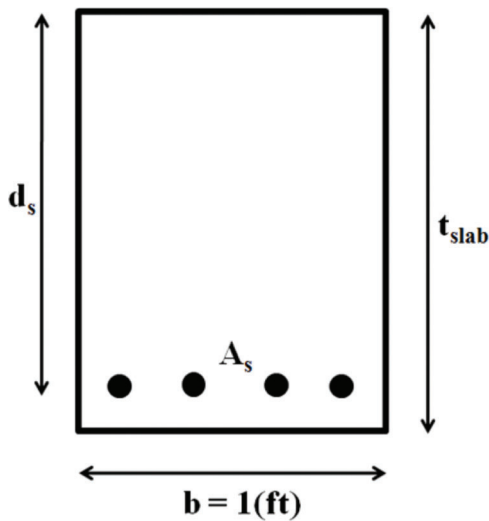


Figure 3.11 Typical beam section of a slab bridge.

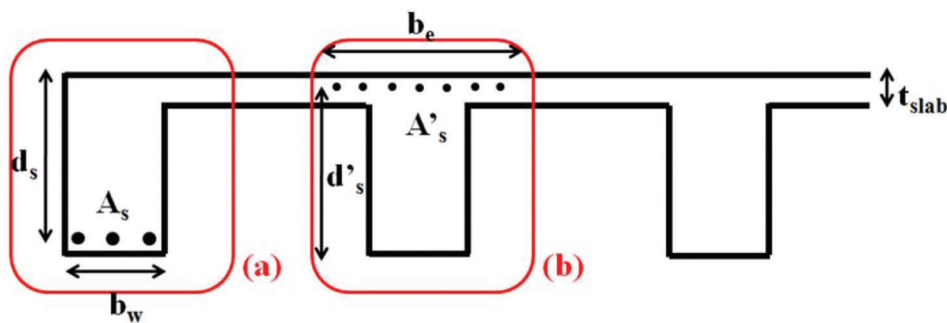


Figure 3.12 Typical beam section of a T-beam bridge: (a) exterior girder (b) interior girder.

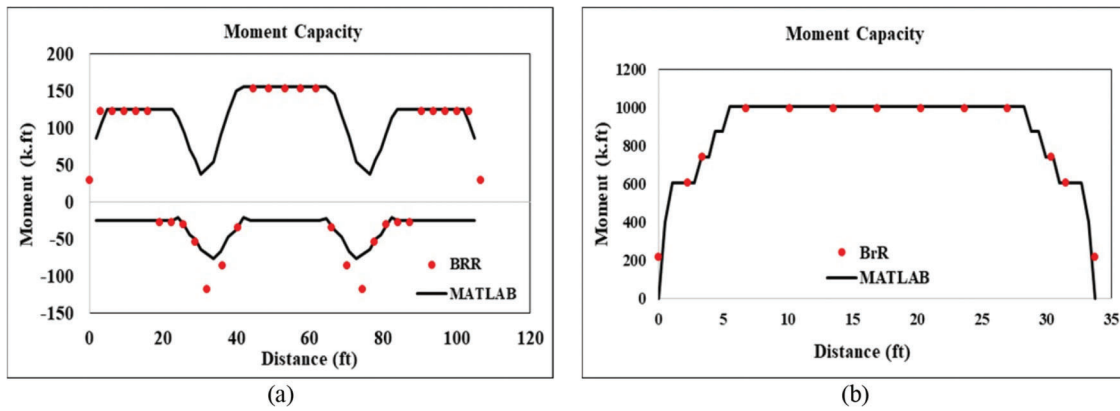


Figure 3.15 Moment capacity comparison between MATLAB and BrR: (a) Sample #5 (slab bridge) (b) Sample #8 (T-beam bridge).

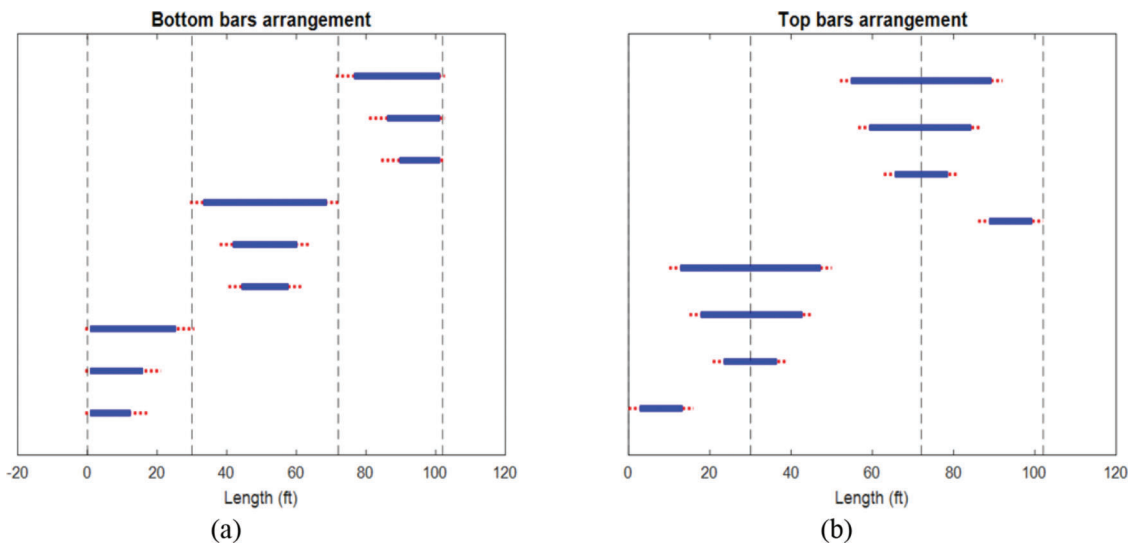


Figure 3.16 Bottom and top reinforcement arrangement over three spans of Sample #3.

results obtained by MATLAB code along the 1-ft. width beam length. Vertical dashed lines indicate middle support positions. Figure 3.15 illustrates comparison between results obtained by MATLAB and BrR software for a flat slab (Sample #5) and a T-beam bridge (Sample #8). As shown in the graphs, there is a good agreement between the results.

3.4.2 Development Length Consideration

To perform a sectional load rating analysis, sectional capacity was computed for rectangular beam of slab bridges and interior/exterior girder of T-beam bridges. Based on information provided in bridge plans about reinforcement configurations, the capacity of each section was calculated considering developed length of reinforcing bar on each side of the considered section. Articles 5.11.2 (LRFR) and 8.25 through 8.29 (LFR) were followed to compute development lengths for tension and hooked reinforcements. Figure 3.16 shows

top and bottom reinforcement arrangements on one 3-span bridge (Sample #1), where dashed lines represent support locations. In the graphs, the portions marked in red show actual lengths of reinforcing bars that are not fully developed and consequently considered to contribute only partially in flexure capacity calculations. For all sample bridges, flexural capacity improvement was observed when the reinforcement is considered as being partially developed beyond the development length instead of being neglected. Figure 3.17 illustrates the improvement in active rebar area for both top and bottom reinforcements when partial development length has been considered for moment capacity calculations for one slab bridge, Sample #1 (green arrows illustrate the rebar area improvement at one specific section). It is noted that development length calculations were based on LRFR 2015 and 2016 interims, which aligns with the approach in BrR software. In all selected T-beam bridges, cranked longitudinal reinforcements were provided in the girders and

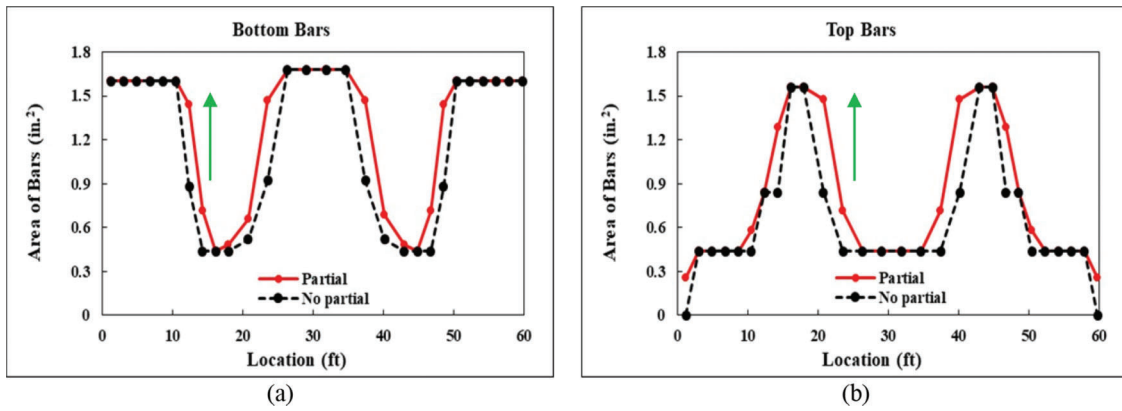


Figure 3.17 Active rebar area improvement when considering partial development length for Sample #1: (a) bottom bars (b) top bars.

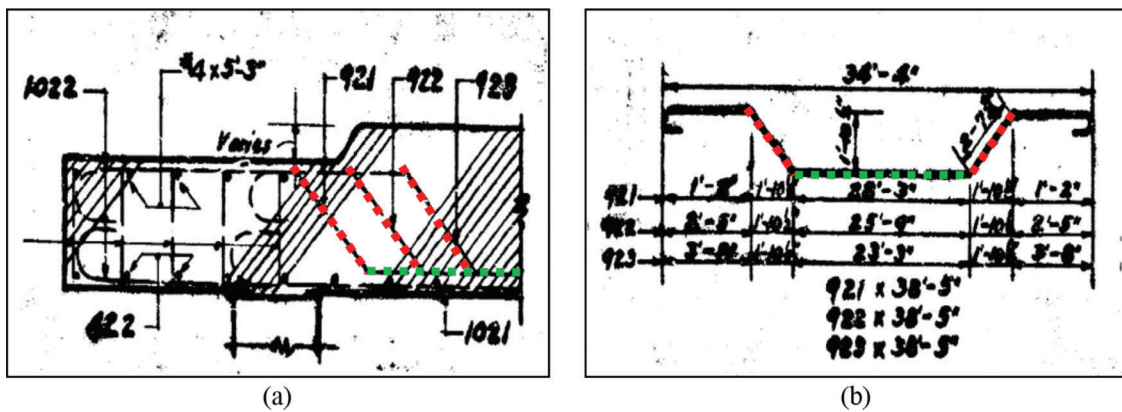


Figure 3.18 Cranked longitudinal reinforcements of Sample #9: (a) arrangement at section view (b) reinforcement configuration.

it is assumed that only straight parts of the rebars were fully developed. This portion is shown with a dashed green line in Figure 3.18. According to the results of a BrR analysis report, it was observed that the same approach is used in the software for longitudinal cranked reinforcements in the development length calculations.

3.4.3 Nominal Shear Resistance

Sectional shear capacity was calculated according to procedures in Article 5.8.3.3 of LRFR and Article 8.16.6 of LFR specifications. Shear capacity was determined by (1) the simplified approach and (2) detailed approach in both LRFR and LFR Specifications. Comparison of the results from two approaches indicated that detailed approach is aligned with BrR software. For slab bridges, only the contribution of concrete was considered in establishing shear capacity since no transverse reinforcement was provided. Transverse bent bars were not considered to act as shear reinforcement according to Articles 5.8.2.6 (LRFR) and 8.19.3 (LFR). However, in the BrR analysis report for a slab bridge Sample #5, it was deemed that the vertical parts of transverse bent bars are assumed to

contribute to shear capacity. For sake of comparison, this approach was followed in the analysis of the same bridge using the MATLAB code (Figure 3.19a) while for others, only concrete is considered to contribute to shear capacity. For your reference, it was confirmed that BrR does not consider these bars as bent longitudinal reinforcement and includes them in shear capacity calculations.

In T-beam bridges, the shear contribution of the inclined portions of longitudinal reinforcements (red dashed lines in Figure 3.18) was added to that provided by stirrups. In the BrR report, this contribution was considered by changing the total number of stirrups and using equivalent spacing in that portion of the girder length. As shown in Figure 3.19b, the results from MATLAB and BrR are in good agreement. For concrete shear capacity, impact of different aggregate sizes was investigated, as there was no information on concrete mix in any bridge plans (Figure 3.20a). The results obtained using MATLAB are in good agreement with those from BrR when using $a_g = 7/8$ in. except for some small differences at both ends. This could be attributed to the trial and error procedure in the shear capacity calculations (Appendix 5B of LRFR (AASHTO, 2014)).

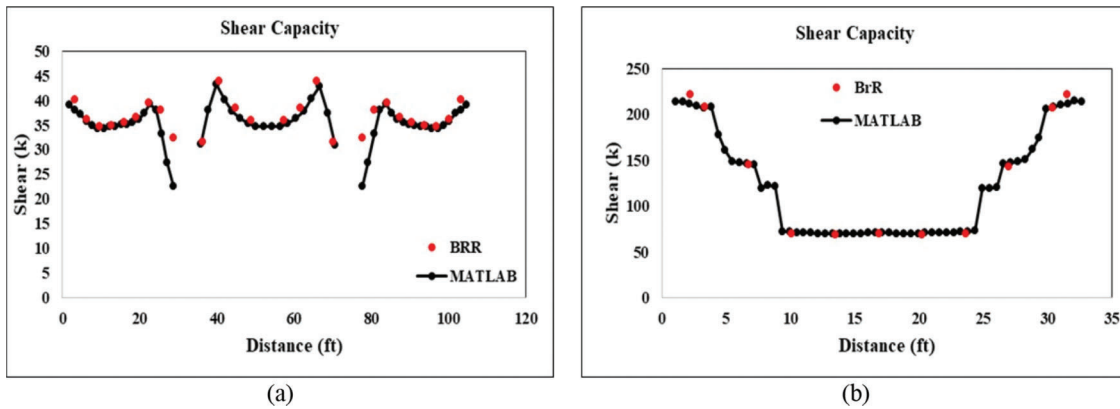


Figure 3.19 Shear capacity comparison between MATLAB and BrR for (a) slab bridge Sample #5 (b) T-beam bridge Sample #8 (LRFR approach, axle load).

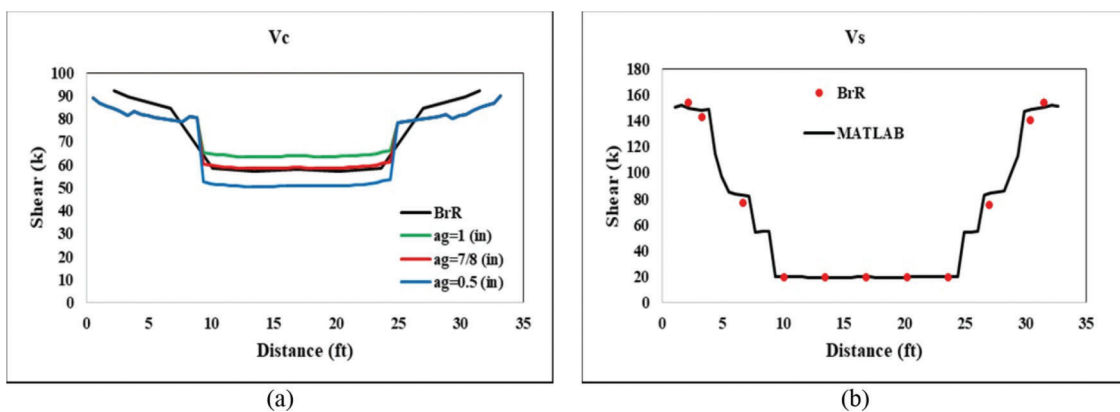


Figure 3.20 Shear capacity comparison between MATLAB and BrR for (a) concrete and (b) steel reinforcement for bridge Sample #8 (LRFR approach, axle load).

3.5 Load Rating Procedure

The superstructure of each bridge was load rated using methodologies consistent with LRFR and LFR approaches. Demand and capacity calculations were explained in previous sections, and in the following sections, the remaining parameters in load rating equations will be discussed.

3.5.1 Load Rating Equations

Rating factor (RF) is a measure of bridge structural condition. Depending on the rating level and rating method, different truck/lane loadings are applied to bridge structure to obtain structural demand. Bridge capacity is evaluated under current structural condition of the bridge. Herein, RF results for LRFR and LFR approaches will be presented for the sample bridges.

LRFR Approach (MBE 6A.4.2.1-1):

$$RF = \frac{\phi_s \phi_c \phi * R_n - \gamma_{DC} * DC - \gamma_{DW} * DW + \gamma_P * P}{\gamma_{LL} * L(1 + IM)} \quad (\text{Eq. 3.1})$$

where RF is the rating factor, R_n is member resistance and DC, DW, P, and L are dead load effect of structural and nonstructural components, dead load

effect of wearing surfaces and utilities, permanent loads effect, and live load effect, respectively.

In Eq. (3.1), system factor ϕ_s and condition factor ϕ_c were selected for both slab and T-beam type bridges according to Tables 6A.4.2.4-1 and 6A.4.2.3-1 of MBE. The bridge condition was assumed to be “good” for all bridges. The resistance factor, ϕ , was chosen for both moment and shear effects in accordance with Article 5.5.4.2 of LRFR specifications. From MBE, values provided in Table 6A.4.2.2-1 were selected for dead load factors, γ_{DC} and γ_{DW} , and the live load factor, γ_{LL} . Dynamic load allowance factor, IM, was selected from Table 3.6.2.1-1. All assumed values for the factors are reported in Table 3.6.

LFR Approach (MBE 6B.4.1-1):

$$RF = \frac{C - A_1 * D}{A_2 * L(1 + I)} \quad (\text{Eq. 3.2})$$

Where RF is rating factor, C is the capacity and D and L are dead and live load effects, respectively.

In Eq. (3.2), dead load factor, A_1 , and live load factor, A_2 , were selected in accordance with the MBE Article 6B.4.3 for both Inventory and Operating load rating levels. Values considered for A_1 and A_2 are provided in Table 3.7.

The impact factor formula from Article 3.8.2 is expressed as

$$I = \frac{50}{125 + L} \leq 0.3 \quad (\text{Eq. 3.3})$$

3.5.2 Load Rating Results

The load rating procedures previously described were applied to all ten bridges. The minimum load rating factor for each sample and its corresponding controlling action (moment or shear) are summarized in

TABLE 3.6
Values Considered for Different Factors

ϕ_s	ϕ_c	ϕ	γ_{DC}	γ_{DW}	γ_{LL}	IM	
1	1	0.9	1.25	1.5	1.35	1.75	33%

TABLE 3.7
Values Considered for Dead Load (A_1) and Live Load (A_2) Factors

Load Rating Level	A_1	A_2
Inventory	1.3	2.17
Operating	1.3	1.3

TABLE 3.8
Detailed Rating Factor Results: Slab Bridges

Sample No. (Spans, ft.)	Approach	Level	M	Loc. (ft.)	V	Loc. (ft.)
1 (18-25-18)	LFR	Inventory	1.51	50.8	2.1	13.6
		Operating	2.52			
	LRFR	Inventory	1.55	50.8	2.59	23.7
		Operating	2.01			
2 (48.9)	LFR	Inventory	0.89	24.4	3.1	5.4
		Operating	1.48			
	LRFR	Inventory	0.73	19	2.62	5.4
		Operating	0.95			
3 ¹ (30-42-30)	LFR	Inventory	1.2	79.3	2.59	68
		Operating	2			
	LRFR	Inventory	1.2	39.7	1.56	34
		Operating	1.55			
4 (21-28-21)	LFR	Inventory	0.99	35	1.95	42.8
		Operating	1.65			
	LRFR	Inventory	0.96	35	2.18	54.4
		Operating	1.25			
5 (32-42.5-32)	LFR	Inventory	0.46	23.7	2.46	35.5
		Operating	0.76			
	LRFR	Inventory	0.47	23.7	1.68	35.5
		Operating	0.61			

¹It should be mentioned that for bridge Sample #3, a rating factor with zero value was observed, at one section for negative moment, and not reported in Table 3.9. This occurred at the section lacking top steel reinforcement based on the bridge drawing detailing information (see Figure 3.14a). In this case, the next minimum value is reported as rating factor value.

Table 3.8 and Table 3.10. It should be noted that for one bridge, different load rating factors according to different scenarios were calculated, including truck/lane loading, moment/shear effects, single/multiple-lane loading, and interior/exterior girders. Detailed results for moment and shear in each bridge are provided in Table 3.8 and Table 3.10. These values serve as the basis for the selection of the rating factors in Table 3.9 and Table 3.11. It should be mentioned that rating factors were evaluated at a distance “d” from the face of the support for shear, and at the support face for negative moment. Moreover, total number of twenty sections were selected to evaluate rating factors along the bridge length for each sample. In the tables, the values reported for locations are measured from the left side of each bridge total length.

TABLE 3.9
Final Rating Factor Results: Slab Bridges

Sample No.	LFR (Inventory)	LRFR (Inventory)	Controlling Effect
1	1.51	1.55	Moment
2	0.89	0.73	Moment
3	1.20	1.20	Moment
4	0.99	0.96	Moment
5	0.46	0.47	Moment

TABLE 3.10
Detailed Rating Factor Results: T-Beam Bridges

Sample No. (ft.)	Approach	Level	Moment		Loc. (ft.)	Shear		Loc. (ft.)
			Int.	Ext.		Int.	Ext.	
6 (36)	LFD	Inventory	1.06	1.25	16.6	1.04	1.26	4.1
		Operating	1.77	2.08		1.74	2.10	
	LRFD	Inventory	1.13	1.19	16.6	1.60	1.90	12.4
		Operating	1.47	1.54		2.07	2.46	
7 (38)	LFD	Inventory	1.26	1.49	17.6	1.26	1.53	35.1
		Operating	2.11	2.49		2.10	2.55	
	LRFD	Inventory	1.32	1.42	17.6	1.35	1.61	15.4
		Operating	1.70	1.84		1.75	2.09	
8 (40)	LFD	Inventory	1.19	1.60	15.4	1.23	1.76	30.9
		Operating	1.98	2.67		2.05	2.94	
	LRFD	Inventory	1.15	1.31	15.4	0.97	1.31	23.2
		Operating	1.50	1.69		1.26	1.70	
9 (28)	LFD	Inventory	1.63	1.74	11.4	0.94	1.00	26
		Operating	2.72	2.90		1.58	1.67	
	LRFD	Inventory	1.58	1.75	11.4	1.80	2.27	27.6
		Operating	2.05	2.26		2.33	2.94	
10 (26)	LFD	Inventory	1.63	1.73	11.4	1.14	1.45	26
		Operating	2.72	2.89		1.91	2.43	
	LRFD	Inventory	1.82	1.58	11.4	1.72	1.67	27.6
		Operating	2.36	2.05		2.22	2.16	

TABLE 3.11
Final Rating Factor Results: T-Beam Bridges

Sample No.	Approach (Inventory)	Int. Girder	Ext. Girder	Controlling Effect
6	LFD	1.04	1.26	Shear
	LRFD	1.13	1.19	Moment
7	LFD	1.26	1.49	Moment
	LRFD	1.32	1.42	Moment
8	LFD	1.19	1.60	Moment
	LRFD	0.97	1.31	Shear
9	LFD	0.94	1.00	Shear
	LRFD	1.58	1.75	Moment
10	LFD	1.14	1.45	Shear
	LRFD	1.72	1.58	Shear/Moment

As an example of each type bridge, load rating factors for LRF (inventory), evaluated at every selected section along the bridge length, are presented in Figure 3.21 for Sample #5 (slab bridge) and Figure 3.22 for Sample #8 (T-beam), compared with results from BrR. As it is observed from the graphs, the results are in good agreement for T-beam bridge and shear rating factors of flat slab while some mismatch exist for flexure rating factors at some locations. Since the capacity and the demand were matched for this case, a possible reason for this inconsistency might be attributed to the fact that results provided from BrR are not necessarily the critical ones and they depend on how user has defined the evaluation sectional points.

3.6 Summary of Findings

The obtained results from 2D study indicate that further actions may be required for those bridges where the associated rating factor is less than one (Samples #3, #4, #5, #8, and #9). Sectional rating factor analysis identifies vulnerable locations and corresponding controlling effect and simplifies possible future strengthening actions. Rating factors obtained from Sample #2 and Sample #5 show significant moment deficiency, which makes them be considered as candidates for possible retrofitting actions, posting, or replacement depending on their current traffic count. These bridges will be examined more closely through

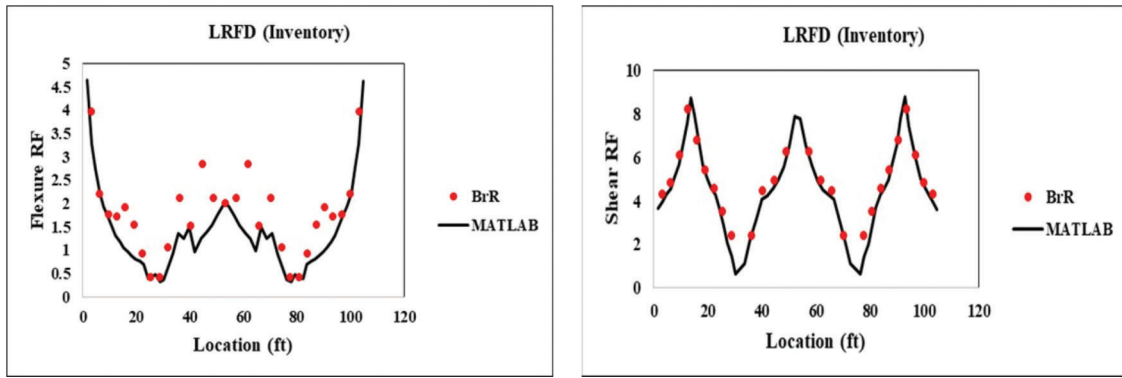


Figure 3.21 Rating factor comparison for LRFR inventory level of design load rating (Sample #5).

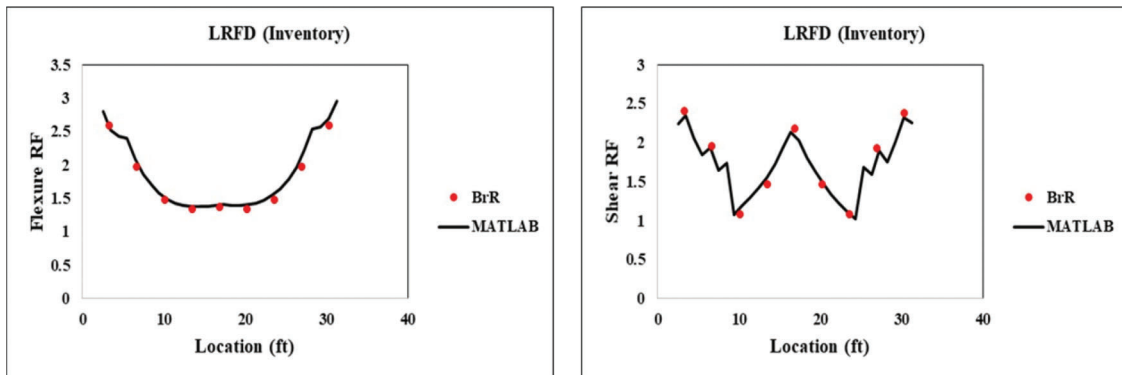


Figure 3.22 Rating factor comparison for LRFR inventory level of design load rating (Sample #8).

finite element analysis, where any potential improvement could be obtained by considering 3D geometries. Based on the results provided in Table 3.8 to Table 3.11, it can be observed that moment is the controlling effect for most of the cases mostly happening in locations where there is lack of reinforcement or where reinforcement is not fully developed. Moreover, smaller rating factors were obtained for interior girders in most of the cases compared to exterior ones in T-beam bridges. This observation could be attributed to larger LLDF of interior girders according to values, as presented in Table 3.4. The findings of this chapter further reveal that some of the approximations in the procedure can play a significant role in the 3D modeling task. First, refined analysis is expected to obtain more realistic responses when analyzing the superstructure as a 3D structure instead of a 2D model. Second, more realistic live load configurations need to be applied to the whole superstructure instead of using “averaged” live load distribution factor, which was observed to significantly affect the load allocation to beam strip in slab bridges and to interior/exterior girder in T-beam ones. Third, as suggested by current specifications, there are parts of the superstructure such as railings and sidewalks that have been neglected to contribute in shear and flexure capacity. The contribution of these components will be considered in 3D modeling, possibly resulting in an increase in the

capacity and consequently improvements in the final rating factors.

4. BRIDGE STRENGTH ASSESSMENT USING 3D FINITE ELEMENT ANALYSIS

4.1 Introduction

As mentioned earlier, the aim of this project is to explore the differences between 2D and 3D analysis in bridge evaluations. In the previous work, each bridge superstructure was analyzed for load rating using CLR, which employs 2D beam analysis. In this chapter, 3D Finite Element models for bridge superstructures were analyzed using ABAQUS. Superstructure features along with actual loading configurations were explicitly represented in the models. Potential modeling factors that may affect FEA results were studied based on AASHTO suggestions and recommendations from available literature, including element type, mesh size, support modeling, and moving load application. A summary of assumptions and verification studies for 3D analysis are presented in the subsequent sections.

4.2 Modeling Assumptions

To set up the 3D modeling methodology using ABAQUS, we start with the analysis of simply

supported beams with rectangular and T-beam cross-sections subjected to uniformly distributed dead load and single moving load (Figure 4.1). The beam with rectangular cross-section has the properties of an existing single-span slab bridge (Sample #2) with a strip width of 1 ft. and depth equal to slab thickness. In the case of the T-section beam, the geometrical properties of one interior girder in a T-beam bridge (Sample #8) were used in the model. These simple beams were studied as verification models to investigate the effect of element type, mesh size, support positions, moving load application, and reinforcement modeling on analysis results when compared to corresponding 2D results. A PYTHON code was developed to calculate moment and shear responses from ABAQUS stress outputs and obtain section-by-section results comparable with the ones obtained from the 2D procedure. After verification of beam models, the same finite element parameters will be applied to the whole superstructure models of the bridges.

4.2.1 Element Type and Mesh Refinement

The effect of different element types and different mesh sizes were investigated for the finite element study. To explore the element type effect, solid and

beam elements were used in the rectangular beam model, while for the T-section beam, solid, shell, and beam elements were considered for deck and girder parts of the section. Figure 4.2 illustrates moment responses for beams subjected to dead load when different element types were used, compared to a reference response obtained with 2D analysis. As it can be seen in Figure 4.2a, when solid elements are used for a rectangular beam, better results were obtained near the support locations. It should be noted that for a T-section beam (Figure 4.2b), due to the geometry effect, the response obtained with solid elements differs significantly from the 2D result. This difference may be attributable to cross-section deformability, an effect not accounted for in 2D beam analysis. To test this hypothesis, the beam length was increased to decrease the sectional geometry effect. Figure 4.3 shows that results converged to the 2D response when larger span length was used compared to the short one. Based on these results, the solid element (C3D8R) was selected for both slab and T-beam superstructure models, as this element type is able to reflect the 3D behavior, with results consistent with 2D analysis when appropriate. Moreover, solid element allows full compatibility between deck and edge components, such as railings with an integral action between them, since the railings

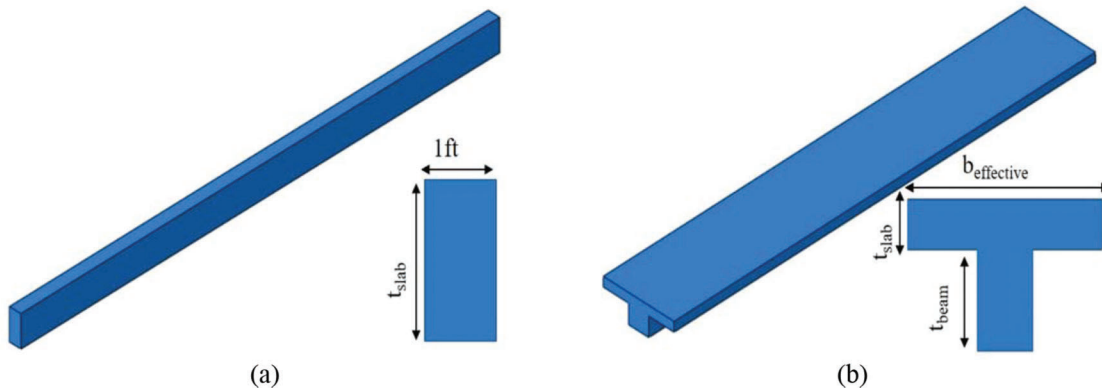


Figure 4.1 Simply supported beams: (a) rectangular (b) T-section.

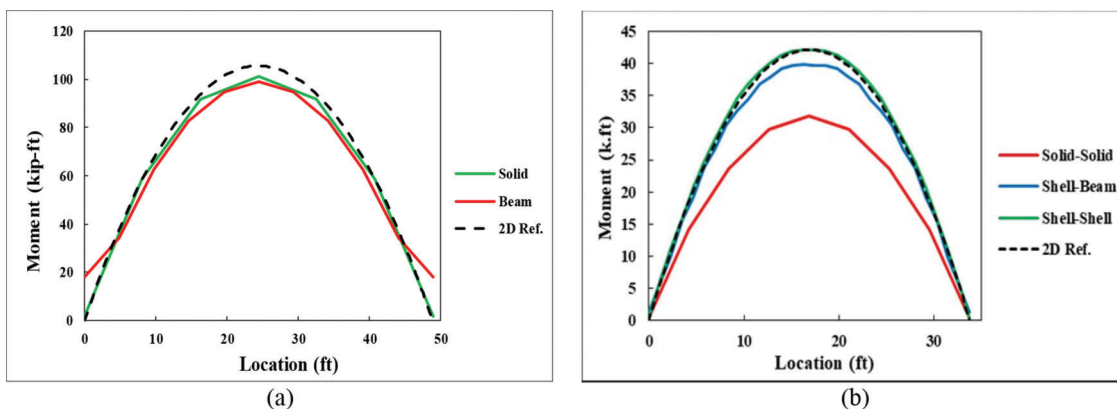


Figure 4.2 Moment response with different element types: (a) rectangular (b) T-section.

could be modeled continuously with slab part to insure the edge participation in longitudinal stiffening. Particularly for T-beam bridge model with solid elements, full composite action could be imposed between slab and girders to prevent any slip and displacement between them.

A convergence study was carried out with variable mesh sizes to find an appropriate element size that achieves a good balance between accuracy and computational time. The convergence study was performed on both a single-beam and full bridge models, comparing the maximum moment values for each refinement level. Figure 4.4 illustrates the moment responses for

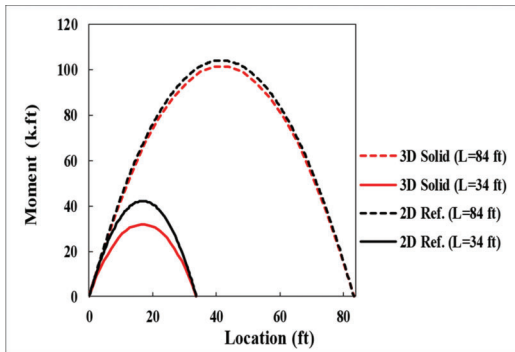


Figure 4.3 T-section beam validation with increased length.

rectangular and T-section beams subjected to a 1-kip concentrated load moving over the beam span using 2-in., 3-in., 6-in., and 10-in. mesh sizes. It is shown that the results did not change significantly beyond the 3-in. mesh, suggesting that this element size is suitable for the purpose of this study. Figure 4.5 shows maximum moment values obtained at different locations along the width of a slab bridge (Sample #2) and interior/exterior girders of a T-beam bridge (Sample #8), when subjected to single truck moving close to the left curb for different mesh refinement levels. The bridge model (Figure 4.5), shows an average error value of about 6% between mesh sizes 6 in. and 3 in. for the slab bridge model, and 3 in. and 2 in. for the T-beam model. Taking computational cost/time (illustrated on Figure 4.5 for slab type bridge) into consideration, element sizes of 6 in. and 3 in. were selected for the FE discretization of slab and T-beam bridges, respectively. Since the element height is critical for the calculation of moment and shear responses and element dimension in longitudinal direction does not affect the results significantly, element longitudinal length was set at 10 in. for computational efficiency.

4.2.2 Model Partitioning

In the 2D approach, the bridge is partitioned into 1-ft. strips for analysis and evaluation purposes. Following a

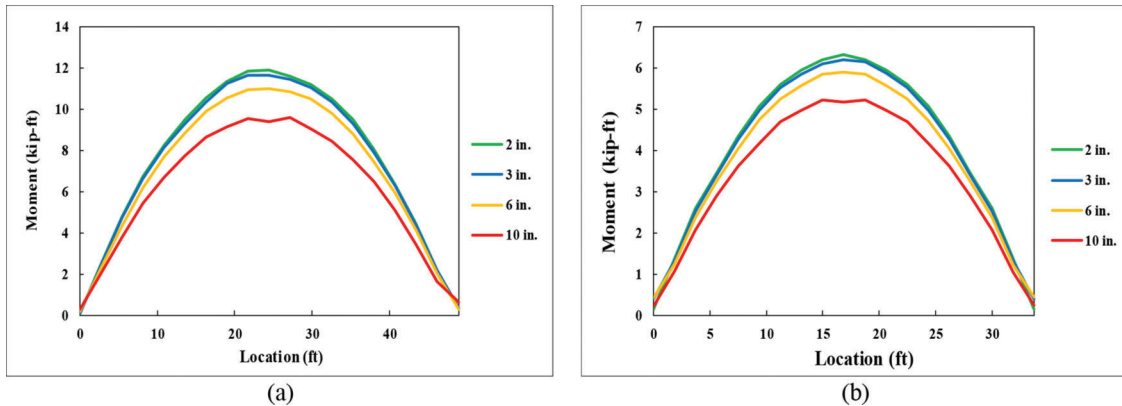


Figure 4.4 Convergence study at beam scale: (a) rectangular beam (b) T-section beam.

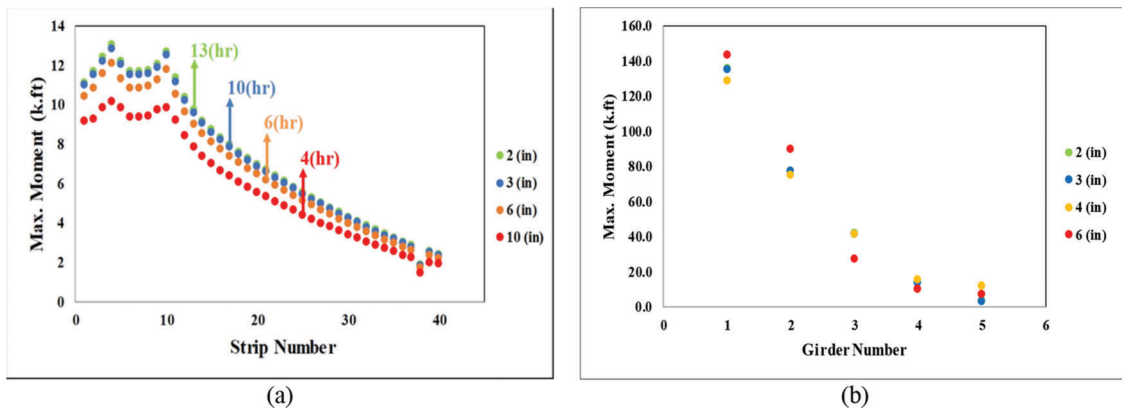


Figure 4.5 Convergence study at bridge scale: (a) slab bridge (b) T-beam bridge.

similar procedure, the superstructure was partitioned with 1-ft. strips in the 3D model such that the moment and shear responses would be comparable with results obtained from 2D analysis. The 1-ft. interior strips comprise sections of the bridge slab, while railing and sidewalk components are included in exterior strips as illustrated in Figure 4.6a. Figure 4.6b shows the interior and exterior girders partitioning approach for T-beam bridges. Like the slab case, an exterior girder in the T-beam model includes the sidewalk and railing.

4.2.3 Modeling Reinforcement

Longitudinal and transverse steel reinforcement was modeled using 3D truss elements with 6 degrees of

freedom at each node to account for the effect of reinforcements on the 3D distribution of stress in the cross-section. The truss elements were fully embedded in concrete elements to reflect a perfect bond between steel and concrete (Figure 4.7). Figure 4.8 shows the influence of including the (transverse or longitudinal) reinforcement on calculated response for a flat slab bridge (Sample #2) subjected to single truck loading. The moment response decreased when including the longitudinal reinforcements in the model (Figure 4.8a), while no significant effect was observed with transverse reinforcement as illustrated in Figure 4.8b. Therefore, for the following bridge models, only longitudinal reinforcements were considered in 3D FE modeling. It should be noted that the graphs represent moment responses for

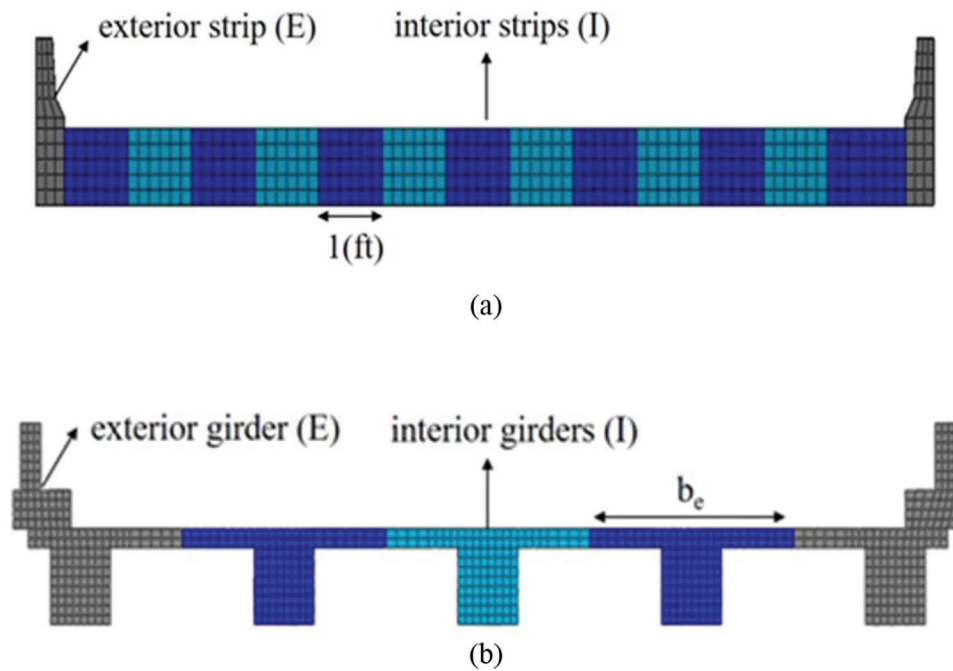


Figure 4.6 Bridge sections showing partitioning approach (a) slab bridge (b) T-beam bridge.

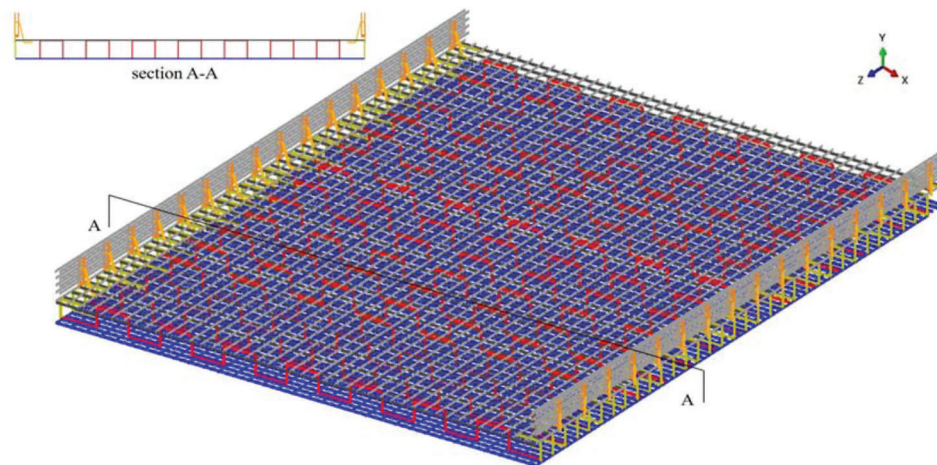


Figure 4.7 Reinforcement modeling (Sample #2).

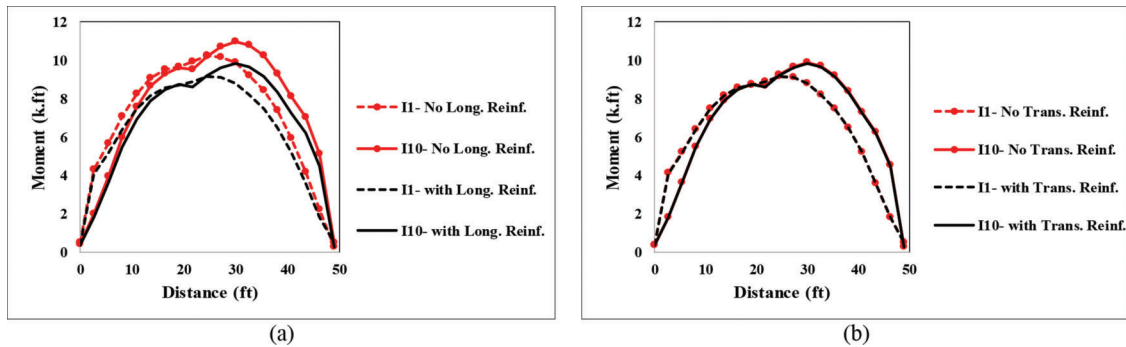


Figure 4.8 Reinforcement effect: (a) longitudinal rebars (b) transverse rebars.

two interior strips located under the truck axles (I-1 and I-10). Moreover, no significant difference was observed in shear envelopes by including/excluding reinforcement.

4.2.4 Modeling Supports

Recent finite element studies conducted on bridges have observed that detailed modeling of supports using rotational or linear springs does not have a significant impact on FE results (Hasançebi & Dumlupınar, 2013; Shahrooz et al., 1994). Therefore, supports were modeled using simple pins at one end and rollers at the other end of the bridge span. In single-beam models, the supports were positioned at the bottom of the cross-section for rectangular beams. For T-beams, the effect of different support locations was investigated by applying the supports once on the slab level and the other time on the centroidal axis of T-beam section. Figure 4.9 illustrates results obtained with these two different support positions in T-beam models discretized with three different element types (i.e., solid-solid, shell-shell, and shell-beam), respectively. The corresponding moment envelopes under uniform dead load are shown in the same figure. As it can be observed from the graphs, changing support locations affects the results significantly for solid element models (Figure 4.9a), while for the others, the differences are small enough to be negligible (particularly for the shell-beam models shown in Figure 4.9c). The model with supports positioned at the centroidal axis generates results closer to the 2D reference. Since beam and shell models assume rigid cross-sections centerline dimensions, with lines and, correspondingly, supports, located at the cross-sectional centroid, it is expected that the results of 2D beam and 3D shell models would produce results consistent with 3D solid models with supports located at the centroid. When the supports are placed at the slab level, the moment reference, and therefore value, is affected. However, for full bridge models, the supports were positioned at the bottom of the girders to be consistent with bridge plans showing beams sitting on the columns/abutments. Moreover, since no significant effect was reported for soil and pier modeling in literature, they were not considered in 3D analysis (Ding, Hao, Xia, & Deeks, 2012; Shahrooz et al., 1994).

4.2.5 Modeling Moving Loads

To apply a moving load in the FEA model, a cylinder-shaped rigid body representing the vehicular load was applied to beam model and moved forward step-by-step (Figure 4.10). A PYTHON code was developed to obtain the final moment and shear envelopes at each section. Figure 4.11a demonstrates the moment response obtained for each loading step, and the final moment envelope obtained using PYTHON code is shown in Figure 4.11b. To validate the moving load modeling approach, the shear and reaction forces obtained for each loading step were compared to corresponding values from 2D analysis. Figure 4.12a indicates a good agreement between the 2D and 3D results for one loading step of three moving 1-kip concentrated loads on a beam with rectangular section. The resultant shear envelope for this case also matched well with 2D results (Figure 4.12b). Figure 4.13 compares the results obtained when the moving load was applied in dynamic and static manners. The difference between the two solution schemes (dynamic and static) is due to the consideration of bridge mass and corresponding inertia forces. The results suggest a clear influence of dynamic loads, with the maximum amplification of 50% at the peak. It is important to point out that both 3D analyses, like the 2D results, do not account for dynamic impact caused by the vertical movements in vehicles, due to the irregularities in roadway surface. This effect was included using the impact factor (IM) of 1.3 per AASHTO specifications.

After verifying the modelling approach for a single moving load, a similar methodology was applied to model the moving trucks. For truck modeling, based on AASHTO recommendations, the wheel loads were applied using a patch measured in 20-in. length and 10-in. width with equivalent pressure uniformly distributed over the contact surface instead of point loads to avoid stress concentration and convergence problems, as reported in the literature (Shahrooz et al., 1994).

The HL-93 and HS-20 truck configurations were used for axle and lane loading in the 3D finite element study. Single and multiple trucks were moved in the longitudinal direction to obtain maximum results and

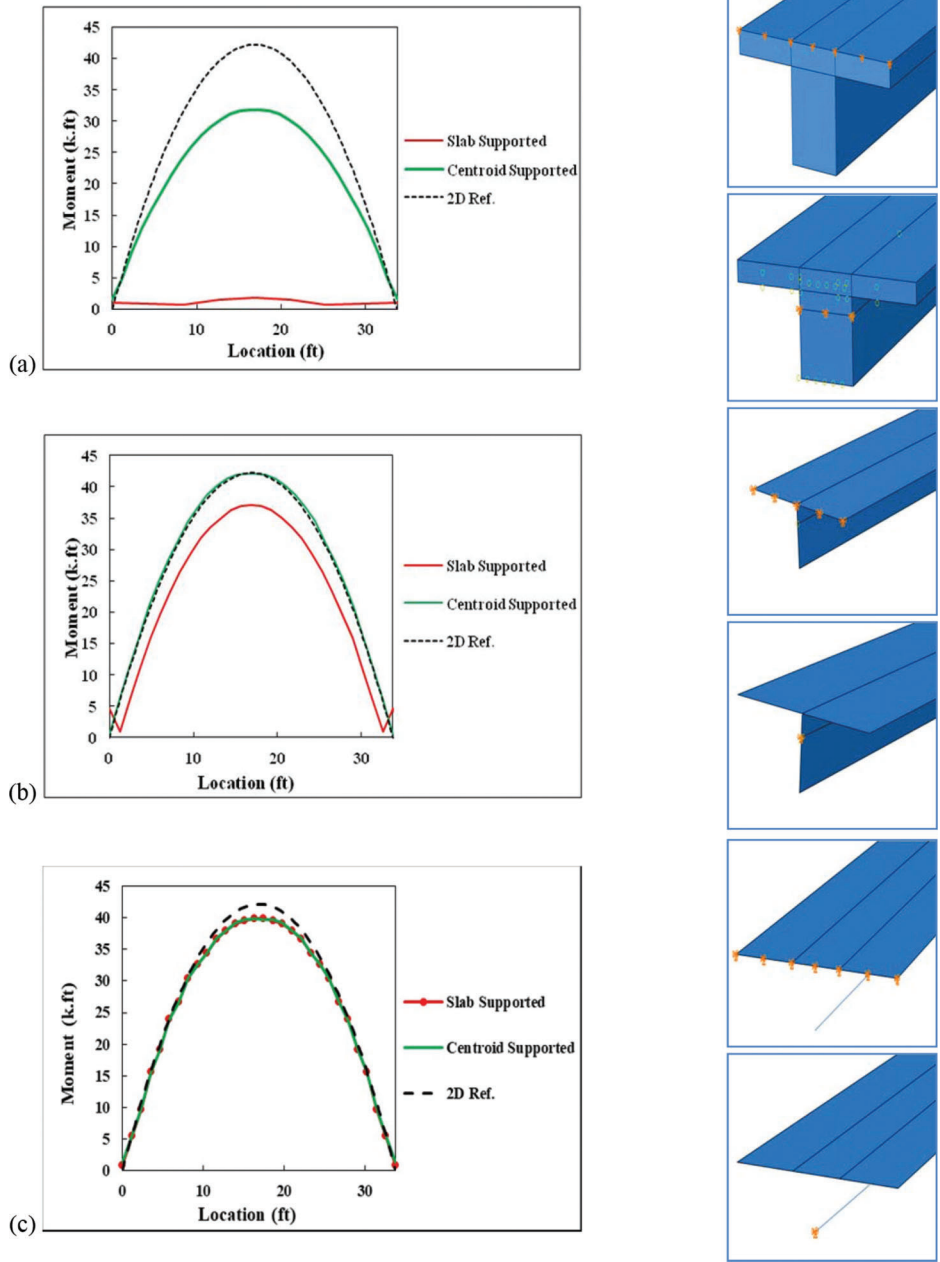


Figure 4.9 Effect of supports modeling for T-beam: (a) solid-solid (b) shell-shell (c) shell-beam.

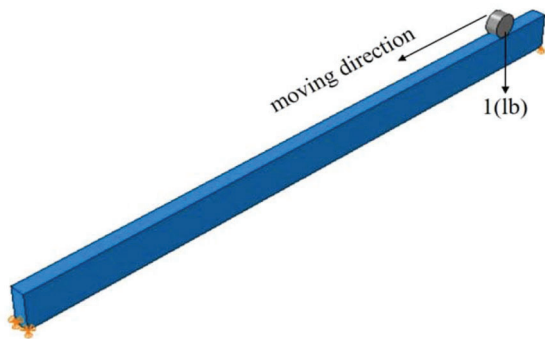


Figure 4.10 Moving load model.

positioned transversely in different locations across the bridge width to investigate the effect of lateral load distribution (see Figure 4.14). Moreover, the trucks were moved beyond the bridge deck to explore effect of partial loading on moment and shear responses. The case of two trucks moving opposite to each other were also considered. The loading was applied considering a 2-ft. distance between the first axle and the sidewalk curb, and a minimum 4-ft. distance between trucks for multiple truck loading cases. Figure 4.14 illustrates a case of multiple-lane loading with trucks positioned 2-ft. from the sidewalk curb and moving in opposite direction on a single-span slab bridge with two traffic lanes.

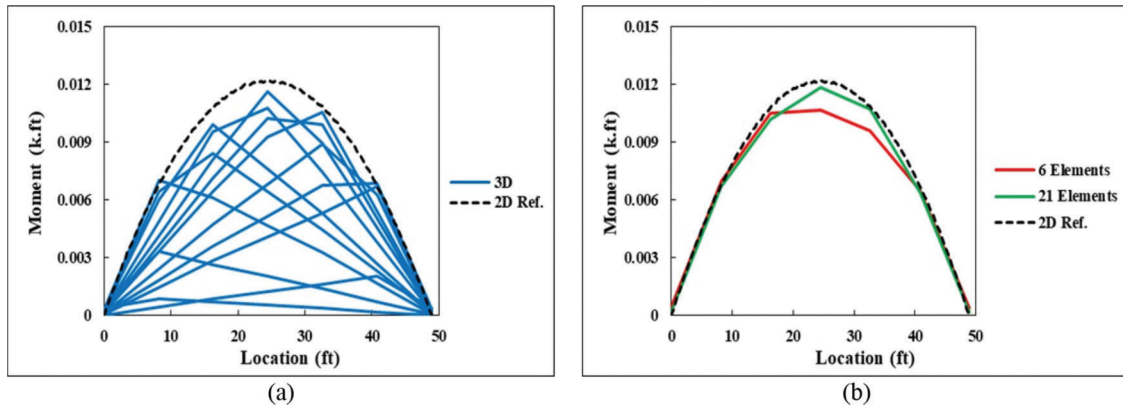


Figure 4.11 Moment response under moving load: (a) step-by-step results (b) final envelope.

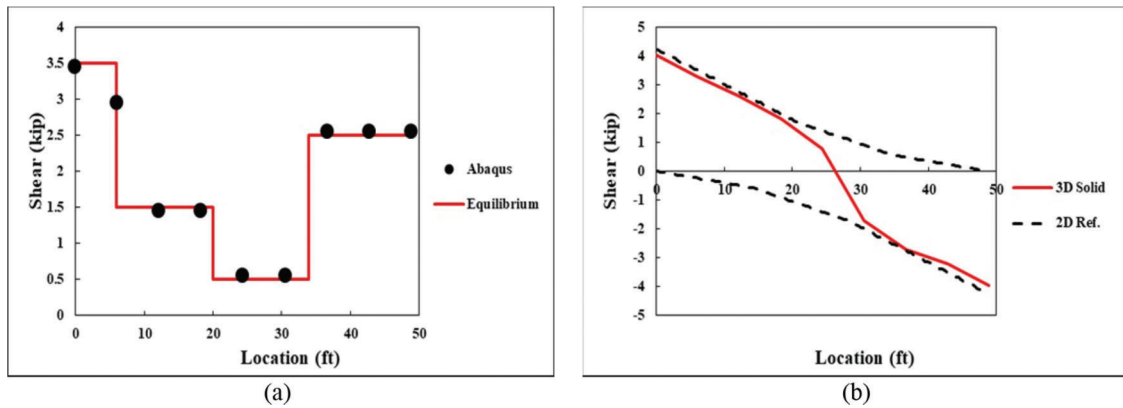


Figure 4.12 Moving load model verification: (a) one loading step (b) shear envelope.

4.2.6 Material Properties

Material properties such as concrete compressive strength (f_c'), steel yield stress (f_y), and corresponding young modulus (E_c , E_s) were extracted from design data if available, otherwise values suggested by the MBE (AASHTO, 2011) were selected based on year of construction. It was assumed that both materials are in elastic range in FE analysis.

4.3 Distribution Factor

For each strip/girder, moment and shear envelopes were obtained under different loading scenarios and the maximum effect was used to calculate the “3D” distribution factor. As expressed in Eq. (4.1), 3D live load distribution factor (3D LLDF) was defined as the ratio of maximum moment/shear effect obtained from FEA to those from 2D analysis based on a simply supported beam.

$$3D \text{ LLDF} = \frac{\text{maximum moment/shear effect from finite element analysis (3D)}}{\text{maximum response of a simply supported beam (2D)}} \quad (\text{Eq. 4.1})$$

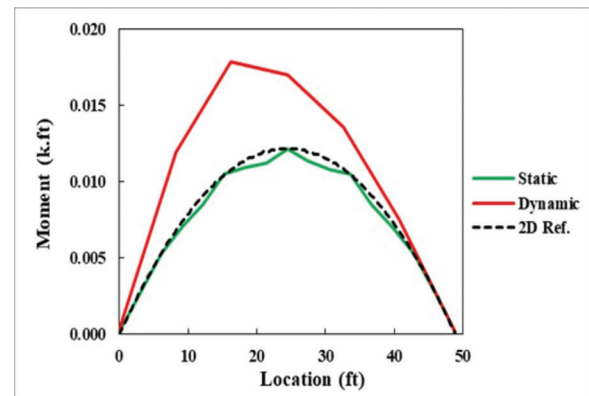


Figure 4.13 Dynamic vs. static loading.

This factor was calculated for interior/exterior strips and girders of each bridge sample, subjected to single/multiple loading lanes or truck/lane loading.

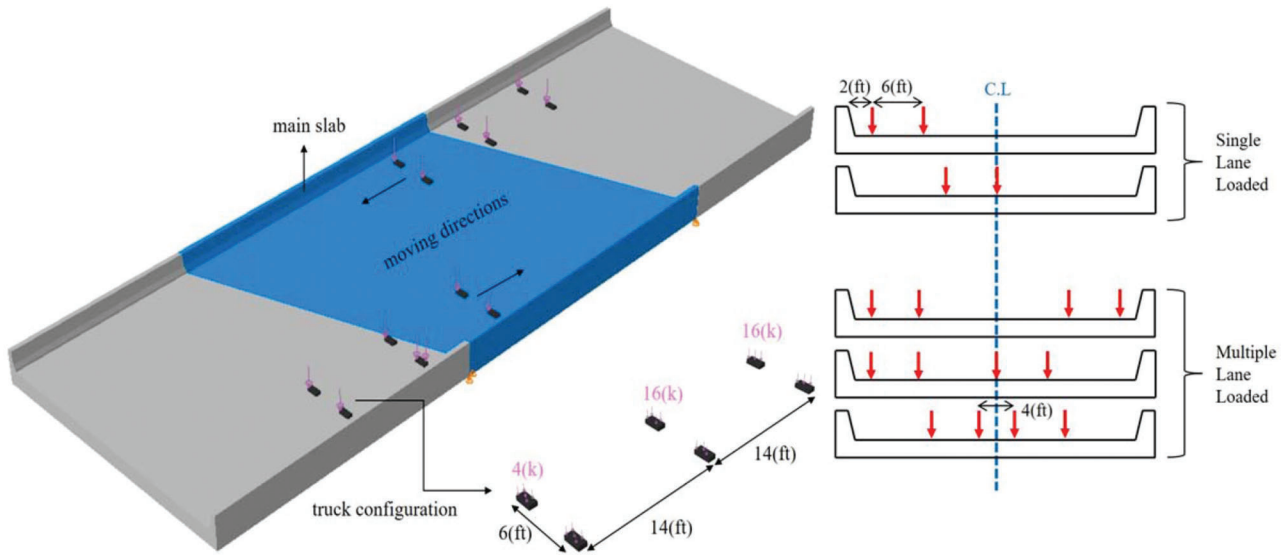


Figure 4.14 Moving truck modeling (Sample #2).

TABLE 4.1
3D LLDFs for Different Loading Configurations, Slab Bridges

Sample No.	Loading Configuration	3D LLDF						By LRFR (2D)	By LFR (2D)
		Int. Strip	Ext. Strip	Int. Strip	Ext. Strip	Int. Strip	Ext. Strip		
		Shear		Positive Moment		Negative Moment			
1	HS-20 (Truck)	0.070	0.241	0.056	0.666	0.021	0.393	0.097	0.098
	HS-20 (Lane)	0.092	0.333	0.042	0.495	0.030	0.655		
	HL-93	0.070	0.259	0.059	0.807	0.023	0.514		
2	HS-20 (Truck)	0.067	0.352	0.037	0.238	–	–	0.080	0.072
	HS-20 (Lane)	0.161	0.431	0.043	0.269	–	–		
	HL-93	0.068	0.362	0.036	0.241	–	–		
3	HS-20 (Truck)	0.075	0.173	0.064	0.249	0.053	0.210	0.084	0.086
	HS-20 (Lane)	0.090	0.180	0.054	0.189	0.046	0.218		
	HL-93	0.074	0.185	0.081	0.312	0.057	0.273		
4	HS-20 (Truck)	0.072	0.307	0.062	1.261	0.020	0.624	0.090	0.095
	HS-20 (Lane)	0.103	0.361	0.050	0.812	0.016	0.616		
	HL-93	0.074	0.382	0.065	1.667	0.022	0.813		
5	HS-20 (Truck)	0.070	0.314	0.033	0.374	0.029	0.471	0.086	0.084
	HS-20 (Lane)	0.086	0.360	0.044	0.328	0.025	0.492		
	HL-93	0.072	0.317	0.036	0.452	0.033	0.628		

The final critical 3D LLDF (per lane) values are reported in Table 4.1 and Table 4.2 for slab and T-beam bridges, respectively. The results reported in Table 4.1 show that 3D LLDFs for exterior strips are significantly larger than those calculated in interior ones. This is due to the increased stiffness of exterior strips, caused by the presence of the railings, when compared to interior ones. A similar pattern can be observed for T-beam bridge distribution factors for moments, while 3D LLDFs for shear are larger in interior strips compared to exterior ones. This can be attributed to the loading configurations, where truck loading is applied on one of the

interior girders, producing large shear response in the corresponding girder (loading was not applied exactly over exterior girders due to 2-ft. distance between axles and curb specified in the code).

4.4 Capacity Calculation

Moment and shear capacities were calculated separately for interior and exterior strips/girders. Figure 4.15a and Figure 4.15b illustrate sections considered for capacity calculation in the 3D approach for exterior strips and girders, respectively, and include any present

TABLE 4.2
3D LLDFs for Different Loading Configurations, T-Beam Bridges

Sample No.	Loading Configuration	3D LLDF				By LRFR (2D)				By LFR (2D)	
		Int.	Ext.	Int.	Ext.	Int.		Ext.		Int.	Ext.
		Moment	Shear	Moment	Shear	Moment	Shear	Moment	Shear	Moment and Shear	
6	HS-20 (Truck)	0.415	0.497	0.517	0.470	0.720	0.899	0.634	0.662	0.750	0.600
	HS-20 (Lane)	0.440	0.588	0.619	0.410						
	HL-93	0.409	0.526	0.527	0.456						
7	HS-20 (Truck)	0.374	0.491	0.522	0.477	0.723	0.882	0.636	0.649	0.743	0.590
	HS-20 (Lane)	0.353	0.441	0.640	0.539						
	HL-93	0.375	0.513	0.535	0.459						
8	HS-20 (Truck)	0.482	0.513	0.499	0.471	0.693	0.729	0.557	0.485	0.673	0.454
	HS-20 (Lane)	0.429	0.450	0.464	0.559						
	HL-93	0.504	0.516	0.483	0.475						
9	HS-20 (Truck)	0.344	0.453	0.524	0.455	0.731	0.847	0.619	0.568	0.730	0.510
	HS-20 (Lane)	0.490	0.561	0.895	0.803						
	HL-93	0.342	0.472	0.540	0.452						
10	HS-20 (Truck)	0.386	0.514	0.553	0.439	0.646	0.836	0.498	0.501	0.689	0.430
	HS-20 (Lane)	0.447	0.802	0.862	0.708						
	HL-93	0.374	0.561	0.555	0.442						

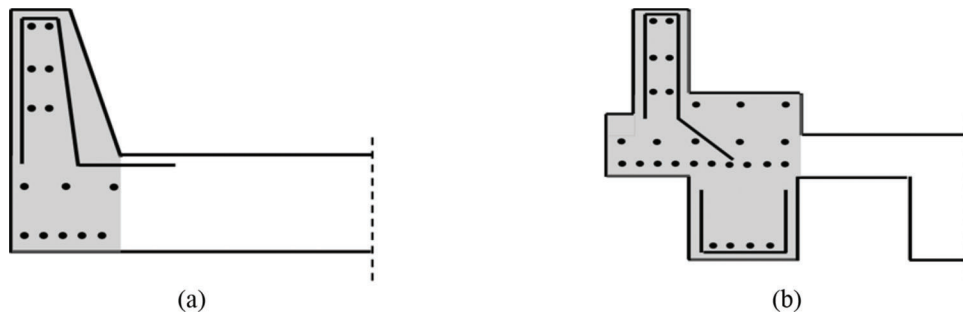


Figure 4.15 Sections considered for capacity calculation for exterior (a) strip (b) girder.

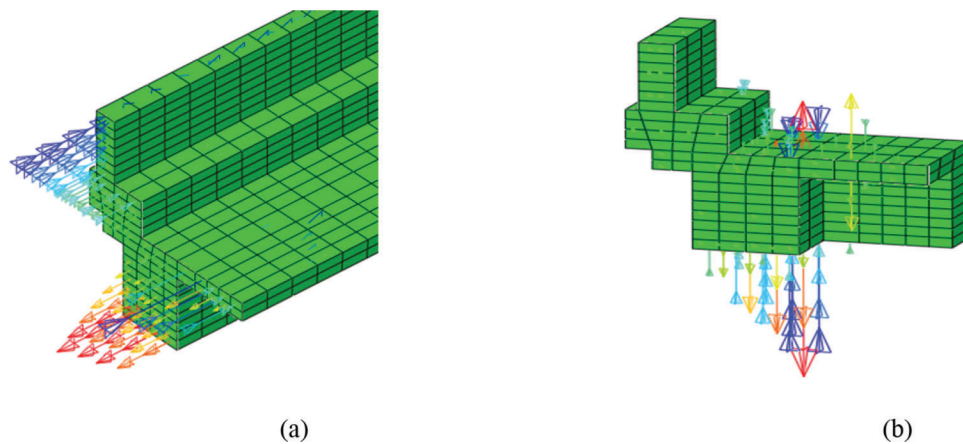


Figure 4.16 Strain distribution: (a) normal (b) shear.

railings or sidewalks. For interior ones, sections used in capacity calculations for the 3D approach are the similar to the ones used in 2D rating. For slab bridges, the railing section was considered to be contributing in

moment and shear capacity for exterior strips, while for T-beam bridges, observed normal and shear strains patterns suggest that railings mainly add to moment capacity. Figure 4.16 displays the strain distribution in

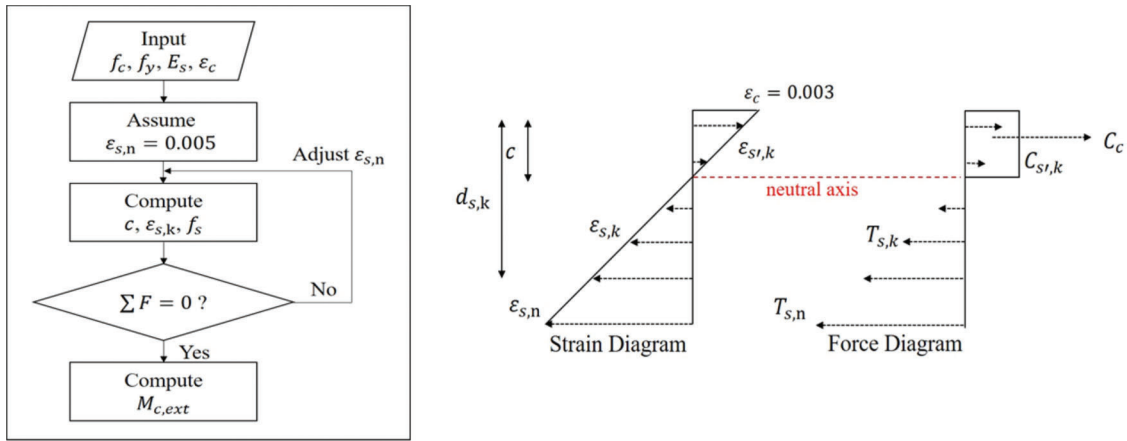


Figure 4.17 Moment capacity calculation procedure for exterior strips/girders.

one exterior girder section, and shows normal strain developed on railing and girder parts while shear strain is mainly developed in the girder web (no contribution from railing in shear). For both types of bridges, moment capacity was improved due to an increase in moment arm length.

Since several layers of reinforcement were provided in the railing sections, the location of the neutral axis was calculated via a trial and error procedure using a flowchart shown in Figure 4.17. After determining the neutral axis location, rebars above and below the axis were considered active in compression and tension, respectively.

4.5 Rating Factor

For each bridge sample, the critical loading scenario and its corresponding controlling effect (moment/shear) was determined based on results obtained from 3D analysis. The load rating factor was calculated following the same equation provided in the 2D approach (Eq. 3.1 and Eq. 3.2) but without LLDF applied to live load responses. For exterior strips/girders, the railing contribution was also included in capacity calculations. Final rating factors are reported in Table 4.3 and Table 4.4 for slab and T-beam bridges, respectively. Comparing rating factor values obtained from 2D and 3D analyses, a noticeable improvement can be observed for both slab and T-beam bridges, with all bridges except one (Sample #2) showing rating factors above one. This bridge (Sample #2) will be further examined in the following sensitivity analysis section to gain further insight on possible improvement in load carrying capacity. With the exception of Sample #2, all bridge samples that had exhibited rating factors below one in 2D analysis, have satisfactory load results when analyzed in 3D. In slab bridges, average rating factors obtained from 3D analysis for moment are 3.7 and 2.7 times larger than the corresponding 2D values for interior and exterior strips, respectively. These ratios are 1.2 and 6.2 for shear. Similarly, in T-beam bridge samples, the ratio between 3D and 2D moment rating

factors are 2.2 and 3.5 for interior and exterior girders, respectively. The corresponding value for shear is 1.5 for both girder types. Moreover, by comparing the values provided in Table 3.8 and Table 3.10 (2D) with Table 4.3 and Table 4.4 (3D), it can be observed that for interior strips of slab bridges and interior/exterior girders of T-beam ones, moment ratings show higher improvements than shear ratings. For interior strips of slab bridge samples, the shear rating factor increased significantly due to contribution of shear reinforcement provided in the railings (see Figure 4.15a).

4.6 Summary of Findings

The results of 3D analysis demonstrate that parameters such as type and size of the element, type of the loading, and load positioning, have a clear impact on FEA results. Based on observed sensitivity of load positioning in lateral direction to live load distribution factor, it seems that considering one single distribution factor for the whole superstructure and all loading scenarios may not be effective to reflect actual lateral distribution of live loads. Based on FE results, the edge stiffening attributed to railings allocates a large portion of the response (both moment and shear) to exterior strips/girders and decreases the share of interior ones significantly. Therefore, the LLDF calculated for interior strips/girders are smaller compared to those obtained from formulation suggested by AASHTO specifications. On the other hand, distribution factors of exterior strips/girders are larger than those obtained from 2D analysis. It should be noted that larger LLDF values for these exterior strips/girders did not lead to critical rating factors since capacity was also improved due to the structural contribution of the reinforced concrete railing. In total, rating factors obtained from 3D analysis are greater than those obtained using the 2D approach for both LFD and LRFD methods. Greater share of demand absorbed by the edges indicates the importance of geometrical feature with large stiffness such as railings in demand distribution. Other bridge geometrical characteristics such as skew

TABLE 4.3
3D Results, Rating Factors of Slab Bridges

Sample No. (Span, ft.)	Approach	Level	Int. Strip				Ext. Strip			
			M	Loc. (ft.)	V	Loc. (ft.)	M	Loc. (ft.)	V	Loc. (ft.)
1 (18-25-18)	LFD	Inventory	4.44	57.6	2.89	23.7	4.30	47.4	14.0	23.7
		Operative	7.41		4.82		7.18		23.5	
	LRFD	Inventory	5.99	27.1	3.13	23.7	3.91	47.4	14.0	37.3
		Operative	7.77		3.81		5.06		18.1	
2 (48.9)	LFD	Inventory	5.05	32.6	3.02	13.6	1.14	29.9	7.93	5.4
		Operative	8.43		5.04		1.91		13.2	
	LRFD	Inventory	4.43	32.6	3.33	8.1	0.87	29.9	6.89	5.4
		Operative	5.74		4.31		1.12		8.94	
3 (30-42-30)	LFD	Inventory	2.37	79.3	1.45	34.0	1.86	11.3	12.7	62.3
		Operative	3.96		2.41		3.10		21.2	
	LRFD	Inventory	2.16	79.3	1.50	34.0	1.64	11.3	11.8	62.3
		Operative	2.80		1.68		2.13		15.3	
4 (21-28-21)	LFD	Inventory	3.86	31.1	1.91	38.9	5.96	31.1	22.8	42.8
		Operative	6.44		3.19		9.95		38.0	
	LRFD	Inventory	3.86	31.1	2.92	38.9	5.52	31.1	23.1	38.9
		Operative	5.00		3.65		7.16		30.0	
5 (32-42.5-32)	LFD	Inventory	1.38	82.8	1.74	71.0	1.64	35.5	8.52	71.0
		Operative	2.30		2.90		2.74		14.2	
	LRFD	Inventory	1.19	82.8	1.82	71.0	1.25	71.0	7.86	71.0
		Operative	1.54		2.04		1.62		10.2	

TABLE 4.4
3D Results, Rating Factors of T-Beam Bridges

Sample No. (Span, ft.)	Approach	Level	Int. Girder				Ext. Girder			
			M	Loc. (ft.)	V	Loc. (ft.)	M	Loc. (ft.)	V	Loc. (ft.)
6 (36)	LFD	Inventory	2.45	14.5	2.22	24.8	4.18	20.7	3.00	24.8
		Operative	4.09		3.71		6.98		5.00	
	LRFD	Inventory	2.50	16.6	2.57	24.8	4.34	20.7	3.62	24.8
		Operative	3.24		3.33		5.63		4.70	
7 (38)	LFD	Inventory	3.11	19.8	1.83	24.1	4.49	21.9	2.13	4.4
		Operative	5.19		3.06		7.49		3.55	
	LRFD	Inventory	3.10	19.8	2.16	24.1	4.67	21.9	2.49	4.4
		Operative	4.02		2.80		6.06		3.23	
8 (40)	LFD	Inventory	2.50	13.5	1.24	23.2	3.80	19.3	1.54	11.6
		Operative	4.17		2.07		6.34		2.57	
	LRFD	Inventory	2.58	15.4	1.49	23.2	3.98	19.3	1.84	11.6
		Operative	3.35		1.93		5.16		2.38	
9 (28)	LFD	Inventory	3.28	11.4	2.05	27.6	6.36	17.9	2.43	1.6
		Operative	5.48		3.42		10.6		4.05	
	LRFD	Inventory	3.40	11.4	2.32	27.6	6.73	17.9	3.01	1.6
		Operative	4.41		3.01		8.73		3.91	
10 (26)	LFD	Inventory	3.77	14.6	2.12	27.6	5.38	16.3	1.53	24.4
		Operative	6.29		3.54		8.98		2.56	
	LRFD	Inventory	3.93	14.6	2.39	27.6	5.65	16.3	2.02	4.9
		Operative	5.10		3.10		7.33		2.62	

angle, slab thickness, support area, and spacing between the girders are also considered as potential factors influencing the LLDF. These observations serve as the basis for sensitivity analysis performed in the following chapter.

5. SENSITIVITY ANALYSIS OF GEOMETRICAL PARAMETERS

5.1 Introduction

The tools of 3D computational modeling allow an accurate representation of the effect of bridge geometry on structural response. This chapter aims at investigating the sensitivity of bridge response to several geometric parameters. Based on the observations made in Chapter 3 and Chapter 4, these study parameters were identified as slab thickness, support area geometry, girder spacing, diaphragm thickness, railing height, and skew angle. Some variables were studied only in slab bridges, such as slab thickness and support area, while others such as girder spacing and diaphragm thickness, were investigated in T-beam bridges. Railing height and skew angle were studied in both. Table 5.1 summarizes the parameters and their corresponding

range of variation, which were determined from the corresponding values in the sample bridges. A sensitivity analysis was conducted on each parameter to observe the impact of changes in parameter value on analysis response.

5.2 Reference Models

The bridge models created in Chapter 4 differ from each other in more than one of the above-identified parameters. Therefore, in order to isolate the effect of each individual parameter in the sensitivity study, reference models were created for each bridge type such that each bridge model created in this study would involve a variation on a single parameter. Two different reference models were created using solid elements (C3D8R) for each bridge type, shown in Figure 5.1. The slab bridge reference model consists of 45 interior 1-ft. strips and two exterior strips, while the T-beam bridge model has four interior girders and two exterior girders. Both reference models are single-span, unless otherwise specified, and their geometrical properties were determined based on average values of the bridge samples studied in Chapter 4. The sensitivity study is

TABLE 5.1
Study Parameters and Ranges

	Parameter Values (or Range)		Unit
	Slab Bridges	T-Beam Bridges	
Railing Height (h_r)	0, 10, 20, 40	0, 10, 20, 40	inch
Skew Angle (\angle)	0, 10, 20, 40, 60	0, 10, 20, 40, 60	degree ($^\circ$)
Slab Thickness (t_s)	15, 20, 30, 20 ^(var)	n/a	inch
Support Modeling	area, line	n/a	–
Diaphragm Thickness (t_d)*	n/a	0, 5, 10, 20	inch
Girder Spacing	n/a	even, uneven (#1 and #2)	–

20^(var): Various thickness along the bridge length, while the average thickness keeps 20.

n/a: Not applicable.

*Thickness = diaphragm area/bridge width.

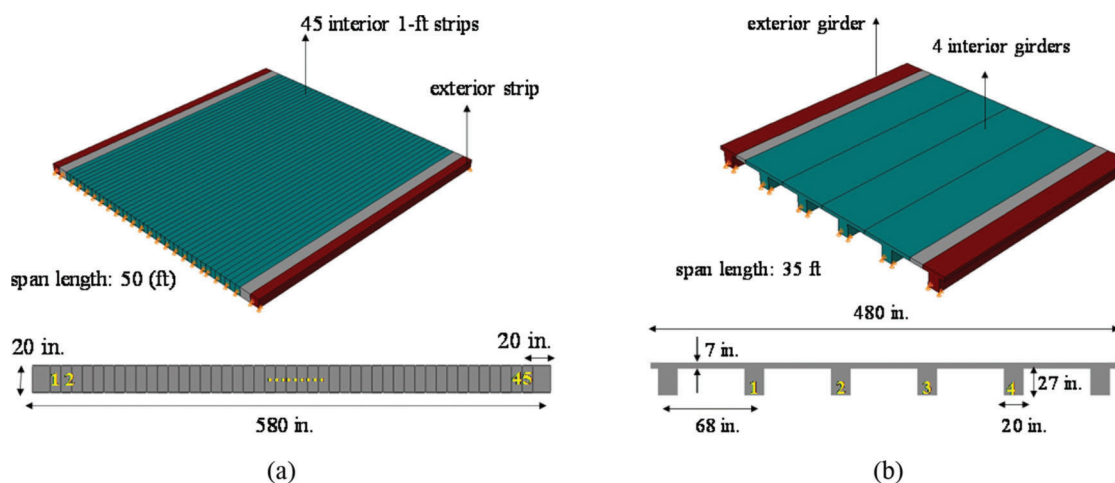


Figure 5.1 Reference models for sensitivity analysis: (a) slab bridge (b) T-beam bridge.

focused exclusively on assessing demand, and therefore capacity calculations, including appropriate reinforcement, are not taken into account. It is useful to keep in mind however, that placement of longitudinal reinforcement may lead to a reduction in moment demand by about 10% to 20%, as observed in Figure 4.8. This is due to the change in stress distribution over the cross-section, with the concentration of tensile stresses in the longitudinal reinforcement and a reduction of maximum tensile and compressive stresses in other parts of the area, which leads to a reduction in moment demand.

For the slab bridge model, supports were positioned at each bottom edge with the lines of pin at one side and roller at the other side, whereas for T-beam model, the same supports were applied on the bottom edges of the girders.

5.3 Railing Effect

To evaluate the effect of railings on bridge demand, railings on each side were added to the reference model.

For reasons discussed in Chapter 4.2.1, solid elements (C3D8R) were used for modeling the railings, allowing for the full compatibility between deck and railing. Railing geometries were determined from average values reported in the sample studied in Chapter 4, based on bridge structural drawings (Figure 5.2). Four different railing heights, specified in Table 5.1, were considered to examine the trend with respect to height.

Figure 5.3 compares moment and shear demands for the reference slab bridges with and without railing of 40 in. The bridges are loaded with a single moving HL-93 truck, and moment and shear demands were obtained for individual strips. In the figures, the moment or shear value reported for a given strip number is the maximum of value along the bridge length on that strip. The two peak moment/shear values observed at two interior strips correspond to the locations of the two truck axles. For moment response, the presence of railings leads to a significant decrease for interior strips and increase for exterior strips, by at most 15.1 kip-ft. (0.3 times reduction) and 112.9 kip (4.3 times increase), respectively. For shear, only exterior strips show an

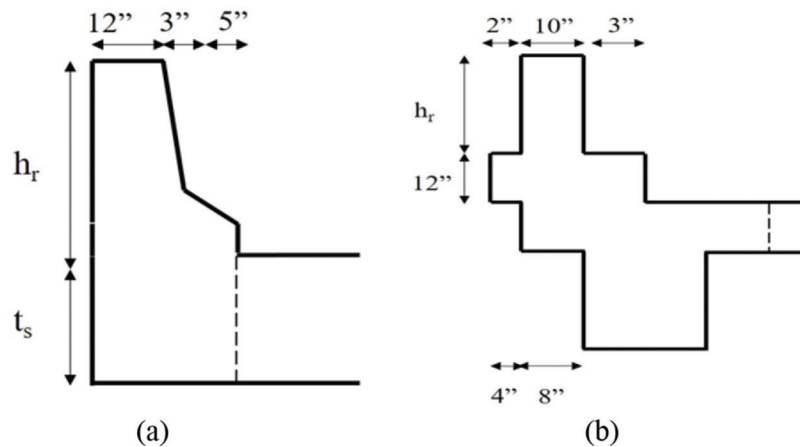


Figure 5.2 Railing geometries at section of (a) slab bridge (b) T-beam bridge.

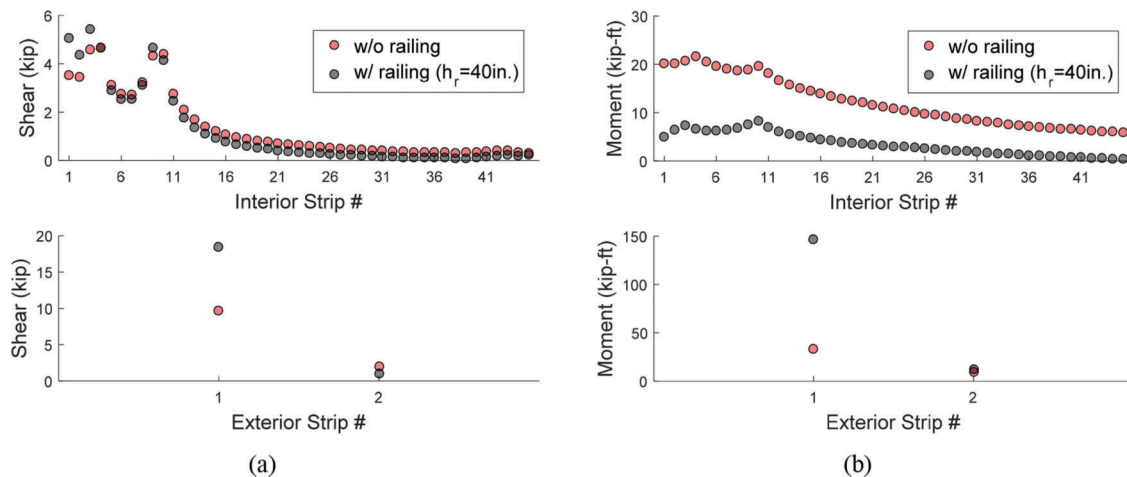


Figure 5.3 Comparison of demand between with and without railings of 40 in. for slab bridge reference model (a) shear (b) moment.

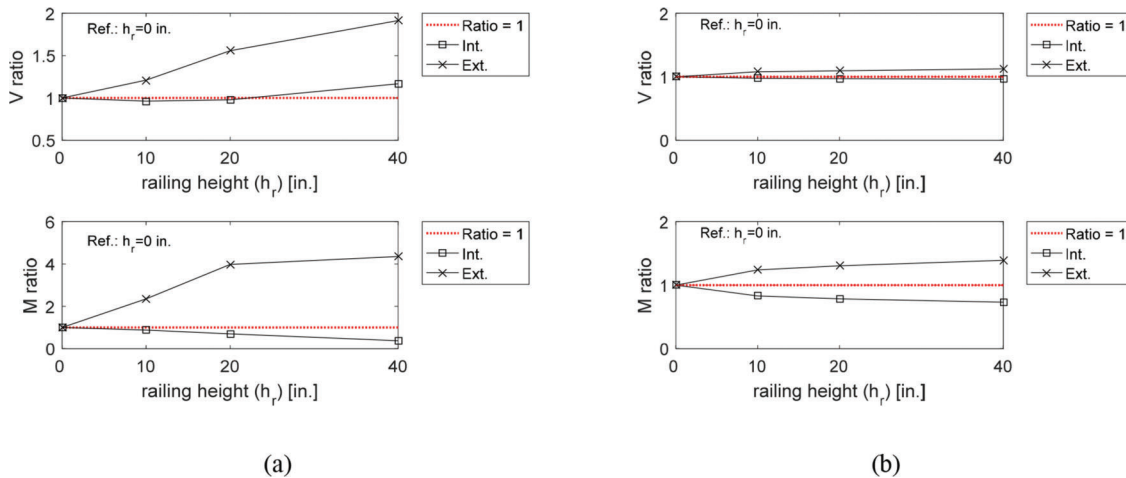


Figure 5.4 Moment and shear change w.r.t railing height (a) slab bridge (b) T-beam bridge.

obvious increase by 8.8 kip (1.9 times increase). This comes from the fact that presence of railings leads to the stiffness increase of exterior strips, and consequent relative decrease of interior ones.

Changes in moment and shear demands for different railing heights are shown in Figure 5.4, where the demand ratio represents a normalized demand value calculated by dividing demand with different railing heights by that in the identical bridge without railings. By such definition, demand ratio without railings (i.e., $h_r = 0$) is always “1”, and thus the trend with increasing railing height can be easily read. In all the following figures, results are expressed in the form of ratios with respect to the reference model to better illustrate the effect of each individual parameter. As observed from the previous example, it is now more obvious that higher railing height results in a bigger increase in moment demand for exterior strips as well as a more obvious decrease in moment of interior strips. Change in shear demand with respect to railing height was shown to be relatively less compared to moment.

In addition, a 3-span slab bridge reference model was examined to study the effect of railing on demand in multiple-span bridges. Figure 5.5 depicts the effect of span numbers on demand in slab bridge with railings, where 1-span and 3-span bridge models with 40-in railings were compared. Unlike the 1-span bridge, positive and negative moments are now separately considered. The comparisons show that all demands (shear, positive and negative moments) were reduced in the 3-span bridge compared to the 1-span case. It should be mentioned that 3-span T-beam bridges were not studied, as all such bridges considered in this study have simply supported condition.

5.4 Skew Effect

Six discrete skew angles ranging from 0 to 60 degrees were considered to assess sensitivity with respect to skew angle. Results shown in Figure 5.6 suggest that bridges with higher skew angles showed degreed

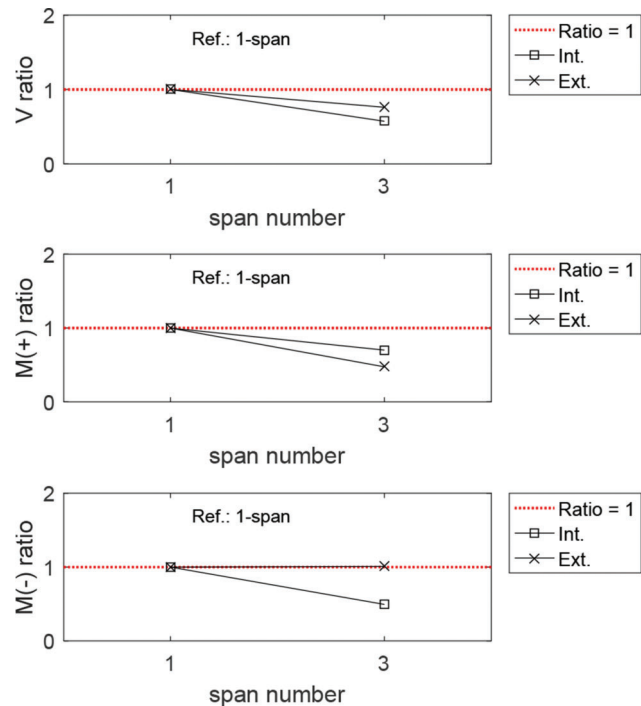


Figure 5.5 Effect of span numbers on demand of slab bridges with railing height of 40 in.

moments in interior and exterior strips for slab and T-beam bridges. The trend for shear demand is not obvious except for the observation that shear for T-beam bridges was less affected by variations in skew angle. For slab bridges with a skew angle of 40 degrees, the effect of span numbers is shown in Figure 5.7, where all demands decreased in bridges with 3 spans compared to 1-span bridges.

5.5 Slab Thickness Effect

For slab bridges, deck thickness could be a critical factor that affects structural demand. Three different deck thickness values of 15 in., 20 in., and 30 in. were

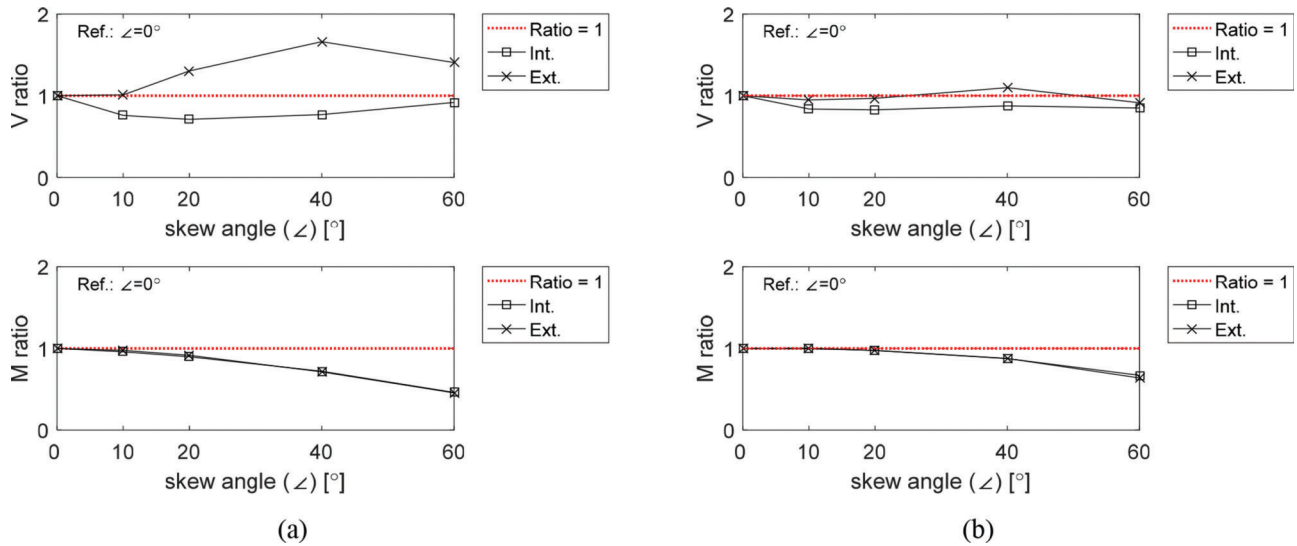


Figure 5.6 Moment and shear change w.r.t skew angle (a) slab bridge (b) T-beam bridge.

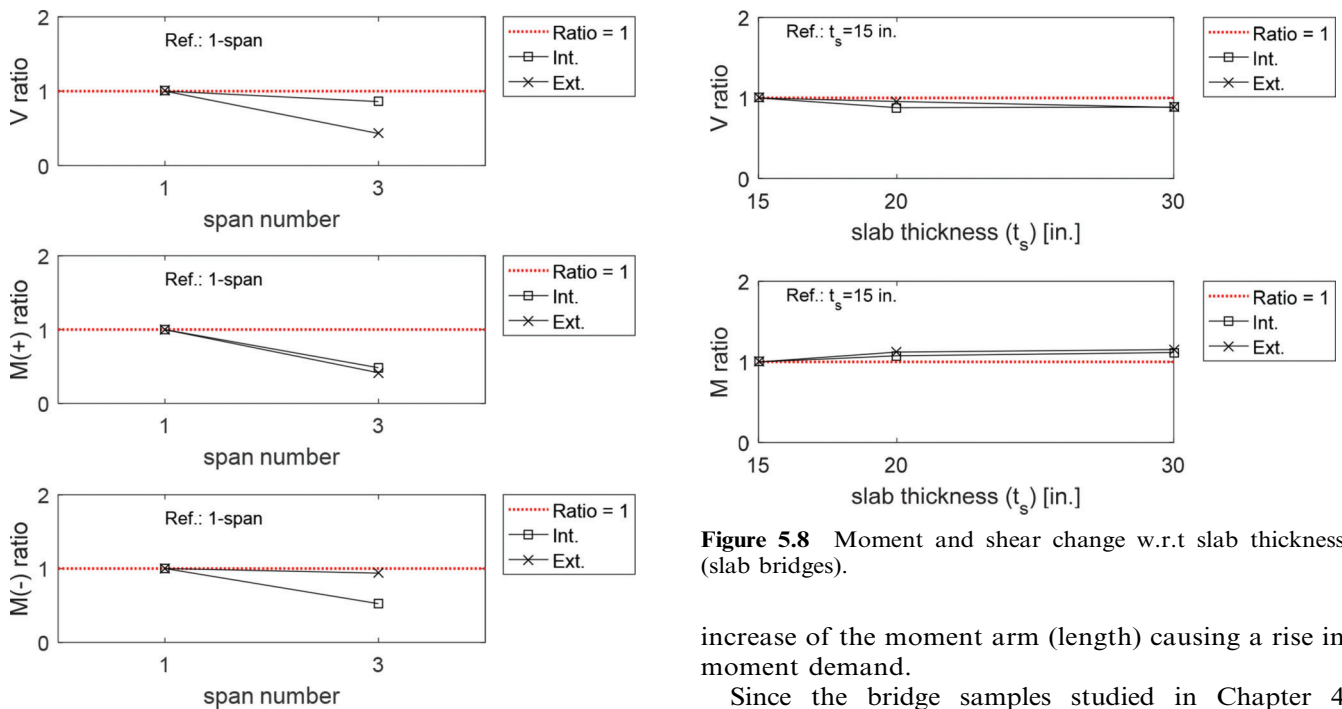


Figure 5.7 Effect of span numbers on demand of slab bridges with skew angle of 40 degrees.

Figure 5.8 Moment and shear change w.r.t slab thickness (slab bridges).

investigated, and the results are given in Figure 5.8. The analyses focused on the effect of increased stiffness without taking into account variations in dead load. It was shown that with increased thickness from 15 in. to 30 in., shear demand decreased to 0.88 (interior) and 0.88 (exterior), while moments increased to 1.11 (interior) and 1.15 (exterior) in the ratio term. Moment and shear trends with respect to slab thickness can be attributed to the fact that an increase of deck thickness leads an increase of the shear depth resulting in shear demand reduction, but also to an

increase of the moment arm (length) causing a rise in moment demand.

Since the bridge samples studied in Chapter 4 included a bridge with variable thickness along the bridge length (Sample 3), we investigate the difference in demand estimates between bridges with constant and variable thicknesses. Figure 5.9 shows the longitudinal sections of 3-span bridge models with either constant or variable thickness. The model with variable thickness was assumed to have the average thickness of 20 in., which corresponds to the constant thickness in the companion model, and both models include railings with height of 40 in. The comparison of the two models indicates that in overall, demand can differ, although their thickness is the same in average (Figure 5.10). For shear, variable thickness resulted in the increase for interior strips and decrease for

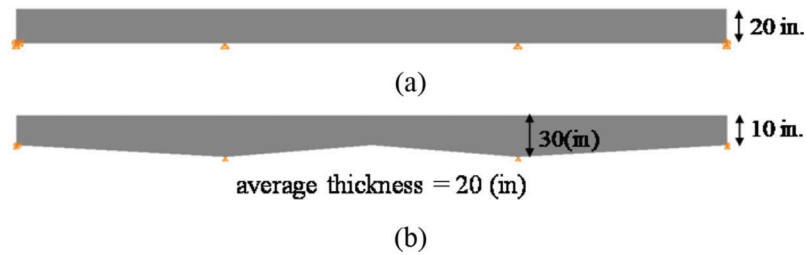


Figure 5.9 Slab thickness type (slab bridge): (a) constant thickness (b) variable thickness.

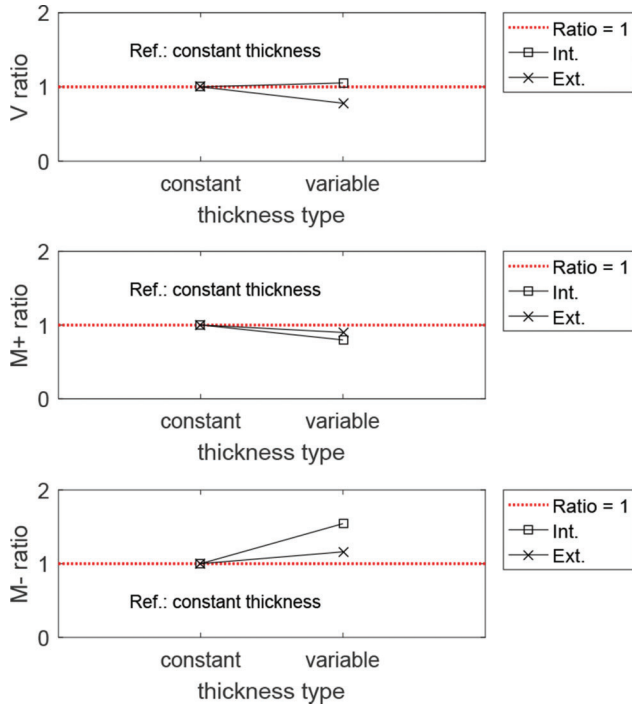


Figure 5.10 Moment and shear change according to slab thickness type (slab bridge with railing height of 40 in.).

exterior strips, 1.05 and 0.78, respectively, in the ratio term. This arises from the shear depth increase in interior strips, leading to the relative stiffness gain of interior strips and lose of exterior strips. The positive moment of both interior and exterior strips decreased to 0.80 and 0.90, respectively, due to the variable thickness effect, while the negative moment increased to 1.54 and 1.16.

5.6 Support Area Effect

As stated earlier, in the slab bridge reference model, supports were modeled with pin and roller lines, which may not be a good representation of real bridge support conditions. A more realistic modeling approach considers a finite contact area between the bridge superstructure and its supports, as described in Figure 5.11. The figure shows the longitudinal section views of the 1-span and 3-span bridge models, indicating the support length (support area divided by bridge width) of each model. According to the drawings of the sample bridges, bridges sit on piers/columns (supports), with

average support length of 24 in. for 1-span, and 30 in. for 3-span bridges. For reference, in the case of line supports, the support area, and therefore equivalent length, becomes zero. The analysis results from line and area supports illustrates that for both 1-span and 3-span bridges, area supports brought about the reduction in both moment and shear in comparison with line supports (Figure 5.12). For instance, shear of 3-span model with area supports reduced to 0.57 and 0.76 (interior and exterior), while positive moment reduced to 0.70 and 0.48 (interior and exterior). In sum, the effect of area support modeling appears to be more prominent in 3-span bridges than in 1-span bridges. The demand reduction effect is caused by the stress distribution over the area.

5.7 Diaphragm Effect

It is usual that T-beam bridges include diaphragm on support position. Figure 5.13 depicts the demand change with respect to four distinct values of diaphragm thickness, where the thickness of zero represents no diaphragm. The results indicate that the diaphragm effect is negligible.

5.8 Girder Spacing Effect

The effect of girder spacing variations was studied using three different cases described in Figure 5.14. In the first case, the girders are evenly spaced, while uneven girder spacing is assumed in the latter two cases. All the three have the same average spacing of 68 in. It is shown from Figure 5.15 that different girder spacing schemes change the shear demand in the order of 0.97 and 1.14 (interior and exterior) for uneven case #1, moment in the order of 0.96 and 1.13 (interior and exterior) for uneven case #2. It is deemed that larger spacing between interior girders makes those girders take more stress, consequently lessening stress in the exterior girders. Furthermore, it indicates that averaging the girder spacing cannot reflect actual load distribution on girders.

5.9 Summary of Findings

In this chapter, a sensitivity study was conducted to assess the impact geometrical parameters, including railing height, skew angle, slab thickness, support area, diaphragm thickness, and girder spacing, on

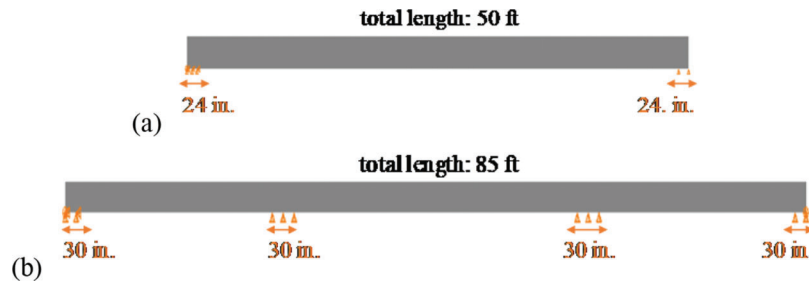


Figure 5.11 Support area for (a) 1-span (b) 3-span slab bridge models.

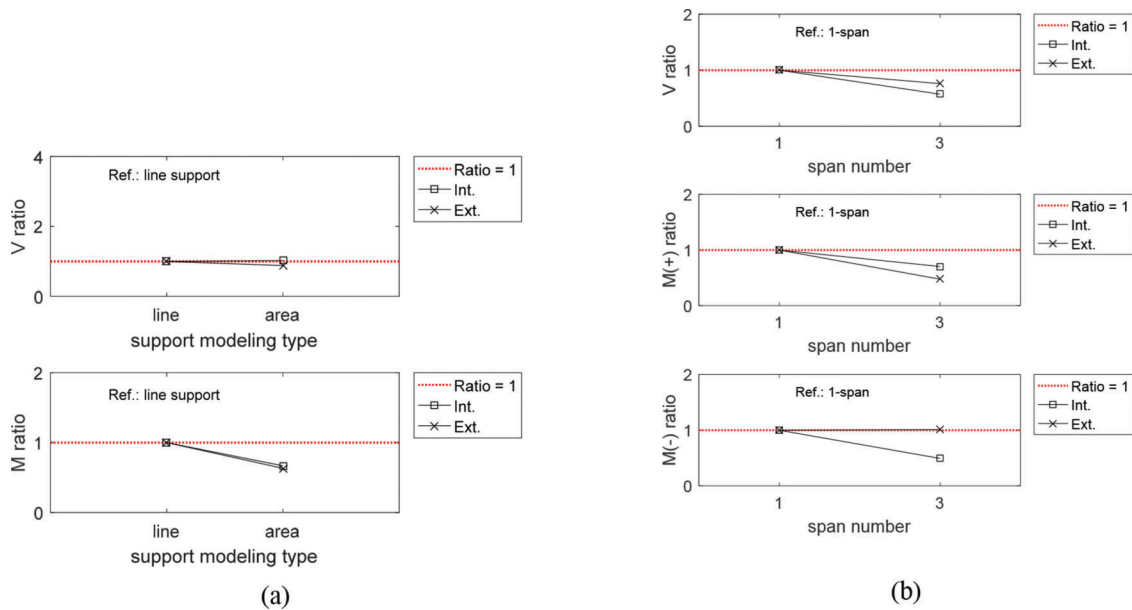


Figure 5.12 Moment and shear change according to support modeling type for slab bridges with (a) 1 span (b) 3 spans.

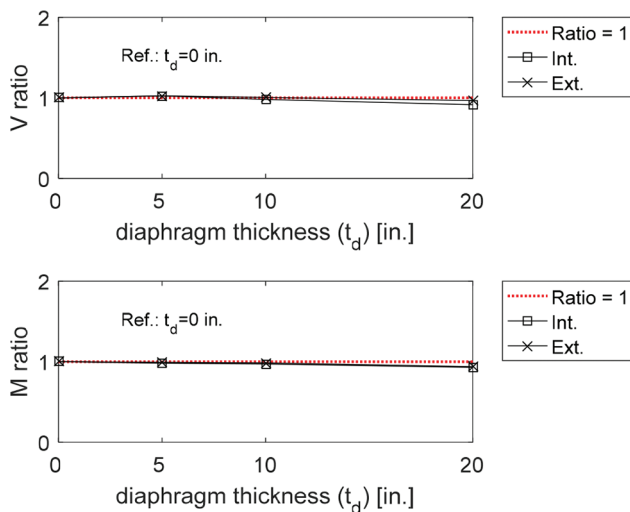


Figure 5.13 Moment and shear change w.r.t diaphragm thickness (T-beam bridge).

demand in flat-slab and T-beam bridges. The following observations were made on the effect of these parameters:

- Railing height was confirmed as a parameter that produced the most drastic change in moment and shear demands of bridges. Particularly, changes in moment and shear demands for exterior strips were more prominent than those of interior strips. This is due to the increased stiffness, caused by the presence of railings, of exterior strips. It follows increasing demand at those locations, and consequently decreasing the relative stiffness and associated demand for interior ones. This increase in demand for exterior strips is counteracted with an increased capacity at these locations.
- An increase in skew angle was found to cause a reduction in moment and increase in shear for both 1-span and 3-span bridges, which is consistent with AASHTO recommendations for skew factor.
- For slab bridges, the effect of slab thickness was relatively small and slab thickness variation along the bridge length showed a slight reduction in moment.
- The importance of modeling the support area was found by comparing the results obtained assuming line supports and models incorporating area support. Models with area support showed a decrease in both moment and shear when compared to the models with line supports. For T-beam bridges, the effect of diaphragm thickness was observed to be negligible.
- Models with uneven girder spacing produced different moment and shear demands depending on the

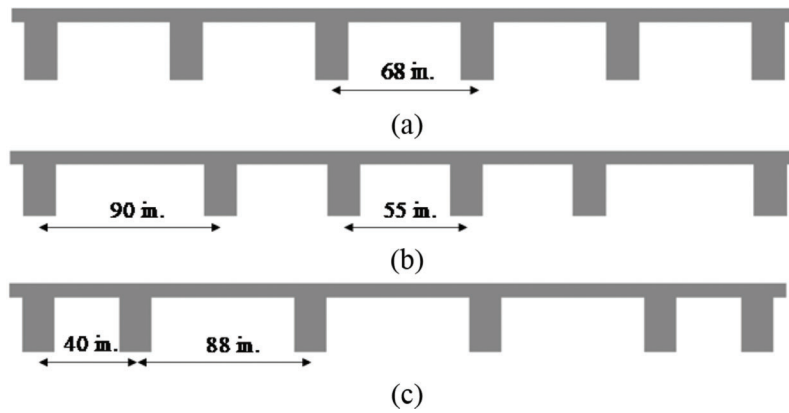


Figure 5.14 Placement of evenly/unevenly spaced girders at section view of T-beam bridge with (a) even (b) uneven #1 (c) uneven #2 girder spacing.

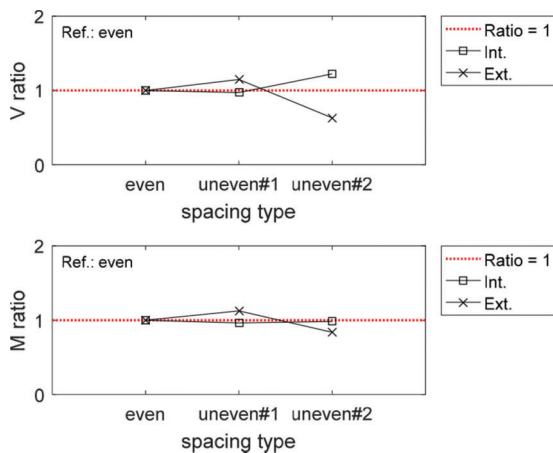


Figure 5.15 Moment and shear change according to girder spacing type (T-beam bridges).

girder locations in comparison with those where girders were spaced evenly at intervals. An uneven girder spacing scheme with larger spacing between interior girders led to higher stresses in those girders, causing higher moment and shear demand. It follows that exterior girders took the relatively lower moment and shear.

In sum, the geometrical characteristics studied above were shown to have a significant impact on structural demand in bridges, with the exception of diaphragm thickness (negligible effect) and the slab thickness (minor effect). Some of these factors are not reflected in the methodology outlined in AASHTO specifications and may potentially be a source of overestimation or underestimation of demands on bridges by current specifications. Above all, effect of railings needs to be properly considered when the deck and railings are properly anchored by reinforcement. A potential improvement of current procedures may be in the form of a modified lateral load distribution factor that reflects the effect of geometric parameters for easy use by structural engineers. These observations form the basis for the discussion and proposed implementation presented in Chapter 6.

6. DISCUSSION OF RESEARCH FINDINGS

6.1 Introduction

In this study, ten RC bridges were evaluated using two different procedures. In the first approach, the bridges were rated using the CLR approach, which relied on 2D beam analysis to estimate demands. The results of CLR were then compared with demand and capacity estimates obtained using 3D finite element analysis of bridge super-structure models. The evaluation of rating factors focused on differences between the two approaches regarding the distribution of live and dead loads as well as capacity calculations, since these are crucial parts of the RF equation. It was observed that modeling the bridge superstructure in 3D with all geometrical features included could affect the distribution of loads and consequently final values of RF. In the following sections, the main differences observed between the two approaches are discussed.

6.2 Demand Estimation

Demand evaluation is one of the key components of load rating procedures. The findings of this study indicate that moment and shear responses estimated in 2D and 3D approaches differ for both dead load and live load applications. In the 2D approach, the dead load was calculated according to geometrical dimensions of the superstructure and evenly distributed over beam-strips (slab bridges) and girders (T-beam), while in 3D, the superstructure weight was considered by the gravity application to the superstructure model. Figure 6.1 illustrates the difference between moment responses obtained from the two approaches for two bridge samples, and results indicate that dead load (DC) response might be overestimated in 2D analysis for interior strips/girders. This finding suggests that distributing the weight of all structural and nonstructural components evenly over the bridge deck could exaggerate the share of interior deck portions, resulting in higher values for DC. In Figure 6.1, the colored graphs indicate interior strip/girder moment envelopes from 3D analysis, and they are compared to the 2D

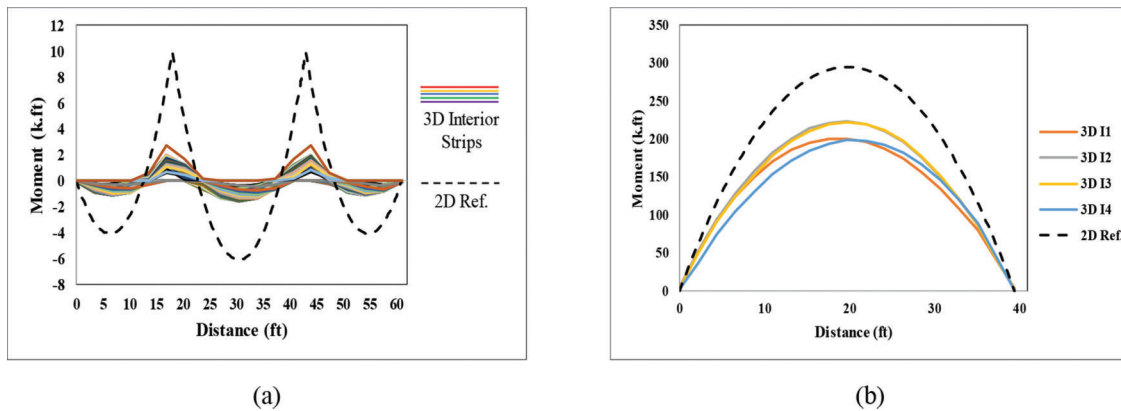


Figure 6.1 Moment response comparison for interior strips/girders: (a) Sample #1 (b) Sample #7.

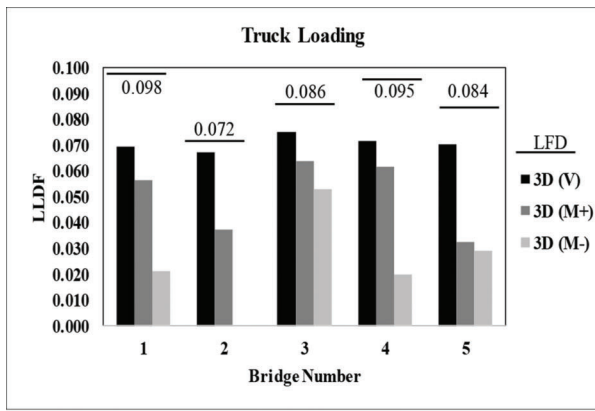
envelope shown with black dashed-line. Only moment envelopes are illustrated in the graphs since such difference was more prominent in moment responses rather than shear.

To investigate differences between live load applications in the two methods, distribution factors calculated based on formulations suggested by AASHTO specifications were compared to those obtained from finite element analysis as explained in Chapter 4.3. Figure 6.2 demonstrates the difference between LLDFs of interior strips/girders obtained from 2D and 3D methods for different load configurations used for the evaluation. The results showed that in most of the cases, the distribution factor obtained from approximate formulas in AASHTO (shown as the horizontal lines in the parts of Figure 6.2) are larger than those from 3D analysis. The one exception is that under lane-load application specified by LFD, the shear distribution factors obtained from 3D analysis are larger compared to 2D ones. This could be attributed to the effect of a large value of point load (26 kips) application over the traffic lane, resulting large shear stresses. Moreover, it is observed that distribution factors for moment were affected more than those for shear when using 3D FEA, resulting in smaller distribution factors for moment compared to those for shear. This result suggests that LLDFs should be given separately for estimation of moment and shear demand. This is an approach presently not recommended for flat-slab bridges in the specifications (AASHTO, 2002, 2014). In flat slab bridges, LLDFs for interior strips decreased by average of about 18, 37, and 62% for shear, positive moment, and negative moments, respectively. In total, the impact of 3D analysis on distribution factors is more significant for negative moment than positive moment, which could be attributed to the effect of continuity of spans in the model. Similarly, in the case of T-beam bridges, 3D distribution factors are smaller than 2D values for interior girders with an average decrease of almost 43% and 37% for moment and shear effects, respectively. Additionally, unlike exterior strips in slab bridges, LLDFs of exterior girders were improved in all cases except for bridge

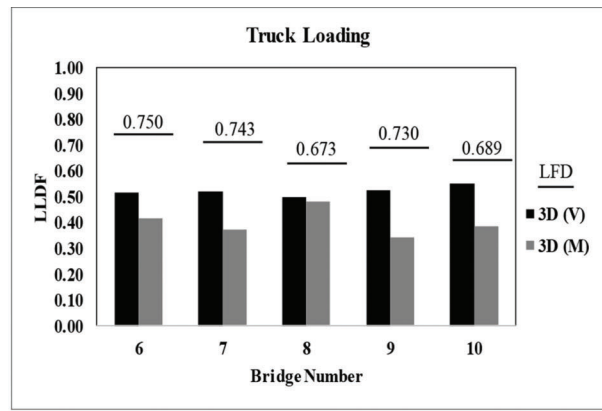
#10, which has the taller railing among all bridge samples.

6.3 Effect of Geometrical Parameters

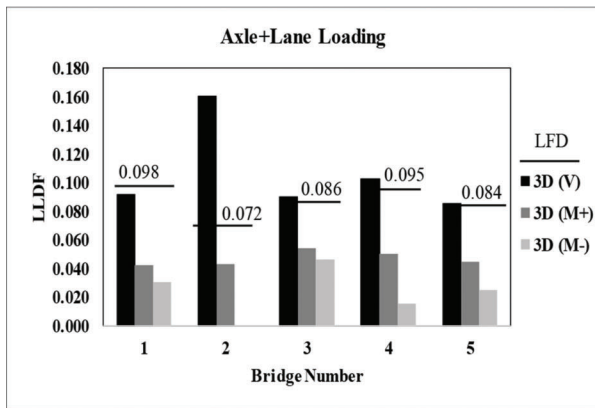
Based on results obtained from 3D analysis, several geometrical parameters influencing the 3D FE analysis results were selected for a more detailed parametric study performed in Chapter 5. Railing height, skew angle degree, diaphragm width, slab thickness, and girder spacing were selected as potential influential geometrical parameters. The parametric study results indicated that railing height and skew angle were the more significant parameters. The increment of both mentioned parameters had a beneficial effect, especially on the moment response of the two bridge types. Figure 6.3 shows maximum moment values obtained for interior strips/girders for different values of railing height and skew angle. In the Figure, the x-axis indicates variable ranges of railing height and skew angle. The results indicated that by increasing both variables, moment response decreases. However, the railing height was the more significant parameter for the bridge types considered. It can be also observed that beneficial contributions due to the presence of the railing decrease beyond a railing height of 40 in. This observation confirms that railing height and skew factor have a discernible impact on demand estimation and, consequently, on load distribution factors. In current distribution factor formulations (AASHTO, 2014, 2002), the presence of railing is neglected, and its weight is distributed on the bridge slab, whereas in the 3D analysis, the results suggested that railings contribute significantly to both demand and capacity calculations for exterior strips. Although skew factor is considered for T-beam bridges, it is ignored for slab type bridges. The findings of the parametric study showed favorable impact of railing/sidewalk and skew features on demand evaluation if implemented in LLDF formulation. Including the RC railing in superstructure modeling could decrease the moment response up to 65% and 27% for slab and T-beam bridges, respectively.



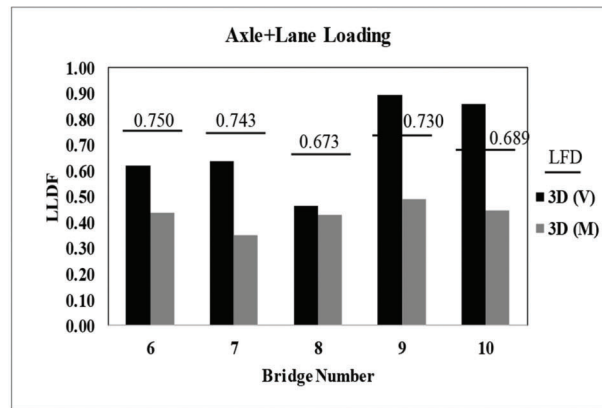
(a-1)



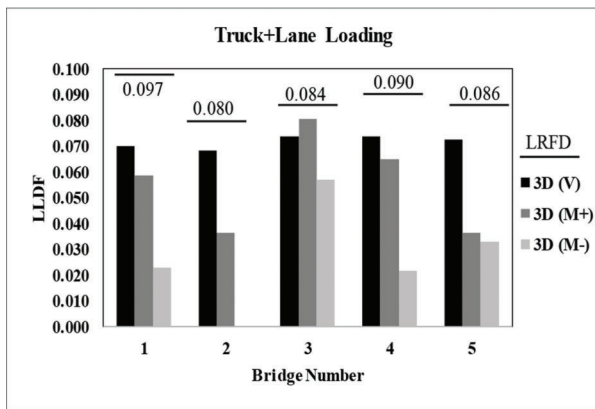
(b-1)



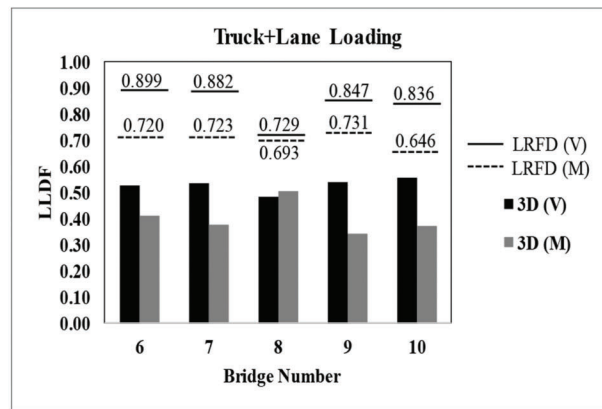
(a-2)



(b-2)



(a-3)



(b-3)

Figure 6.2 LLDFs comparison for interior strips/girders: (a) slab bridge (b) T-beam bridge.

Additionally, implementing the skew factor in deck modeling resulted in 58% and 33% reduction in moment values obtained for slab and T-beam bridges, respectively.

By comparing the moment responses obtained for 1-span and 3-span slab bridge models (Figure 6.4), it can be observed that the moment reduction is more significant for 1-span bridges (larger slope) when increasing the railing height from 0 to 40 in. It follows

that number of spans could play a role in effectiveness of geometrical features and consequently the LLDFs.

6.4 Capacity Calculation

In the evaluation of rating factors, moment and shear capacities were calculated for interior and exterior strips/girders, separately. With the inclusion of railings, exterior strips attracted higher stresses, due to an

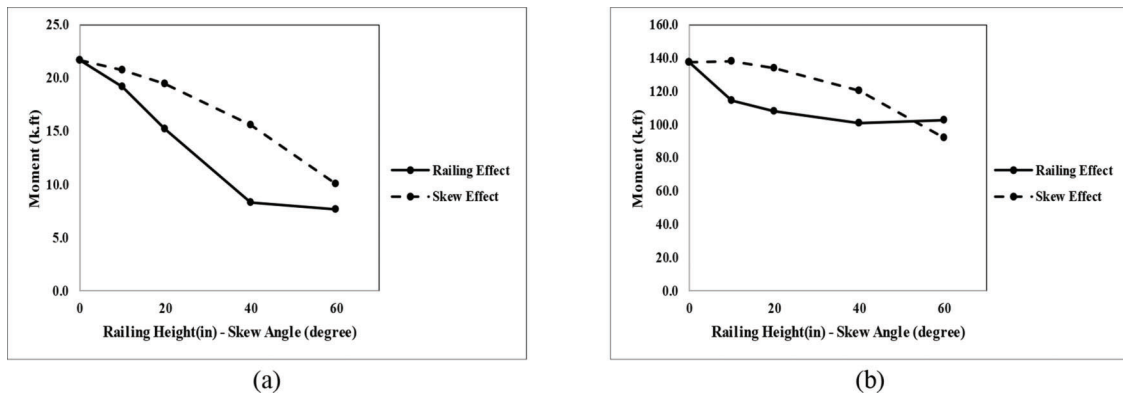


Figure 6.3 Railing and skew effect: (a) slab bridge (b) T-beam bridge.

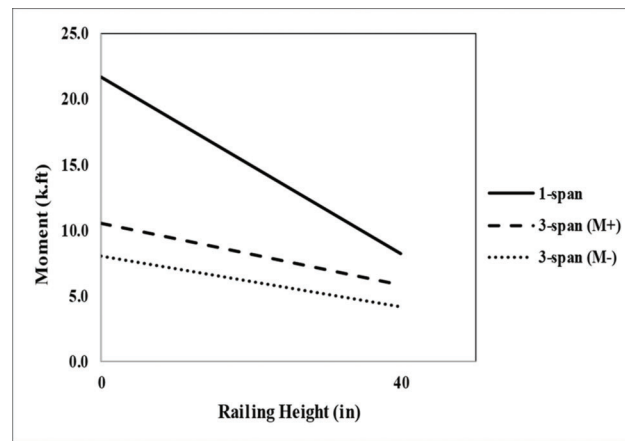


Figure 6.4 Moment reduction for 1-span and 3-span bridges with railing of 40 in.

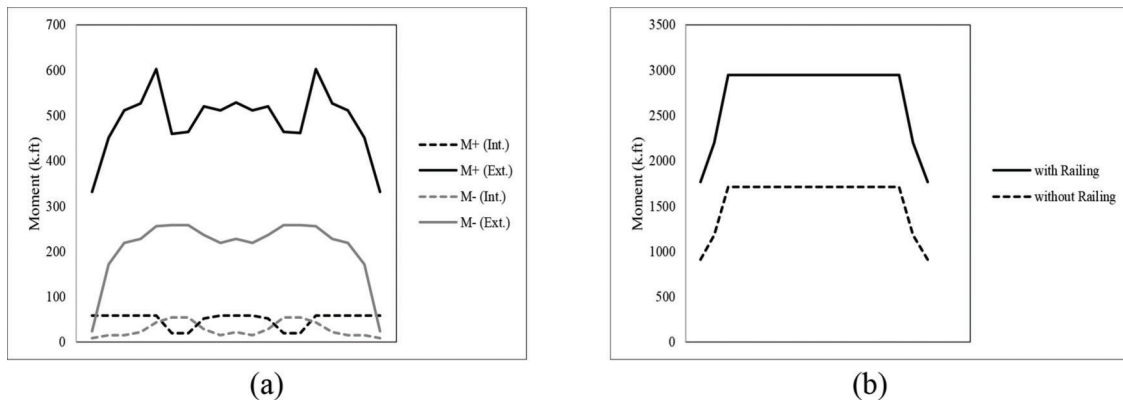


Figure 6.5 Moment capacity of interior and exterior strips/girders: (a) slab (b) T-beam.

increased stiffness, and were therefore allocated a greater share of loads. Despite the increase in demand, an increase in capacity led to rating factors above the critical value of one. Figure 6.5 demonstrates the moment capacity of exterior strip/girder incorporated with railing compared to one without. Larger cross-section of the edge beams and a great amount of reinforcement provided in them resulted in significant increases in capacity as shown in the figure. As

discussed in Chapter 4, the contribution of edge strip/girder cross-sections in moment and shear capacity was determined based on observation of normal and shear strain developments in finite element model. Therefore, in slab bridges, railing section could be considered contributing in moment and shear capacity of exterior strips while for T-beam bridges, the railing part was considered being active only in moment with negligible contribution in shear.

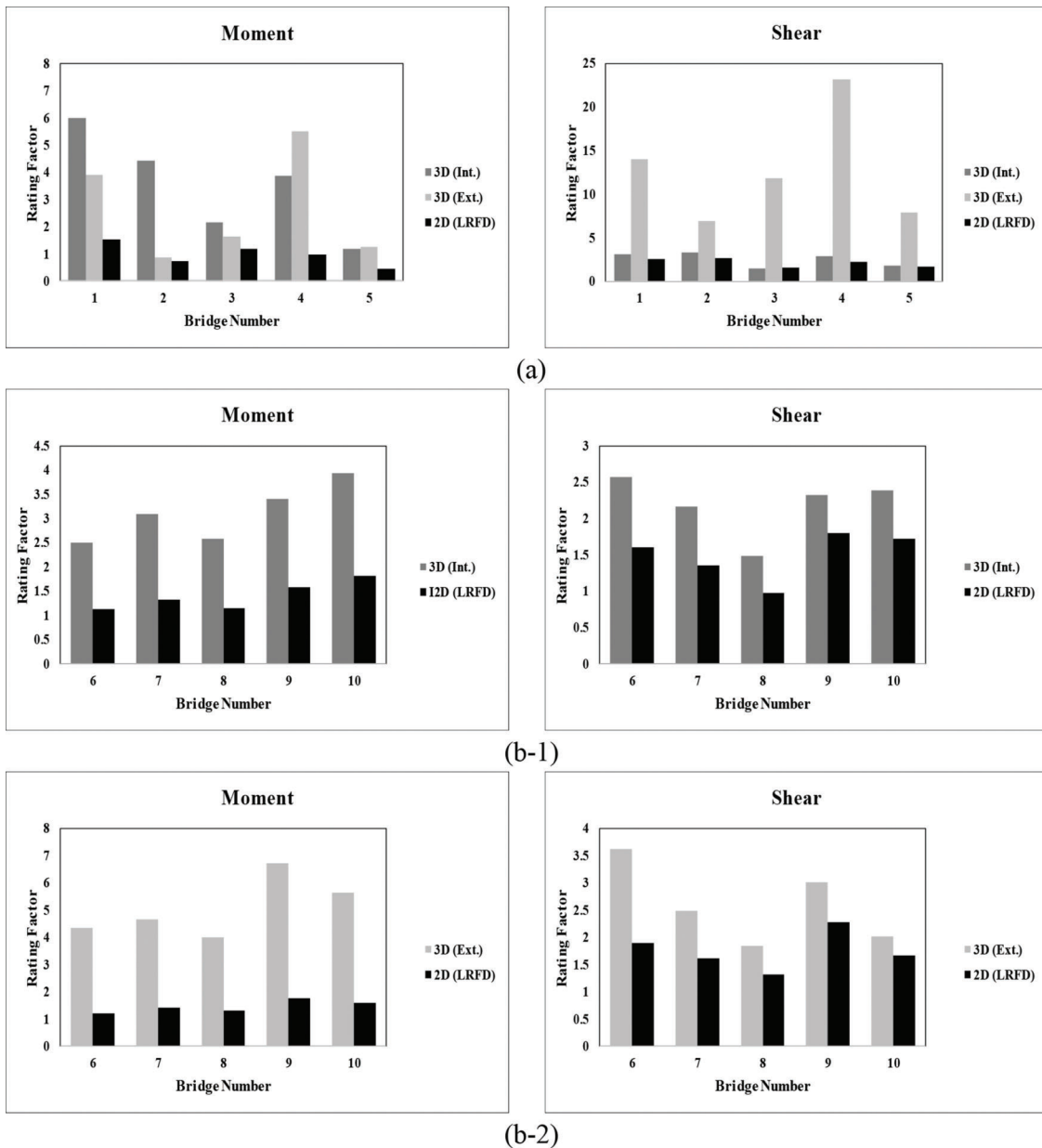


Figure 6.6 2D and 3D rating factor comparison: (a) slab (b-1) interior of T-beam (b-2) exterior of T-beam.

6.5 Improvement in Rating Factors

Final rating factor values estimated following 2D approach and using 3D finite element analysis were presented in Chapter 4.5. Figure 6.6 illustrates graphically the differences between the two methods. In slab bridges, average rating factors obtained from 3D analysis for moment are 3.7 and 2.7 times larger than the corresponding 2D values for interior and exterior strips, respectively. These ratios are 1.2 and 6.2 for shear. Similarly, in T-beam bridge samples, the ratio between 3D and 2D moment rating factors are 2.2 and 3.5 for interior and exterior girders, respectively. The corresponding value for shear is 1.5 for both girder types.

6.6 Summary of Findings

The findings of this study indicated that the simplified analysis methodology for load rating provided by AASHTO, called CLR, underestimates the load rating in RC slab and T-beam bridges. Rating factors obtained based on 3D FEA increased significantly as a result of using 3D superstructure models where structural and nonstructural features are represented explicitly. It was also shown that the main factor affecting the results was demand distribution across the bridge (LLDF). Additionally, a parametric study associated with demand estimation showed a substantial influence of geometric features on load distribution, and consequently moment and shear responses. These features are railing height,

deck skew angle, and support area. The inclusion of end diaphragm in T-beam bridges improved the results slightly. Variable deck cross-section and girder spacing changed the results significantly. It was concluded that neglecting these parameters in LLDF formulation could lead to overestimation of load assigned to strips/girders.

7. SUMMARY AND PROPOSED IMPLEMENTATION

7.1 Summary of Findings

The goal of this project was to investigate a potential improved methodology for the load rating evaluation of flat-slab and T-beam reinforced concrete (RC) bridges in Indiana using the tools of 3D analysis. To this end, five tasks were conducted, and the findings of each task are summarized below.

Task 1. Selection of representative bridges. Five representative bridges for each bridge type were selected from the NBI database for Indiana. Among many structural/nonstructural features, the followings were considered to identify the bridge samples—year built, span length, number of spans, number of lanes, curb-to-curb roadway width, skew angle, and depth of decks (or beams/girders).

Task 2. Bridge strength assessment using conventional rating method. The selected bridges were assessed using the 2D-based CLR methodology currently in practice in Indiana to establish the basis for comparison with the refined 3D FEA results. The rating factors calculated for the bridges in the sample indicate that some bridges (Sample #2 and Sample #5) exhibit moment deficiency, which makes them candidates for possible retrofitting actions, posting, or replacement depending on their current traffic count. It is also observed that moment is the controlling effect as a result of locations lacking sufficient steel reinforcement or where reinforcement is only partially developed. In most of T-beam bridges, smaller rating factors were obtained for interior girders compared to exterior ones, mainly due to the larger live load distribution factors (LLDF) of interior girders.

Task 3. Bridge strength assessment using 3D finite element analysis. For a more detailed assessment of the selected bridges, 3D FEA was conducted with a detailed model of the bridge superstructure geometry (railings, skew angle, slab thickness, girder spacing, etc.). The observed sensitivity of load positioning in lateral direction to evaluate live load distribution factors indicates that considering one single distribution factor for an entire superstructure and all loading scenarios may not be effective to reflect actual lateral distribution of live loads.

Concrete railings, when properly anchored for monolithic action, play a significant role in allocating a large portion of the response (both moment and shear) to

exterior strips/girders. This subsequently decreases the share of interior ones. Therefore, the LLDFs calculated for interior strips/girders are smaller compared to those obtained by the formulation in AASHTO specifications, while distribution factors of exterior strips/girders are larger. It is found that larger LLDF values for exterior strips/girders did not lead to critical rating factors since capacity was also improved due to increased stiffness. In summary, *rating factors obtained from 3D FEA are greater than those obtained using the 2D approach for both LFD and LRFD approaches.* Greater share of demand absorbed by the edges indicates the importance of considering railings in LLDF evaluation.

Task 4. Sensitivity analysis of geometrical parameters. Bridge geometrical characteristics such as railings, skew angle, slab thickness, supports area, and spacing between the girders were considered as potential factors having an impact on LLDF. Railing height was confirmed as a parameter that produced the most drastic change in moment and shear demands of bridges. Particularly, changes in moment and shear demands for exterior strips were more prominent than those of interior strips. An increase in skew angle was found to cause a reduction in moment and increase in shear for both 1-span and 3-span bridges. The effect of slab thickness of slab bridges was relatively small and slab thickness variation along the bridge length resulted in a slight reduction in moment. Models with area support showed a decrease in both moment and shear when compared to the models with line supports, indicating the importance of area support modeling in 3D FEA. For T-beam bridges, the effect of diaphragm thickness was observed to be negligible. Lastly, T-beam bridge with uneven girder spacing affected moment and shear demand in comparison with even girder spacing, and the effect was dependent on the girder spacing scheme, which stresses the importance of the consideration of actual girder spacing in LLDF calculation.

Task 5. Discussion of Research findings and proposed implementation. The comparison of rating factors obtained from CLR and 3D FEA indicate that CLR according to AASHTO specifications results in lower estimates of load rating factor in RC slab and T-beam bridges. LLDF is the main parameter affecting the results. Furthermore, a parametric study associated with demand estimation showed a substantial influence of geometric parameters on LLDF. Railing, deck skewness, and support area had substantial beneficial impact on demand response. It follows that neglecting these parameters in LLDF formulation could lead to overestimation of load shares assigned to strips/girders.

7.2 Proposed Implementation

Based on the study results and conclusions, the following recommendations are presented for consideration and possible implementation.

1. The comparison of rating factors obtained from CLR and 3D FEA indicated that the CLR methodology provided in AASHTO specifications results in lower load rating factor in RC slab and T-beam bridges and the live load distribution factor (LLDF) was shown to be the main parameter affecting the results. All sample bridges showed an increase in rating factors when evaluated using the 3D FEA-based load rating method compared to CLR values. Notably, three out of four bridges that rated unfavorably, with load rating results below 1 using CLR, showed ratings above 1 with the 3D FEA approach (compare the results of Task 2 and Task 3). The remaining bridge with the rating factor less than "1" (Sample #2) was further improved with the consideration of support area in 3D FE modeling, as shown in Task 4.
2. Given the improved load rating estimates, it is recommended that bridges that exhibit border-line load rating results be analyzed using the 3D FEA-based procedure, while the standard rating methods (CLR) may continue to be used for a conservative estimate of bridge rating.
3. Further improvements can be made to CLR to incorporate 3D effects while maintaining the simplicity of load rating procedures. The presence of railing has a substantial influence on stress distribution in the bridge super-structure, causing higher stress concentrations in exterior strips and reduces stresses in interior ones. It is therefore recommended that, in dead-load demand estimations using CLR, railing weight be allocated entirely to the exterior strips, instead of distributing it evenly across the bridge, as is done current practice using BRR.
4. The study also showed that on the capacity side, an important consideration is the inclusion of the reinforced concrete railing in the estimation of capacity for flexure and shear in RC slab bridges and for flexure in T-beam bridges. Therefore, it is recommended to include reinforced concrete railings properly anchored into the bridge superstructure in the determination of capacity of exterior strips and girders.
5. A parametric study associated with demand estimation showed a substantial effect of geometric features on LLDF. The study showed that railing height, deck skew, and support area had substantial impacted obtained values of moment and shear. It was also concluded that neglecting these parameters in LLDF formulation could lead to overestimation of load assigned to strips/girders. To simplify the incorporation of these geometric features in load rating calculations by INDOT or structural engineers using current 2D rating methods, a modified live load distribution factor formula, where the effect of these parameters could be taken into account would improve rating estimates. A more extensive parametric

study in support of the development of a modified live load rating factor is recommended.

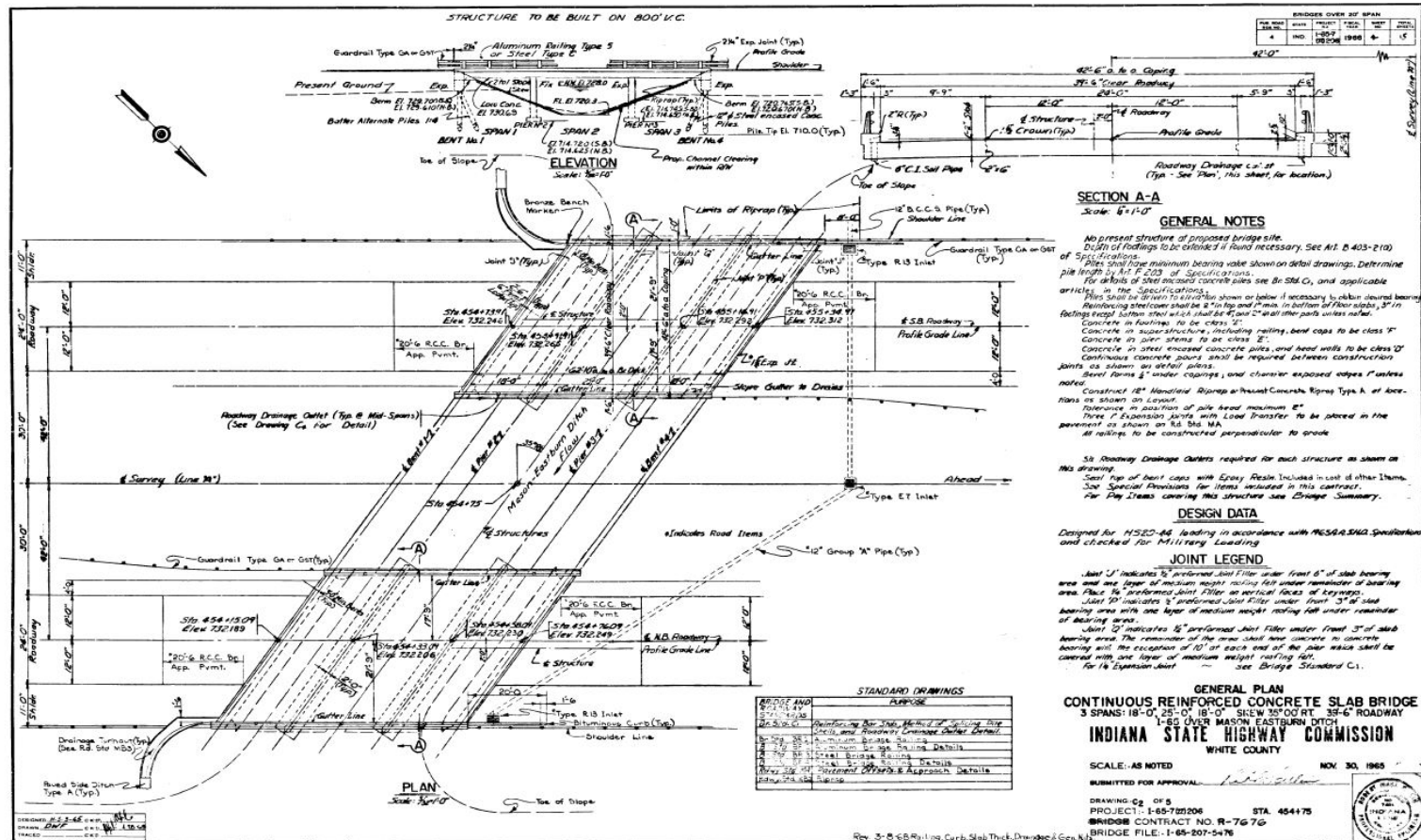
REFERENCES

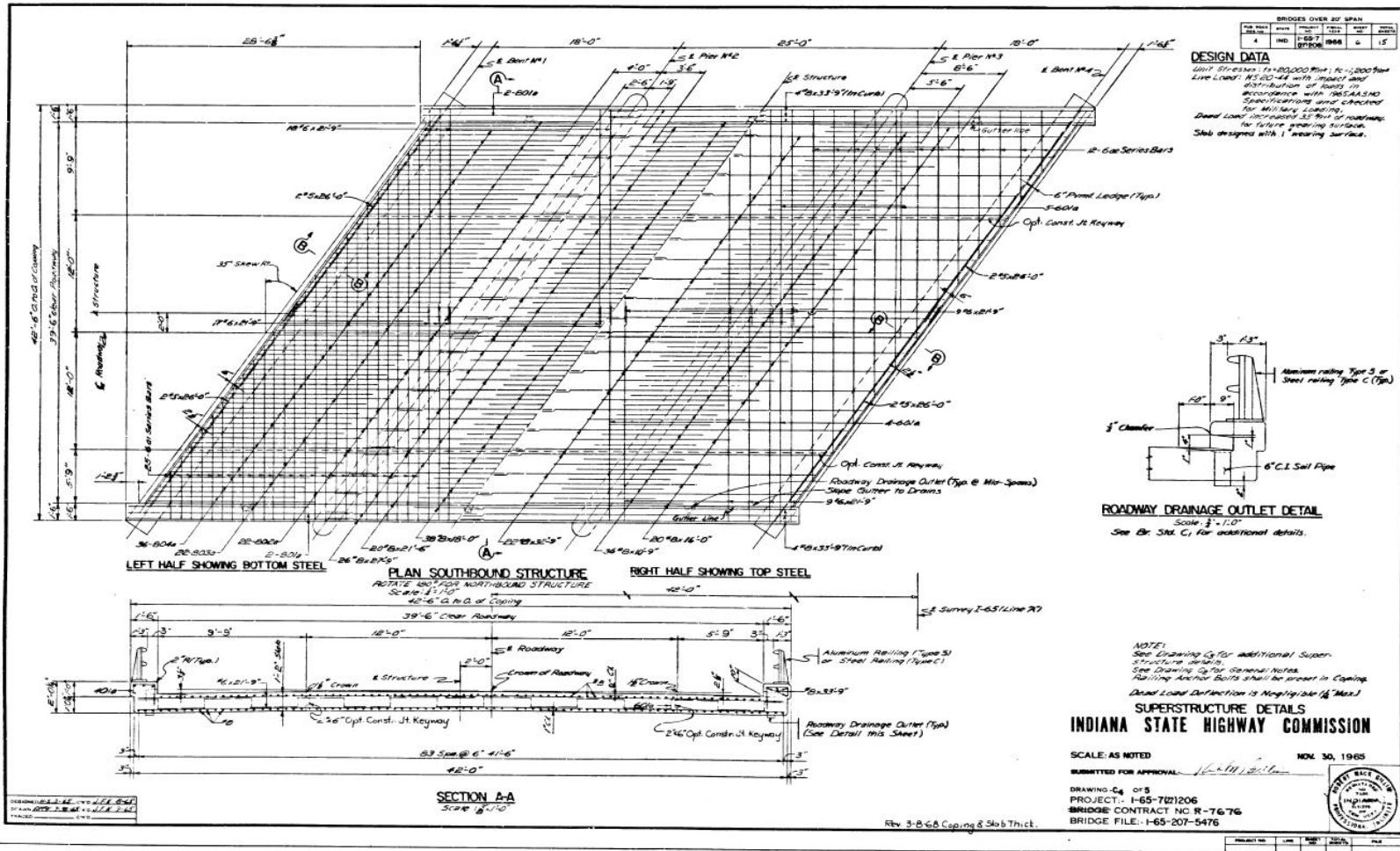
- AASHTO. (2002) *AASHTO standard specifications for highway bridges* (17th ed.). Washington, DC: American Association of State Highway and Transportation Officials.
- AASHTO. (2011). *2011 interim revisions to the manual for bridge evaluation*. Washington, DC: American Association of State Highway and Transportation Officials.
- AASHTO. (2014) *AASHTO LRFD bridge design specifications* (7th ed.). Washington, DC: American Association of State Highway and Transportation Officials.
- American Society of Civil Engineers. (2013). 2013 report card for America's infrastructure findings: Roads [Web page]. Retrieved from <http://2013.infrastructurereportcard.org/>
- Barker, R. M., & Puckett, J. A. (2013). *Design of highway bridges: An LRFD approach* (3rd ed.). Hoboken, NJ: John Wiley & Sons.
- Cai, C. S., & Shahawy, M. (2003) Understanding capacity rating of bridges from load tests. *Practice Periodical on Structural Design and Construction*, 8(4), 209–216. [https://doi.org/10.1061/\(ASCE\)1084-0680\(2003\)8:4\(209\)](https://doi.org/10.1061/(ASCE)1084-0680(2003)8:4(209))
- Catbas, F. N., Ciloglu, S. K., Hasançebi, O., Popovics, J. S., & Aktan, A. E. (2003). *Re-qualification of aged reinforced concrete T-beam bridges in Pennsylvania*. Philadelphia, PA: Drexel University. Retrieved from <https://pdfs.semanticscholar.org/af33/82f9d7b00458ba9303459f2fecb7e8ca39b3.pdf>
- Ding, L., Hao, H., Xia, Y., & Deeks, A. J. (2012). Evaluation of bridge load carrying capacity using updated finite element model and nonlinear analysis. *Advances in Structural Engineering*, 15(10), 1739–1750. <https://doi.org/10.1260/1369-4332.15.10.1739>
- Hasançebi, O., & Duşlupınar, T. (2013). Detailed load rating analyses of bridge populations using nonlinear finite element models and artificial neural networks. *Computers & Structures*, 128, 48–63. <https://doi.org/10.1016/j.compstruc.2013.08.001>
- Sanayei, M., Reiff, A. J., Brenner, B. R., & Imbaro, G. R. (2016). Load rating of a fully instrumented bridge: Comparison of LRFR approaches. *Journal of Performance of Constructed Facilities*, 30(2), 04015019-1–04015019-7. [https://doi.org/10.1061/\(ASCE\)CF.1943-5509.0000752](https://doi.org/10.1061/(ASCE)CF.1943-5509.0000752)
- Shahrooz, B. M., Ho, I. K., Aktan, A. E., de Borst, R., Blaauwendraad, J., van der Veen, C., ... Miller, R. A. (1994). Nonlinear finite element analysis of deteriorated RC slab bridge. *Journal of Structural Engineering*, 120(2), 422–440. [https://doi.org/10.1061/\(ASCE\)0733-9445\(1994\)120:2\(422\)](https://doi.org/10.1061/(ASCE)0733-9445(1994)120:2(422))

APPENDIX

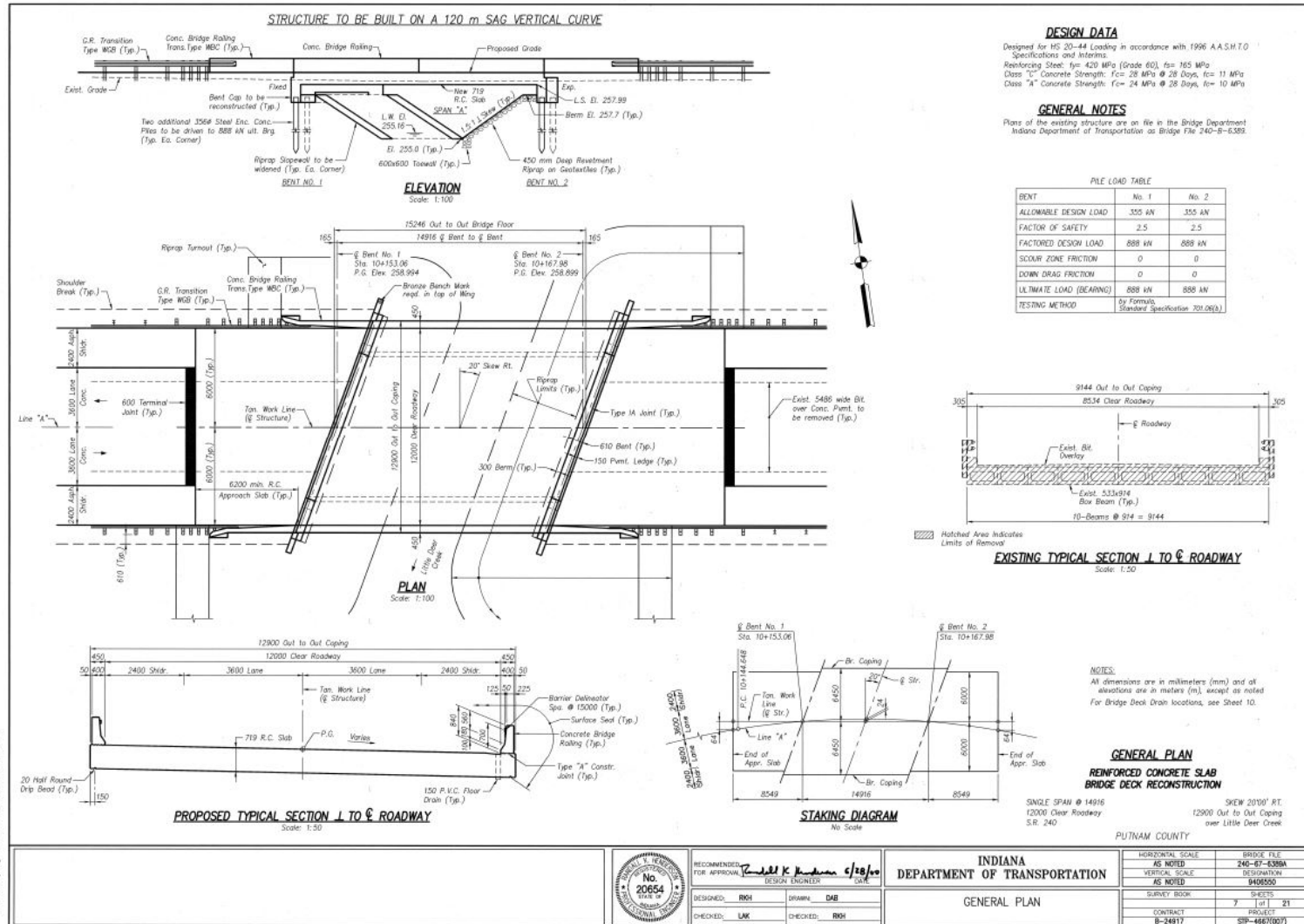
SUPERSTRUCTURE PLANS AND REINFORCEMENT DETAILING OF SAMPLE BRIDGES

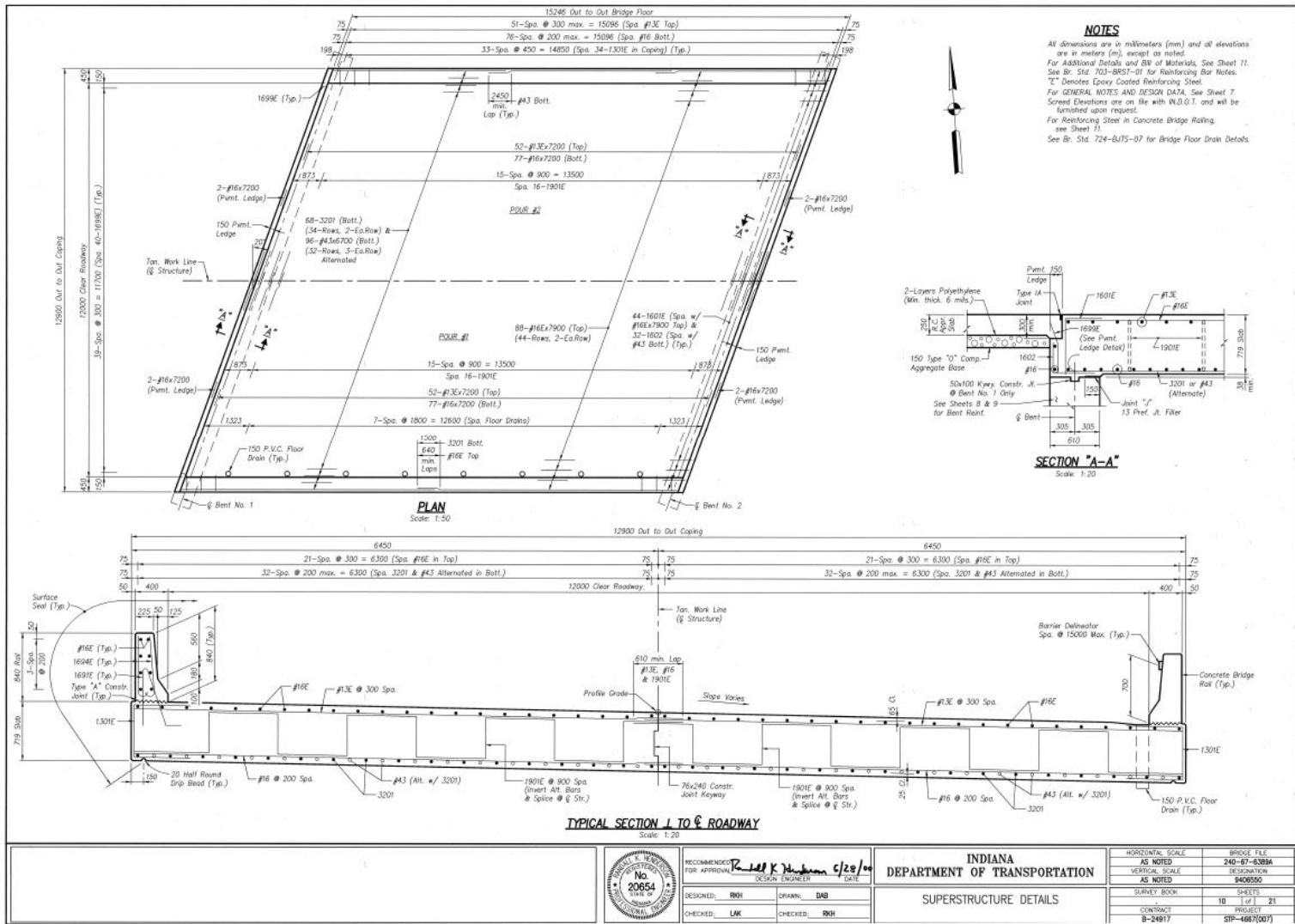
Sample #1





Sample #2





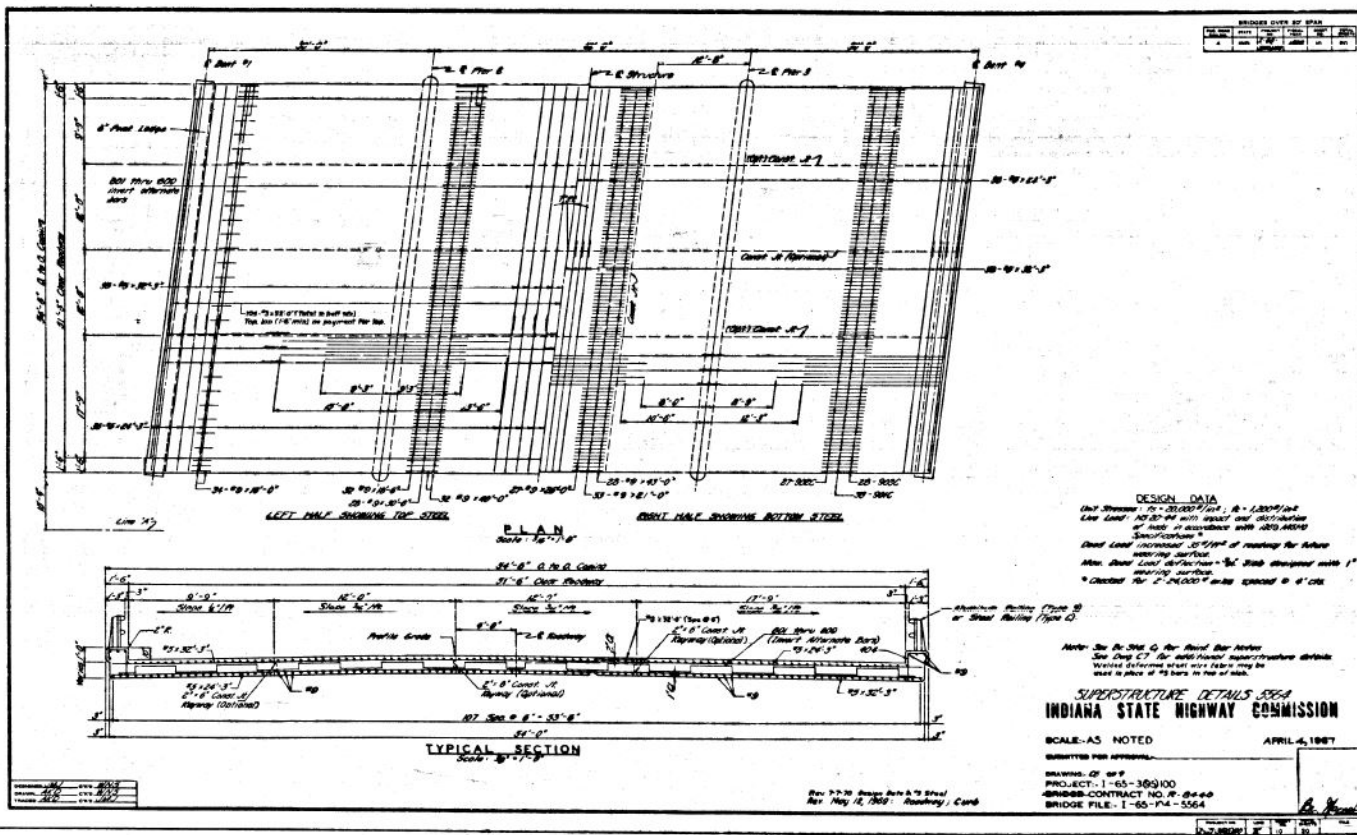
FILENAME: hsp1.dwg DATE: JAN 11, 2000 TIME: 11:43 AM



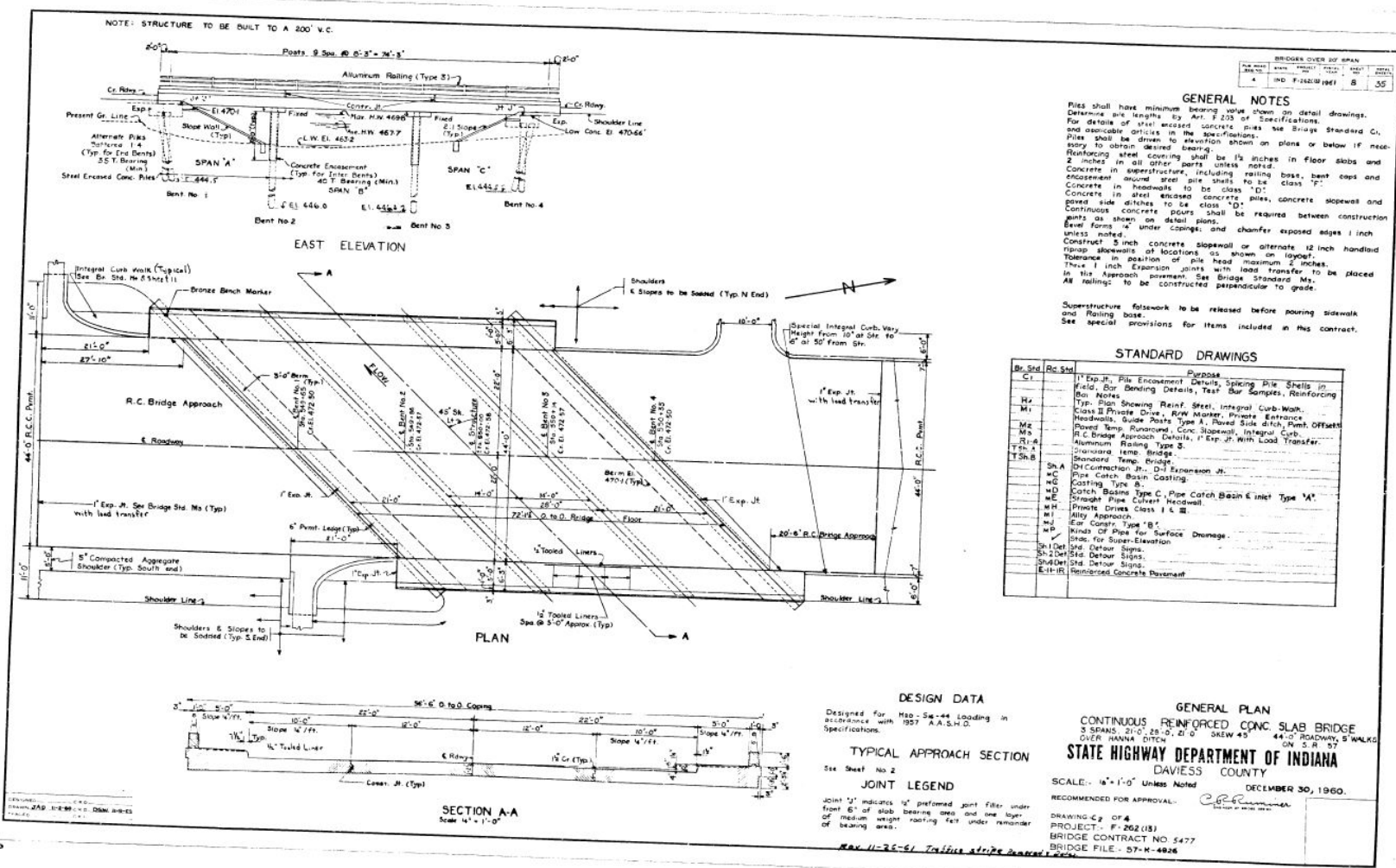
RECOMMENDED FOR APPROVAL: *Robert K. Johnson* 6/28/00
 DESIGN ENGINEER DATE
 DESIGNED: RGH DRAWN: BAB
 CHECKED: LAK CHECKED: RGH

INDIANA
 DEPARTMENT OF TRANSPORTATION
 SUPERSTRUCTURE DETAILS

HORIZONTAL SCALE	BRIDGE FILE
AS NOTED	240-61-6388A
VERTICAL SCALE	DESIGNATION
AS NOTED	9406550
SURVEY BOOK	SHEETS
10	1 OF 21
CONTRACT	PROJECT
B-24917	STP-4667(007)



Sample #4



GENERAL NOTES

Piles shall have minimum bearing value shown on detail drawings. Determine pile lengths by Art. 2.23 of Specifications.

For details of steel encased concrete piles see Bridge Standard C1, and applicable articles in the specifications.

Piles shall be driven to elevation shown on plans or below if necessary to obtain desired bearing.

Reinforcing steel covering shall be 1 1/2 inches in floor slabs and 2 inches in all other parts unless noted.

Concrete in superstructure, including raising base, bent caps and encasement around steel pile shells to be class "D".

Concrete in roadways to be class "D".

Concrete in steel encased concrete piles, concrete slopewalls and gored side ditches to be class "D".

Continuous concrete piers shall be required between construction joints as shown on detail plans.

Level forms to be used on gorges and chamfer exposed edges 1 inch unless noted.

Construct 3 inch concrete slopewall or alternate 12 inch handhold riprap slopewalls of locations as shown on layout.

Tolerance in position of pile head maximum 2 inches.

Three 1 inch expansion joints with load transfer to be placed in the Approach pavement. See Bridge Standard M5.

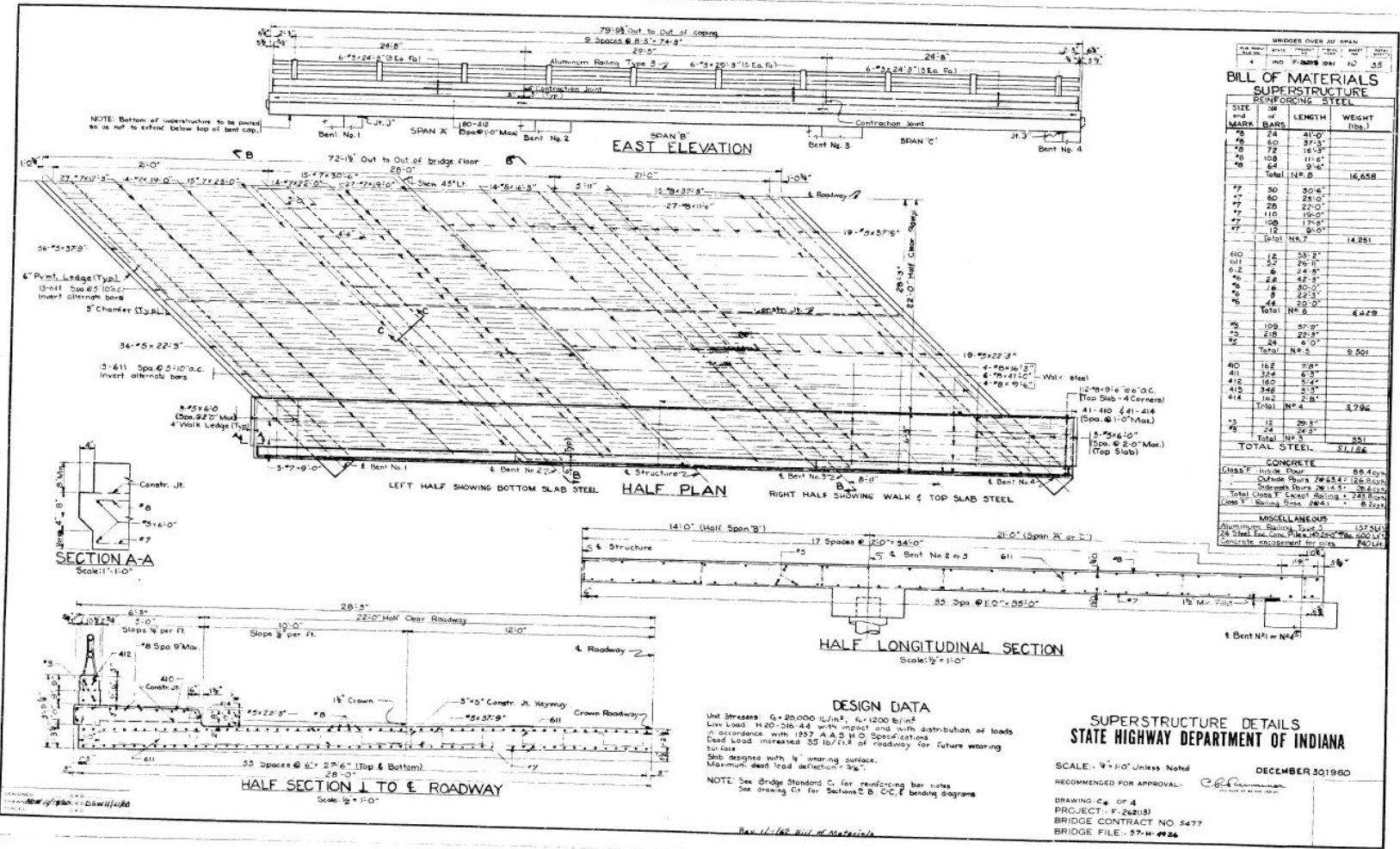
All fillings to be constructed perpendicular to grade.

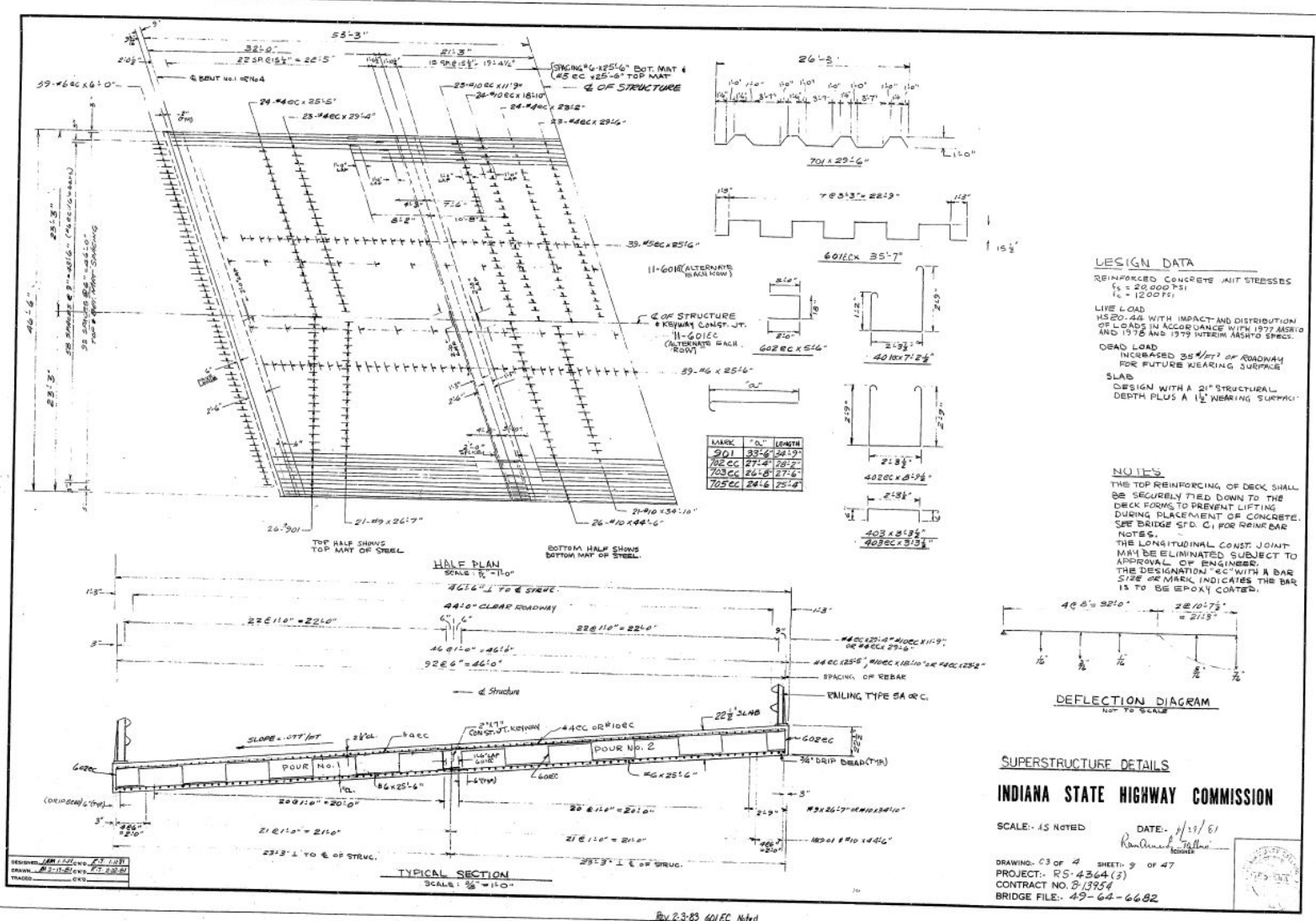
Superstructure falsework to be released before pouring sidewalk and raising base.

See special provisions for items included in this contract.

STANDARD DRAWINGS

Br. Sec.	Re. Sec.	Particulars
C1		Pile Encasement Details, Piling Pile Shells in Field, Bar Bending Details, Test Bar Samples, Reinforcing Bar Notes
M5		Type: Plan Showing Reinf. Steel, Integral Curb-Walk, Class II Private Drive, Run Marker, Private Entrance Headwalls, Guide Posts, Type A, Road Side ditch, Pile Offsets
M6		Road Temp. Roundabout, Conc. Slopewall, Integral Curb
M8		R.C. Bridge Approach Details, 1' Exp. Jt. With Load Transfer
R1-A		Aluminum Railing Type S
T1-A		Standard Temp. Bridge
T1-B		Standard Temp. Bridge
SN		Dr. Connection Jt., Dr. Expansion Jt.
WC		Pipe Catch Basin Coating
WC		Coating Type B
WD		Catch Basins Type C, Pipe Catch Basin E inlet Type "A"
WE		Straight Pipe Culvert Headwall
WH		Private Drive Class I & II
WI		Alley Approach
WP		Kind of Pipe for Surface Drainage
Z		Shds. for Super-Elevation
SH1-D		Std. Detour Signs
SH2-D		Std. Detour Signs
SH3-D		Std. Detour Signs
E11-1R		Reinforced Concrete Pavement





DESIGN DATA

REINFORCED CONCRETE UNIT STRESSES
 $f_c = 20,000 \text{ PSI}$
 $f_s = 12,000 \text{ PSI}$

LIVE LOAD
 MS20-44 WITH IMPACT AND DISTRIBUTION
 OF LOADS IN ACCORDANCE WITH 1977 MSRB
 AND 1978 AND 1979 INTERIM MSRB SPEC.

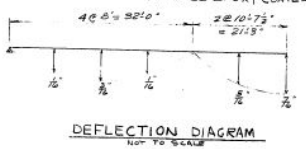
DEAD LOAD
 INCREASED 35% OF ROADWAY
 FOR FUTURE WEARING SURFACE

SLAB
 DESIGN WITH A 2" STRUCTURAL
 DEPTH PLUS A 1/2" WEARING SURFACE

NOTES

THE TOP REINFORCING OF DECK SHALL
 BE SECURELY TIED DOWN TO THE
 DECK FORMS TO PREVENT LIFTING
 DURING PLACEMENT OF CONCRETE.
 SEE BRIDGE S.F.D. C FOR REINBAR
 NOTES.

THE LONGITUDINAL CONST. JOINT
 MAY BE ELIMINATED SUBJECT TO
 APPROVAL OF ENGINEER.
 THE DESIGNATION "EC" WITH A BAR
 SIZE OR MARK INDICATES THE BAR
 IS TO BE EPOXY COATED.



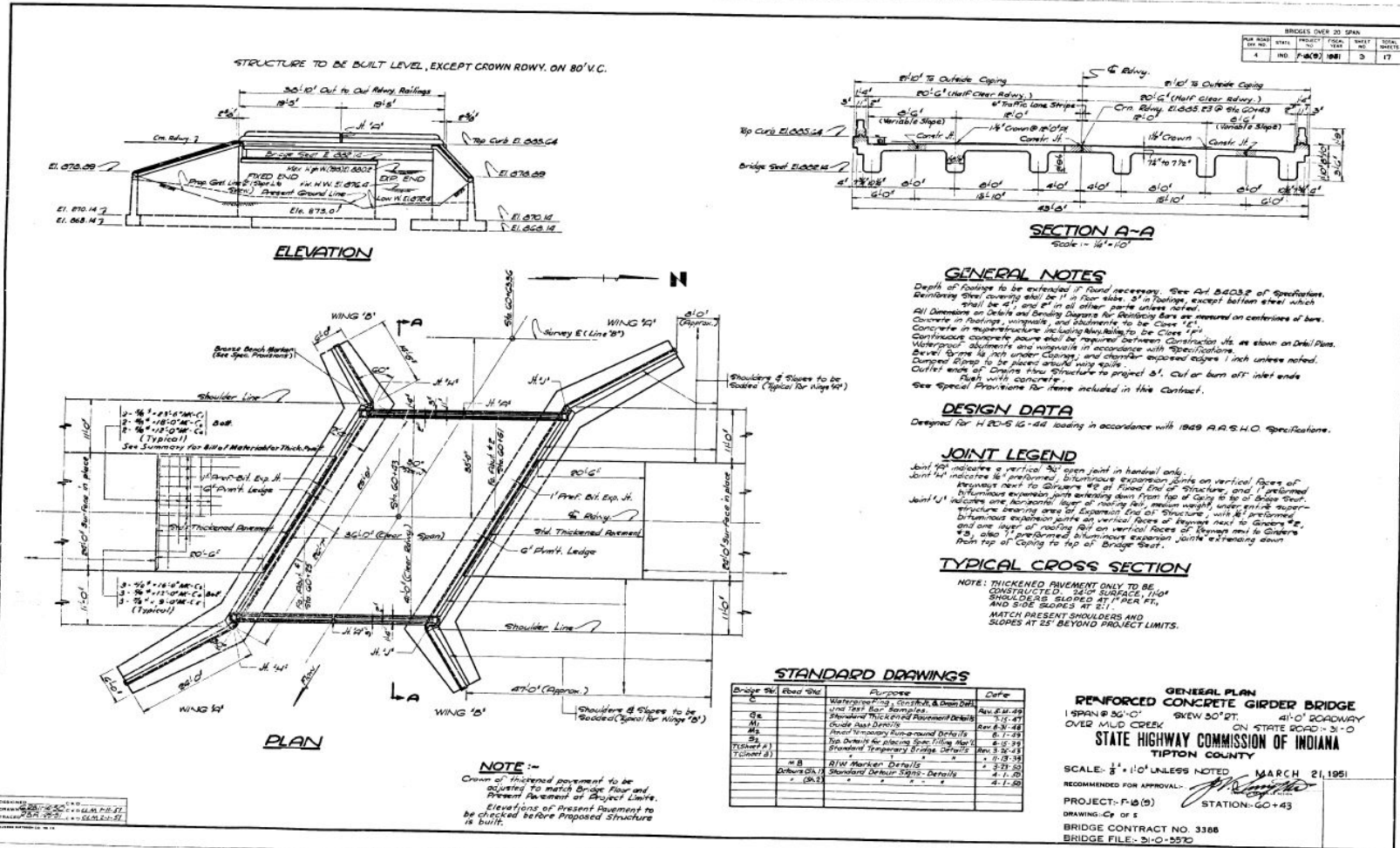
SUPERSTRUCTURE DETAILS
INDIANA STATE HIGHWAY COMMISSION

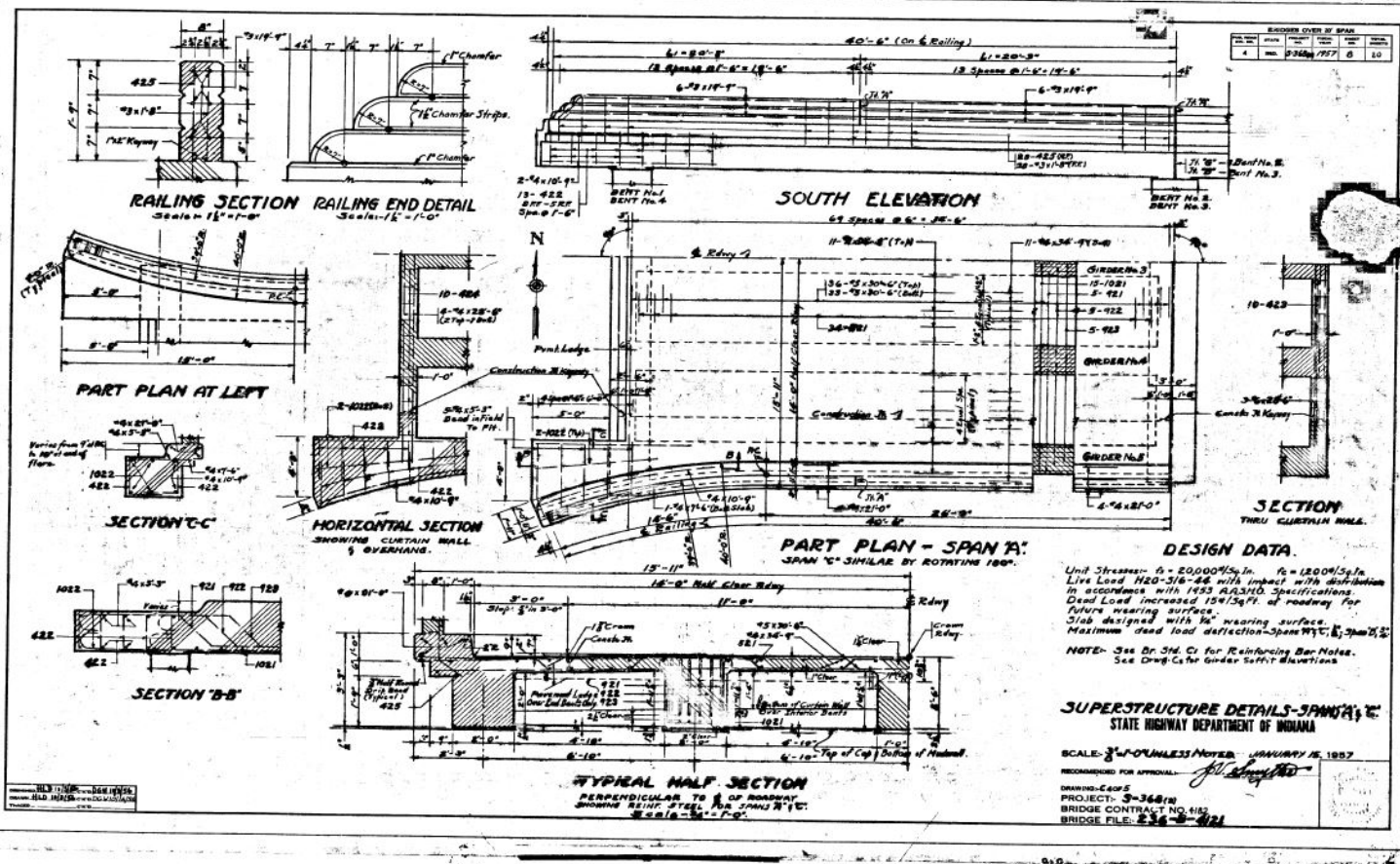
SCALE: AS NOTED DATE: 1/11/81

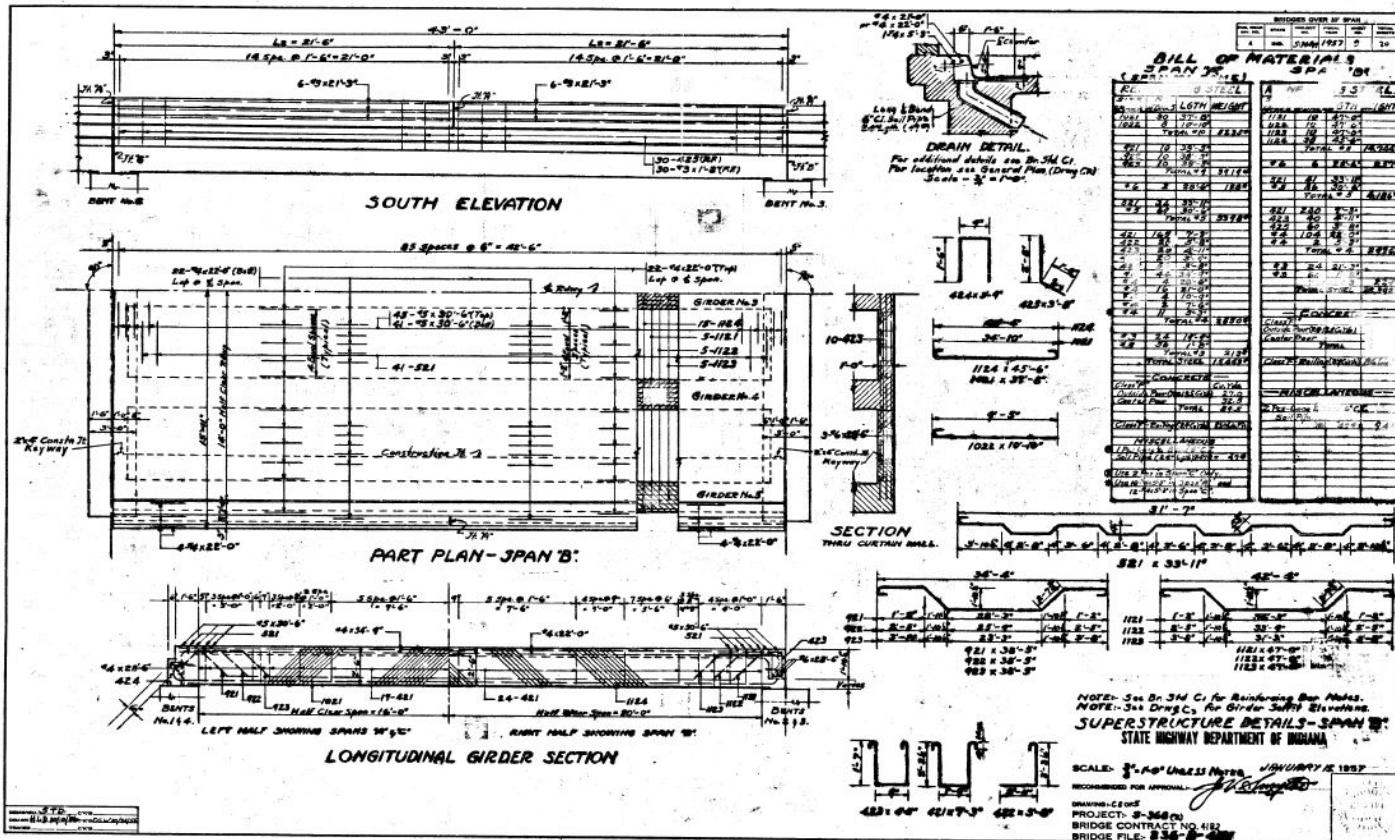
DRAWING: CS OF 4 SHEET: 9 OF 47
 PROJECT: RS-4364(S)
 CONTRACT NO. B-13754
 BRIDGE FILE: 49-62-6682

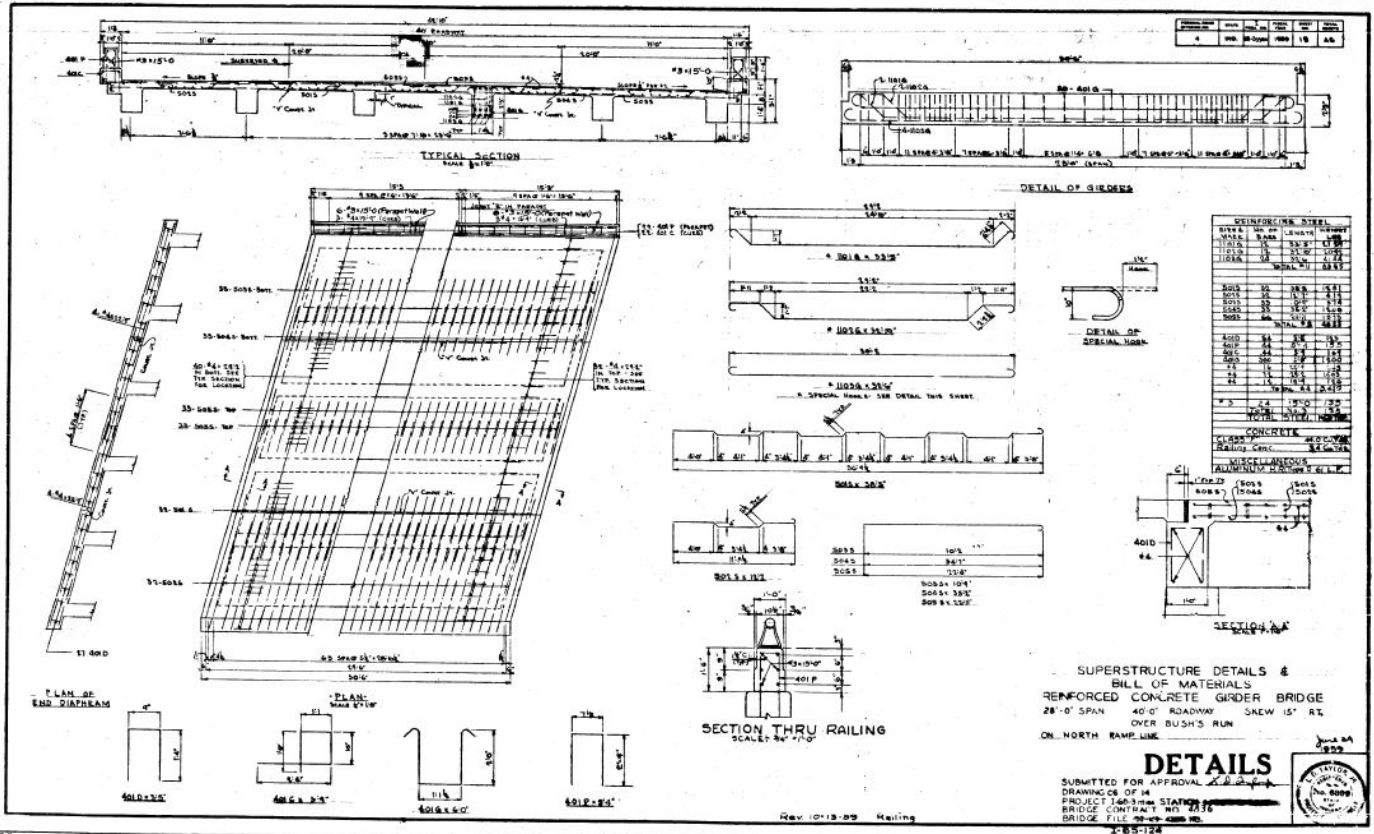
By 2-85 601EC Mtd

Sample #6









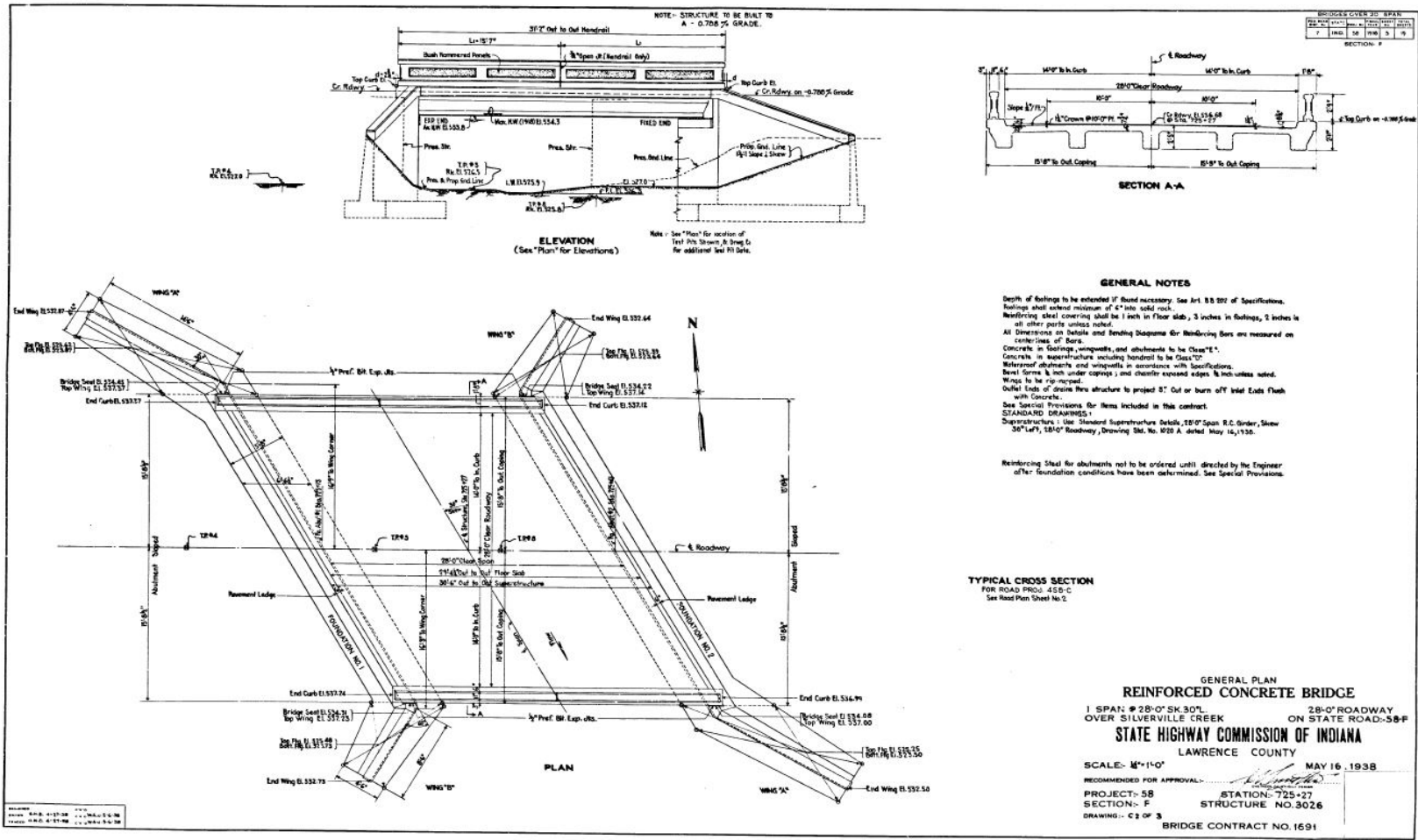
SUPERSTRUCTURE DETAILS &
BILL OF MATERIALS
REINFORCED CONCRETE GIRDER BRIDGE
28'-0" SPAN 40'-0" ROADWAY SKEW 15° RT.
OVER BUSH'S RUN
ON NORTH RAMP LINE

DETAILS

SUBMITTED FOR APPROVAL
DRAWING NO. OF 14
PROJECT: I-40/100 STATION
BRIDGE CONTRACT NO. 2336
BRIDGE FILE NO. 100-100-100



Sample #10



About the Joint Transportation Research Program (JTRP)

On March 11, 1937, the Indiana Legislature passed an act which authorized the Indiana State Highway Commission to cooperate with and assist Purdue University in developing the best methods of improving and maintaining the highways of the state and the respective counties thereof. That collaborative effort was called the Joint Highway Research Project (JHRP). In 1997 the collaborative venture was renamed as the Joint Transportation Research Program (JTRP) to reflect the state and national efforts to integrate the management and operation of various transportation modes.

The first studies of JHRP were concerned with Test Road No. 1 — evaluation of the weathering characteristics of stabilized materials. After World War II, the JHRP program grew substantially and was regularly producing technical reports. Over 1,600 technical reports are now available, published as part of the JHRP and subsequently JTRP collaborative venture between Purdue University and what is now the Indiana Department of Transportation.

Free online access to all reports is provided through a unique collaboration between JTRP and Purdue Libraries. These are available at <https://docs.lib.purdue.edu/jtrp/>.

Further information about JTRP and its current research program is available at <https://engineering.purdue.edu/JTRP>.

About This Report

An open access version of this publication is available online. See the URL in the citation below.

Seok, S., Ravazdezh, F., Haikal, G., & Ramirez, J. A. (2019). *Strength assessment of older continuous slab and T-beam reinforced concrete bridges* (Joint Transportation Research Program Publication No. FHWA/IN/JTRP-2019/13). West Lafayette, IN: Purdue University. <https://doi.org/10.5703/1288284316924>